Politecnico di Milano
SCHOOL OF INDUSTRIAL AND INFORMATION ENGINEERING
Master of Science – Energy Engineering

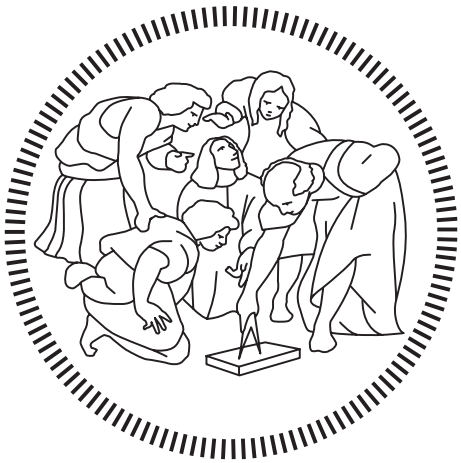

Synthetic methane production in high-RES remote regions: design and techno-economic evaluation of a large-scale PtG plant

Supervisor
Prof. Giulio GUANDALINI

Co-supervisor
Dr. Paolo COLBERTALDO

MSc Thesis by
Emilio BOSI – Matr. 905778

Academic Year 2019 – 2020

Acknowledgements

Per prima cosa vorrei ringraziare il Professor Guandalini e il mio correlatore Paolo Colbertaldo, non avrei potuto chiedere di meglio. Mi sento anche di ringraziare il Professor Valenti che è stato il mio mentore nelle mie prime esperienze lavorative in Novelis. Sempre lì in Novelis devo molto anche a Pierangelo per il tanto tempo passato insieme e che ha speso per trasmettermi tanta esperienza. Un ringraziamento particolare va anche a mio zio Emilio che per il mio percorso è un faro e il mio punto di riferimento. Non posso che ringraziare tutta la mia famiglia, che mi ha sempre fornito un supporto emotivo e soprattutto un confronto culturale, fondamentale per la mia crescita. Ci tengo anche a ringraziare tutti i miei più cari amici e gli affetti, senza di voi questi anni sarebbero stati molto bui.

Infine dedico una nota particolare a mio nonno Dino, senza alcun dubbio ho scelto di fare l'ingegnere nella mia vita per via di tutto il tempo passato insieme a costruire archi e balestre insieme. A 8 anni mi hai regalato un trapano della Bosch, dicendomi che quando sarei cresciuto avrei potuto usarlo, all'inizio non capivo... poi mi sono reso conto che lui invece già aveva capito tutto di me. Anche se non sei qui con me ti dedico questa tesi perché è a te che devo tutto questo.

Sommario

I più recenti valori di LCOE rilevati da fonti rinnovabili situate in regioni remote aprono la possibilità di sfruttare tale energia anche per usi diversi, ad esempio produrre gas sintetico. Tale processo rientra nella tecnologia chiamata Power to Gas (PtG), che prevede la trasformazione di acqua e anidride carbonica in metano, consumando energia elettrica nel passaggio intermedio di elettrolisi.

L'obiettivo di questo lavoro è stato il dimensionamento di un grande impianto PtG situato in una zona ad alto potenziale rinnovabile scollegata dalla rete elettrica e di valutarne i costi, in particolare il costo del gas prodotto.

L'analisi ha considerato il fotovoltaico per la produzione di elettricità e la tecnologia Alkaline electrolyte (AEK) per il processo di elettrolisi, mentre per il processo di metanazione si è adottata la tecnologia dei reattori a letto fisso adiabatico. Come fonte di anidride carbonica sono state valutate due alternative: la prima prevede l'acquisto di CO_2 catturata in un impianto industriale limitrofo (CC), la seconda integra la cattura direttamente della CO_2 dall'atmosfera con la tecnologia Direct Air Capture (DAC).

L'impianto è stato dimensionato in tre differenti configurazioni: una usa la CC e le altre due usano la DAC; quella che usa la CC e una delle due DAC, usano un pacco batterie agli ioni di litio mentre l'altra prevede una turbina a gas alimentata a idrogeno per produrre energia elettrica. Le tre configurazioni sono state valutate in tre casi: il primo (Full Load) prevede che il metanatore lavori sempre alla potenza nominale, richiedendo grandi accumuli per gestire l'intermittenza della fonte primaria; nel secondo caso (Full Load and Recovery) il calore disperso dal metanatore viene recuperato e utilizzato; nel terzo caso (Partial Load with Recovery and Oversizing) il metanatore viene sovradimensionato e viene aggiunta la possibilità di operare a carico parziale.

Lo studio ha investigato l'efficienza energetica delle nove configurazioni insieme al costo del gas prodotto, evidenziando un'efficienza di conversione da energia elettrica a gas tra il 31% (DAC con turbina a gas) e il 39% (CC) .Poi sono stati calcolati i due prezzi breakeven

della CO_2 che facevano allineare LCOM del caso CC con quello delle altre due filiere DAC. Questa analisi è stata fatto solo per il caso migliore (Partial load). Un'analisi di sensibilità sul CAPEX dei componenti dell'impianto ha permesso di valutarne l'effetto sul costo finale del gas, mostrando che il maggior responsabile dei costi è il PV seguito dall' AEK. Il costo finale del gas è stato confrontato con un prezzo di riferimento del gas naturale mostrando che il gas sintetico costa più di dieci volte l'equivalente fossile.

Parole chiave: Power to Gas; Metanazione; Stoccaggio dell'energia; Gas naturale sintetico

Abstract

The low values of LCOE achieved recently by RES in remote location opens the possibility to use electricity-derived fuels as energy carriers to exploit such affordable energy source. The process for the synthesis of these fuels stays within the Power to Gas (PtG) technology, involving the conversion of water and carbon dioxide to methane by means of electric energy for the intermediate electrolysis process.

The objective of this work is to design and evaluate the economic potential of a large PtG plant located in a region offering high RES potential while not being connected to the electric grid.

In the analysis, photovoltaic is used as source of power, alkaline electrolyte (AEK) is used for electrolysis and adiabatic fixed bed reactors is the technology considered for methanation. As source of carbon dioxide, two alternatives are studied: capturing CO_2 from the exhaust gases of nearby industrial facilities (CC) or capturing carbon dioxide directly form atmosphere (Direct Air Capture, DAC).

The PtG plant is designed in three configurations, one using CC and the other two using DAC. The one using CC and one of the two DAC use Lithium-ion batteries for energy storage, the other uses a hydrogen-fed gas turbine to generate electric energy. These three configurations are evaluated in three cases: in the first (Full Load) the methanator always works at full load, requiring larger storage systems; in the second (Full Load and Recovery) the waste heat of the methanator is recovered and used; the third case (Partial Load with Recovery and Oversizing) oversizes the methanator and adds the possibility to operate at partial load.

First, the analysis assesses the efficiency of each configuration as well as the corresponding Levelized Cost of Methane (LCOM), evidencing that the electric to gas efficiency goes from 31% (DAC with gas turbine) to 39% (CC). Then, it is calculated the breakeven price of carbon dioxide that aligns the LCOM of the three supply chains in Partial load case, as it revealed the most convenient. A sensitivity analysis has been performed on the CAPEX of

the system components to evaluate the impact on the LCOM, showing that the most critical element is PV followed by AEK. The final cost of synthetic gas compared to a reference price of natural gas shows that the renewable gas costs more than ten times its fossil alternative.

Keywords: Power to Gas; Energy storage; Methanation; Synthetic methane.

Extended Abstract

Introduction

In the last years the levelized cost of electricity from renewable sources has reached values that are competitive with those of the fossil alternatives. Modern renewables, like photovoltaic (PV) and wind, located in high-RES locations can reach extremely low cost of production, leading to consistently high profits. One example is the record low bid of 2.34 c$/kWh for the 300 MW PV power plant in Sakaka (Saudi Arabia) in 2018 [1]. The most appealing areas in the world are South America, western Sahara and northern Russia for onshore wind farms, while Middle East and North Africa show an impressive potential for PV. In some regions the two technologies are both high performing, such as western Sahara and Andes. If used in combination, they can provide a more stable load. Unfortunately, most of these high-RES regions are also remote areas, so the potential low cost of electricity has no role since there are no consumers nearby; therefore, this high potential remains trapped.

The key to unlock this high potential is energy storage. One option is to transform the electric energy generated by renewables into liquid or gaseous fuels that can then be transported to consumers elsewhere. This supply chain can take advantage of the low cost of electric energy to synthetize a stable energy carrier. The technology is called Power-to-Gas (PtG). The simplest option is to synthetize hydrogen by means of water electrolysis. However, hydrogen requires a significant energy effort to be transported especially on great distances due to low volumetric energy density, while hydrocarbons are easier to be transported. To synthetize hydrocarbons, hydrogen is still needed, becoming an intermediate product of the supply chain. The other essential element for hydrocarbon synthesis is the carbon source. One possibility is to use carbon dioxide, which reacting with molecular hydrogen produces hydrocarbon products. The use of carbon dioxide is of particular interest as carbon dioxide could be extracted from the atmospheric air or recovered from exhaust gases of industrial facilities. In both cases the synthetic fuels will result carbon neutral from a life-cycle point of view.

The objective of this work is to design and evaluate the economic feasibility of a large PtG plant located in a high-RES region.

Methodology and configurations

Considering hydrogen production from RES electricity by electrolysis, in principle, every RES could be used. Wind and PV gather great attention as they show an impressive theoretical potential, especially in remote regions. PV power output is far more predictable than wind power and the construction of a wind farm is more complex, with the need to undergo long-term on-site measurements to verify the actual potential. Consequently, PV technology is selected preferred in this work as the primary energy source of the simulated PtG plants, due to easier location selection and parameters influence evaluation.

The location selection is a crucial milestone of the analysis, since the site should satisfy the following requirements:

- access to water for electrolysis feed;
- proximity to Oil & Gas distribution channels for product delivery;
- high RES potential;
- presence of industrial facilities as source of carbon dioxide is also an asset.

In addition, for practical applications of this concept, political stability is a requirement for safe investments. Yanbù, Saudi Arabia, has been selected after an accurate screening. It is a strategic hub for the Oil & Gas supply chain and its harbor is one of the most important channels of oil distribution and export. The estimated power output of a PV system in such area is really one of the highest in world (1922 kWh/y from Solar Global atlas). Water supply is ensured by the desalting of sea water. In addition, the site is full of industrial facilities that could behave as good source for carbon dioxide source. The high stability of the government and the fact that the area is highly industrialized is a good feature for a large-scale installation. Saudi Arabia government also promoted utility scale PV projects (like the one in Sakaka mentioned above). From all points of view, Yanbù is a very strategical position for a very large scale PtG plant.

Given the electricity source, the main unit to be selected is the electrolysis system. As of today, there are mainly two commercial electrolysis technologies: alkaline electrolyte electrolyzers (AEK) and polymeric membrane electrolyzers (PEM), whereas solid oxide electrolyzers (SOEC) are promising but only available as prototype or in the small scall. For this work, alkaline technology (AEK) is selected as it is the most mature and economical technology at the current state of art.

Since the PtG plant is intended to operate off-grid and connected to intermittent electricity sources, an electric energy storage system for input smoothing and peak shaving is mandatory. For this purpose, Lithium-ion batteries are used due to their commercial maturity. Furthermore, storage systems (tanks) for the local accumulation of chemical products (hydrogen, CO2) are needed.

As concerns the methanation system, chemical methanation is an established technology and has been preferred in this work. The alternative is biological methanation that has been tested in a few lab and pilot plants, while its feasibility for large-scale commercial plants still needs to be proved [2]. Among the different options for chemical methanation systems, the adiabatic fixed bed reactors have been used in this work to design the plant, since it is the most established technology.

As source of carbon dioxide for the methanation process, two alternatives have been studied in this work: capturing CO_2 from exhaust of nearby industrial facilities (Carbon Capture, CC) or capturing carbon dioxide directly from the atmosphere (Direct Air Capture, DAC). Two groups of technologies can be identified for direct air carbon capture: the first uses a water solution containing a hydroxide sorbent with a strong affinity to CO_2, the second relies on the use of amines bonded on a porous solid support. The main difference is the operational temperature: the capture using liquid sorbent requires high temperature ($T > 800°C$) [3], while the solid sorbent technology requires temperature around 100°C. For the purpose of this work, the solid sorbent technology is considered as it is possible to use the waste heat of the methanator to feed the heat demand of the DAC system, thus improving the energy efficiency of the plant. A schematic representation of the proposed PtG plant is displayed in Figure 1.1.

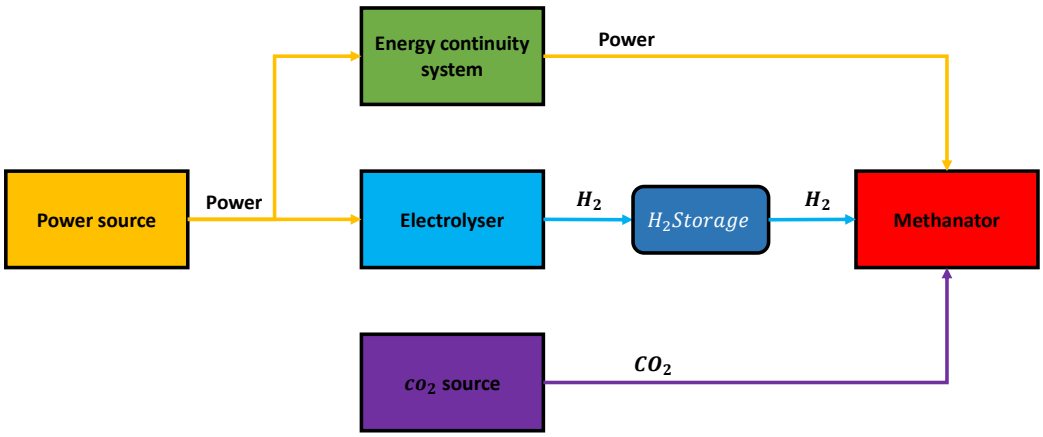

Figure 1.1 Schematic representation of a PtG plant for synthetic methane production.

In this work, three configurations are analysed:

1. *PV-CC-BES*, in which carbon dioxide is purchased from nearby industrial plants that are equipped with carbon capture. The plant is powered during the night by electric energy stored in a lithium ion battery package.
2. *PV-DAC-BES*, which is similar to the previous one in terms of plant component, with the difference that carbon dioxide is locally captured from atmospheric air using a DAC system. Thermal demand of the DAC is provided with electric resistances, so both electric and thermal demand are provided by the battery package when the plant is off.
3. *PV-DAC-GT*, in which the batteries are removed and a gas turbine is installed to generate electricity and heat by burning hydrogen from the electrolyzer.

This set of configurations is evaluated in three different cases, leading to a matrix of nine configurations. The first case is the Full Load case (FL), in which the methanator is intended to work always at full load throughout the year, so the BOP (Balance of Plant) needs to be designed to guarantee such conditions, in particular affecting the storage systems. The second case is the Full Load with heat Recovery case (FLR), which differs from the FL case by the fact that the waste heat of the methanator is recovered and used. In the PV-CC-BES

configuration, the waste heat powers an ORC system in order to generate additional electric energy that is consumed internally in the plant. In the other two supply chains the heat is used to partially cover the heat demand of the DAC system. The third case is the Partial load and Oversizing (PLRO) in which it the methanator is oversized and the plant can run at halved load. This case is an extension of the FLR so even in this case the heat recovery is done.

A model called *Days clustering* is used to create three prototype generation daily profiles, corresponding to a "worst day", an "average day" and a "best day". The "worst day" is of particular interest as it is the day on which the plant is sized. The sizing procedure considers only mass and energy balances on a daily basis, meaning that the size of AEK and PV plant ensure the production of a constant steady stream of 100 MW_{LHV} of SNG during the "worst day". Since there is not a unique combination of PV and AEK sizes that guarantees a steady production of 100 MW_{LHV} it is introduced the economic factor to find the cheapest solution that complies with the technical constraints. The model uses the independent variable $R_{AEK/PV}$ which is the rate between the nominal power of the AEK over the nominal power of the PV plant. For each $R_{AEK/PV}$ are univocally found the two sizes of PV and AEK that allows to synthetize a steady stream of 100 MW. Then it is conducted a sensitivity analysis on the investment cost of the sum of these two components as function of the $R_{AEK/PV}$ and the lowest is picked.

The size of the H_2 storage and of the batteries are assumed unlimited in this first phase. The actual size of the storages is assessed with a detailed model considering hourly steps in a second design iteration. This *hourly model* takes as input 8760 measured values of power production of the PV plant. Then energy balances are solved for each hour according to the defined layout and components operating rules. The resulting size of the storages is the minimum that guarantees that the plant avoids any shutdown during the year.

For the last case (PLRO), it is also used an additional daily model to evaluate the optimal size of the oversized methanation unit. The model basically evaluates the tradeoff size in which the additional investment cost is payed back by the yearly additional productivity, considering a realistic combination of the three prototypical days.

From the economic point of view, a WACC of 8% is assumed, the lifetime of the plant is estimated to be 20 years and the availability is set to 95%. For each of the nine cases it is

evaluated the LCOM (Levelized cost of Methane), including the investment cost of PV system, conversion plant and DAC if required.

FL case: methanator operating always at full load

For the first case (Full Load case, FL), the results of such analysis are reported in Table 1.1, showing that the PV-DAC-BES configuration has the lowest values of $R_{AEK/PV}$. An important fraction of the energy produced by the PV plant goes to the DAC, reducing the load of electrolysis unit. In PV-DAC-GT, instead, the gas turbine burns hydrogen, so the AEK has a higher nominal power and $R_{AEK/PV}$ increases as well. In this solution, no heat recovery from methanator is considered.

Table 1.1 Main finding in the design and economics of FL.

	PV-CC-BES	**PV-DAC-BES**	**PV-DAC-GT**
$R_{AEK/PV}$	0.5	0.35	0.5
PV size [MW]	1458	1649	2122
AEK size [MW]	729	660	1061
LCOM [$/MW]	267	362	379

Looking at the levelized cost of methane (LCOM) of each supply chain, it appears that the most economical solution is by far the PV-CC-BES chain, meaning that the presence of the DAC system has the highest impact on the final cost of methane. In the LCOM the weight of the OPEX is low (10% on average), confirming that these solutions are highly CAPEX intensive.

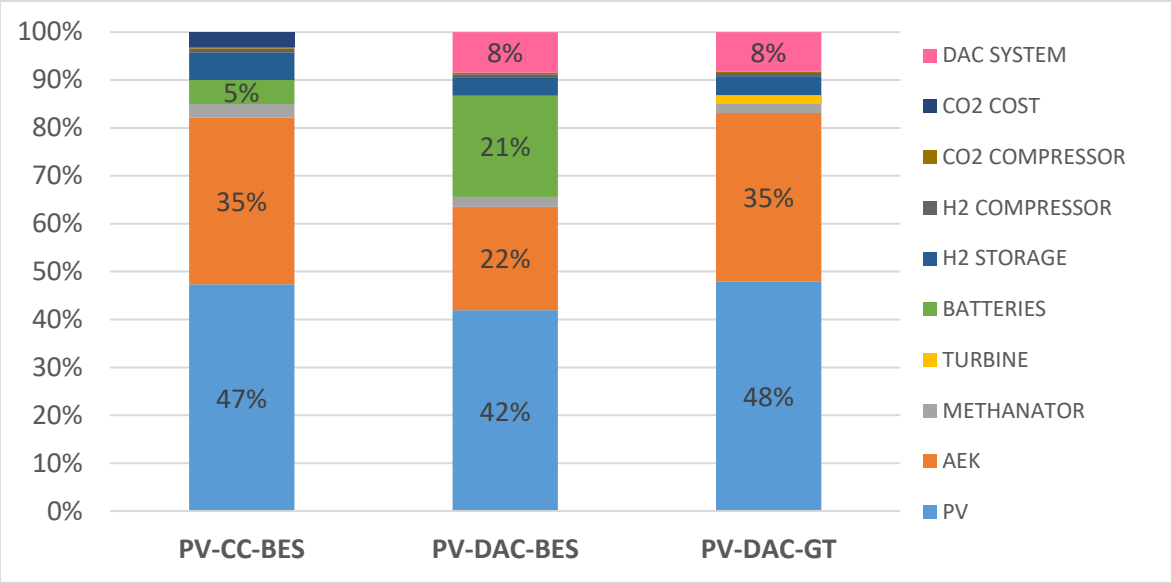

Figure 1.2 Share of the LCOM for each supply chain in FL case.

Among the voices of the total CAPEX in Figure 1.2 the two major items are PV accounting 42-48% and AEK 22-35%. The only exception is for PV-DAC-BES configuration in which batteries accounts for 21 % of CAPEX. So, the impact of the DAC is both related with its high investment cost and, especially, with the energy required for its operation.

FLR case: additional heat recovery of the methanator waste heat

Since the methanation process is a highly exothermic process (the hydrogen-to-methane efficiency is about 78%, meaning that the 22% of energy is extracted throughout the high temperature cooling circuit), the heat recovery potential is high. In this work, the methanator is assumed to be a three adiabatic reactor type with four intermediate coolers, as presented in Figure 1.3. The available heat for recovery and the ranges of temperature for each heat exchanger are reported in Table 1.2.

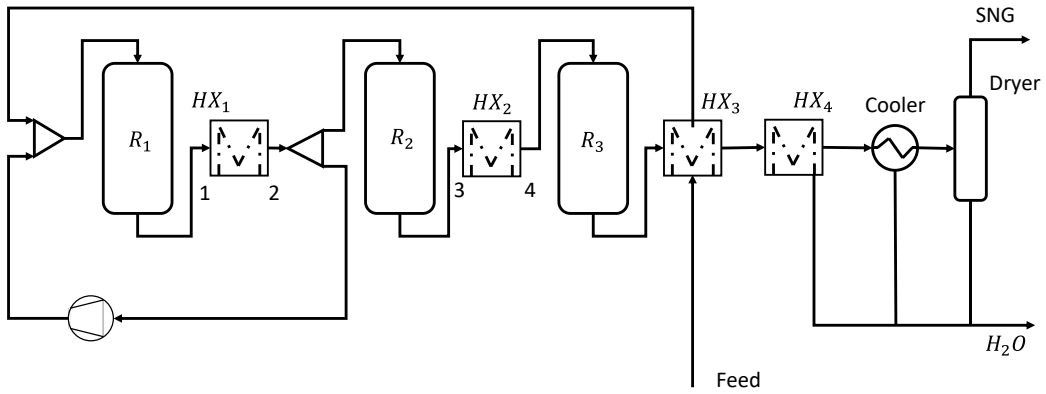

Figure 1.3 Methanator process flow scheme

Table 1.2 Available heat for recovery for a 100 MW Methanator scaled from [2]

SIZE 100 [MW]	HEAT [KW]	T [C°]	T [C°]
HX4	7245	135	192
HX1	13603	255	665
HX2	4754	195	511
Cooler	2490	135	45
TOT for recovery	**28094**		

In PV-CC-BES the heat available is used to power an ORC system to produce additional electric energy. Only HX_1 and HX_2 are used for this purpose as they successfully comply with the temperature requirements for the ORC system.

In PV-DAC-BES and PV-DAC-GT the final user for heat recovery is the DAC system. The DAC system needs a constant flow of hot pressurized water around 100 °C to drive the regeneration process of the solid sorbent. This temperature allows a higher heat recovery, in fact in this case also HX_4 temperatures complies with DAC temperatures.

In PV-DAC-BES case, the introduction of heat recovery turns into a lower capacity of the battery pack and a higher $R_{AEK/PV}$, while for PV-DAC-GT it means smaller gas turbine and more hydrogen available for gas synthesis.

$R_{AEK/PV}$ in PV-DAC-BES increases from 0.35 of the FL case to 0.45 with heat recovery. In the other two cases, there is not a perceptible difference. Looking at the LCOM, the use of ORC causes a cost reduction of 5% in PV-CC-BES case, while in the other two cases the cost reduction is between 11-13%. The greater advantage in the last two cases is justified by

a combination of higher energy efficiency in the heat recovery (as HX_4 is involved and the final user temperature is lower) and a lower cost of using a simple heat exchanger for steam generation, compared to the cost of a complete ORC system. In any case, the heat demand of the DAC has to be satisfied.

PLRO case: oversized methanator unit and partial load operation

In the previous two cases (FL and FLR), the whole plant was designed on the "worst day" in order to guarantee always the production of 100 MW_{LHV} of SNG. In this way, for most of the time, the PV and AEK provide more hydrogen than the quantity that the methanator can convert. Consequently, it could be beneficial to oversize the methanator and all the related systems. However, oversizing the methanator and operating it with a full load logic, will bring the plant to consume faster the hydrogen in the stocks during worst-like days causing the shutdown of the plant. In order to avoid such scenario, detrimental for efficiency and plant lifetime, it is introduced the possibility for the methanator to work at partial load. The concept is to operate at maximum load when AEK produces enough hydrogen, and switching at partial load if the storage of hydrogen go below a critical threshold or if the PV plant is producing less energy due to bad climate conditions. Hence, the oversizing procedure must be followed by an increase in operational flexibility.

To manage this flexibility a new algorithm is introduced. This algorithm is used to decide whether to work at partial load or at full load. The plant operates at full load and switch to 50% operation when one of two 'alarms' is on. The first alarm simulates to the availability of PV production forecasts and a precautionary approach can be adopted, if the incoming whether conditions are bad. In this analysis, the sum of the energy that the PV plant will produce in the following 24 hours is calculated and, if the value is lower than a certain threshold, the plant works the next hour with halved load, the next hour the process is repeated. The second alarm forces the plant to operate at partial load if at least one of the two storages (batteries, if present, and H_2 storage) has a level under a certain threshold. So, the alarm that looks the forecasts is useful to manage particular events, while the second alarm operates more periodically stabilizing the plant operation.

The advantage of producing more SNG thanks to the oversizing process is counterbalanced by the major investment cost of the methanator. Clearly, there is a tradeoff size in which

these two effects are balanced that is assessed through a sensibility analysis. The model (*Daily model*) calculates mass and energy balances on daily basis using in combination the three selected prototype days for a yearly simulation. The model conducts a sensitivity analysis calculating the expected LCOM [$/MWh] as a function of the size of the methanator. In Table 1.3 are reported the sizes from the model with the resulting LCOM.

Table 1.3 Nominal capacity of the methanator in the PLRO case, and technical and economic performance.

	Size [MW]	*η_{EE-CH4}*	*LCOM [$/MWh]*
PV-CC-BES	*132*	*39%*	*197*
PV-DAC-BES	*130*	*35%*	*259*
PV-DAC-GT	*136*	*31%*	*268*

The correct operation of all systems is checked even at partial load. The DAC system is modular-type so no problems are expected, but the heat integration of the methanator is influenced by the load and it must be evaluated the correct synergy at partial load. In the detailed analysis, it results that both heat exchanger for heat recovery and ORC system can operate with the load of the methanator halved.

The output of this final case is higher than the previous one and the LCOM experienced a reduction from 18% (PV-DAC-BES) to 23% (PV-CC-BES) with respect to the FL case.

Configurations comparison

A first sensibility analysis on the cost of carbon dioxide is performed to assess which is the breakeven cost that align the LCOM of PV-CC-BES to the LCOM of the other two supply chains using the DAC technology. This analysis is done on the PLRO case since it has demonstrated the most economical effectiveness. The breakeven cost is 355 $/t$CO_2$ for PV-DAC-BES and 400 $/t$CO_2$ for PV-DAC-GT.

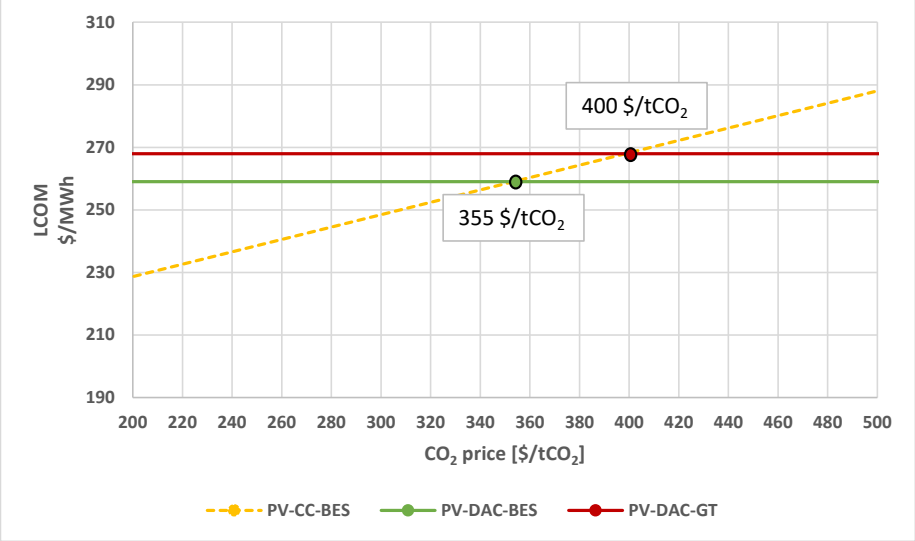

Figure 1.4 Breakeven cost of CO_2 purchased that levelized the LCOM of PV-CC-BES to the other two supply chain in PLRO case

Finally, the energy performance of the plant for all nine configurations are compared. The efficiency from solar to electric energy is the same in all cases, as they use the same PV technology, while the efficiency from electric energy to SNG depends on many factors.

In Table 1.5 are gathered the main results of the analysis. Globally both the LCOM and the electric to CH_4 conversion always improves from FL case to PLRO. Among the cases, the most economical supply chain is always the one that purchase carbon dioxide instead of capturing it from the air.

Since most of the advantage is due to the investment cost, a sensitivity analysis on the CAPEX of the major components of the plant is presented. This analysis considers PV, AEK, Batteries and DAC. In the evaluation, each of these components is reduced in CAPEX of a factor of 20% and 40 %, calculating the resulting new size of the plant. In fact, the plant is designed by new using the procedure to consider the fact that a lower cost of one component could result in different sizes. It turns out that the major reduction in LCOM occurred with the major items such as PV and AEK with the recalculated LCOM reported in Table 1.4.

Table 1.4 LCOM after CAPEX reduction of PV and AEK.

CAPEX reduction		PV-CC-BES	PV-DAC-BES	PV-DAC-GT
0%	-	197	259	268
-20%	PV	178	237	243
	AEK	183	245	250
-40%	PV	158	216	219
	AEK	169	230	232

Table 1.5 Resume table of configurations.

		Investment [mln $]	Production [GWh/y]	LCOM [$/MWh]	$\eta_{EE\text{-}CH4}$
FL	PV-CC-BES	1935	833	267	30%
	PV-DAC-BES	2582	833	362	26%
	PV-DAC-GT	2847	833	379	21%
FLR	PV-CC-BES	1875	833	253	30%
	PV-DAC-BES	2278	833	314	29%
	PV-DAC-GT	2530	833	338	25%
PLRO	PV-CC-BES	1847	1044	197	39%
	PV-DAC-BES	2264	1004	259	35%
	PV-DAC-GT	2574	1083	268	31%

It is finally compared the price of natural gas (NG) with expected LCOM. In Figure 1.5 it is compared a reference price of NG with the LCOM for each supply chain in their best case (PLRO). It is visible that in all cases the SNG is far more expensive than NG.

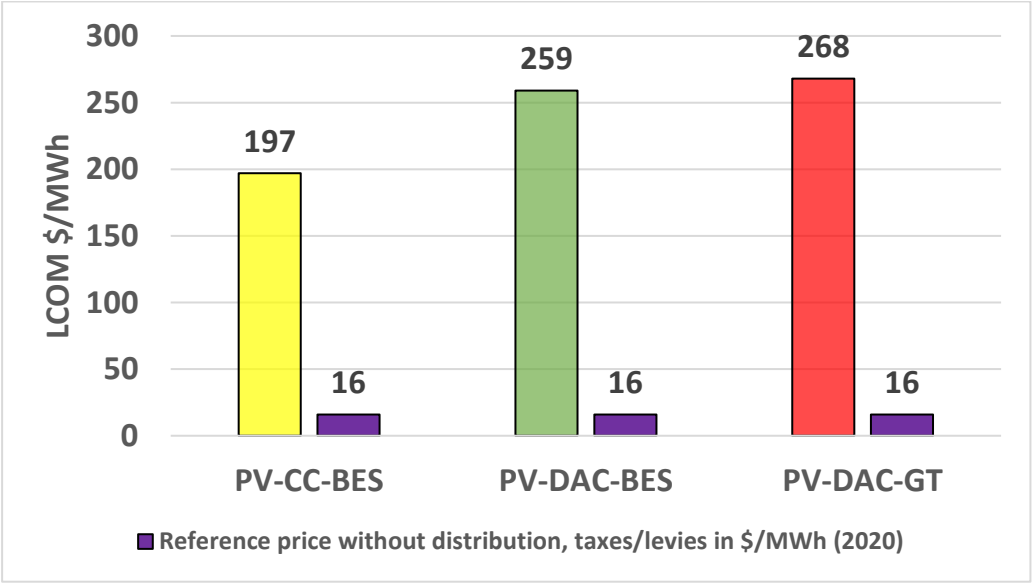

Figure 1.5 Levelized cost of synthetic methane (LCOM) in the PLRO case of each configuration (without transport), compared to the reference cost of imported natural gas (without distribution, taxes/levies).

Conclusions

In this study, the feasibility and the performance of a large scale PtG plant in a remote location have been demonstrated. The possibility to exploit the high RES potential still fights with the high costs of this kind of plants. In fact, it results that the SNG costs more than ten times its fossil alternative.

Nevertheless, the possibility to synthetize gaseous or liquid hydrocarbons in general is capturing more and more attention as it could be a reliable renewable energy source an important game changer in the automotive sector for the decarbonization process. Consequently, as shown by the final sensitivity analysis, a strong reduction in investment costs of PV and AEK is mandatory for reducing the cost, to be competitive with the fossil gas market the CAPEX should be decrease at of 90%.

Among the proposed plant configurations, the preferred is the PV-CC-BES in PLRO, with an LCOM of 197 $/MWh, because of the absence of the DAC which not only has high CAPEX but its energy consumption causes an increase in size of PV, Batteries and AEK (only in PV-DAC-GT).

Attention should be paid to the heat integration. It decreases the LCOM of PV-CC-BES of 5% while the reduction is stronger for the DAC supply chains, with a reduction of 13% for PV-DAC-BES and 11% for PV-DAC-GT.

Finally the oversizing coupled with possibility to run at partial load has demonstrated very effective to reduce the costs driving down the LCOM of 17-22 % compared to the operation at full load with heat recovery.

Table of Contents

List of Figures

List of Tables

Chapter 1 Introduction

To deal with the crisis of the climate change, the electric power industries are transiting to sustainable energy systems. In most parts of the world today, renewables have

become the lowest-cost source of new power generation. As costs continue to fall for solar and wind technologies, this will be true in a growing number of countries [4].

However, with the growing capacity of modern renewables in the energy mix, it becomes more crucial the role of energy storage systems. Regarded as a long-term, large capacity energy storage solution, commercialized power-to-gas (PtG) technology has attracted much research attention in recent years. PtG plants and natural gas-fired power plants can form a close loop between an electric power system and a natural gas network [5], power to gas plants can use the carbon dioxide extracted from the exhausts of natural gas fired plants to produce the fuel. In this way a carbon neutral loop can be established.

PtG represents a process that converts water and carbon dioxide into methane, while consuming energy provided by the electricity. This process generally consists of two steps, namely electrolysis and methanation, the first transform water into molecular hydrogen and oxygen consuming electric energy, and the latter combine carbon dioxide with hydrogen to obtain methane throughout an exothermic process. There are some regions in which renewables can reach extreme low generation costs, but often these regions are remote areas where there are no loads to power.

This very cheap electric energy could be indeed converted into chemical energy using PtG process. In this way the abundant electric energy can be used to synthetize methane which could then be transported and in principle create a biunivocal exchange of methane and carbon dioxide between natural gas power plants and PtG plants.

Synthetic fuels have a large disadvantage, however: low energy efficiency. Large volumes of electricity are needed for their production due to conversion losses [6].

This work will examine techno-economical analysis of a 100 MW PtG plant powered by PV panels in off-grid condition. Off-grid bound is made in order to evaluate if it is possible to establish in future a mutual exchange of CO_2-CH_4 between gas fired plants and off-grid PtG plants.

In this work it will done at first a technology review of the technologies involved, with particular focus on DAC systems followed by the location selection of the plant. In this analysis three configurations will be explored, each in three cases leading to a matrix of nine combinations. The three cases define the three steps of the analysis:

- at first, the plant is assumed to work at full load all the time, minimizing the possibility of shutdown;
- the second cases analyse if the waste heat of the methanator could be exploited in a useful way in the plant;
- at the end, it is removed the bound to work always at full load, and the plant can change the load depending on the situation in order to optimize the capacity of the storages, also the methanator is oversized in order to exploit the energy during the days in which the PV plant produce more energy than the quantity that the methanator can transform into syngas.

Then are described the models used in the work, followed by the design phase in which each component of the plant is modeled. This is done both for the technical aspect and for the economical side.

From chapter 2 to chapter 4, each chapter focuses on one case, from the FL (Full load), through FLR (Full Load with Recovery), to PLRO (Partial Load with Recovery and Oversizing). For each case it is done the sizing of the plant and it is evaluated the LCOM (Levelized cost of Methane). For chapter 3 and chapter 4 it is also assessed the technical feasibility of the introduction of a recovery system on the methanator to verify if the system could be integrated succesfully with the rest of the plant. The PLRO case, since it include the possibility to work at partial load, needs the evaluation of the recovery system to ensure the correct operation even at partial load.

In chapter 5 there is also a section in which it is evaluated the global efficiency of the plant from solar energy to the syngas for all the nine cases. Then it is done a sensitivity analysis

on the reduction of the specific investment cost of each component, in order to assess which components the LCOM is more sensible at. Finally it is compared the resulting LCOM with the reference price of natural gas on the market.

Chapter 2 Methodology

In this section a technology review will be carried out in order to summarise the technologies involved in the power-to-gas process. Technologies are divided into five blocks because they answer for five main tasks: power generation, CO_2 capture, electrolysis, methanation, and others. As Figure 2.1 suggests, the PV plant generates power for the electrolyzer and for the energy continuity system. Then the electric energy is converted into hydrogen through water electrolysis and finally hydrogen reacts with carbon dioxide in the methanator procuding synthetic methane. The energy continuity system guarantee that all electric appliances are fed when the PV plant is off.

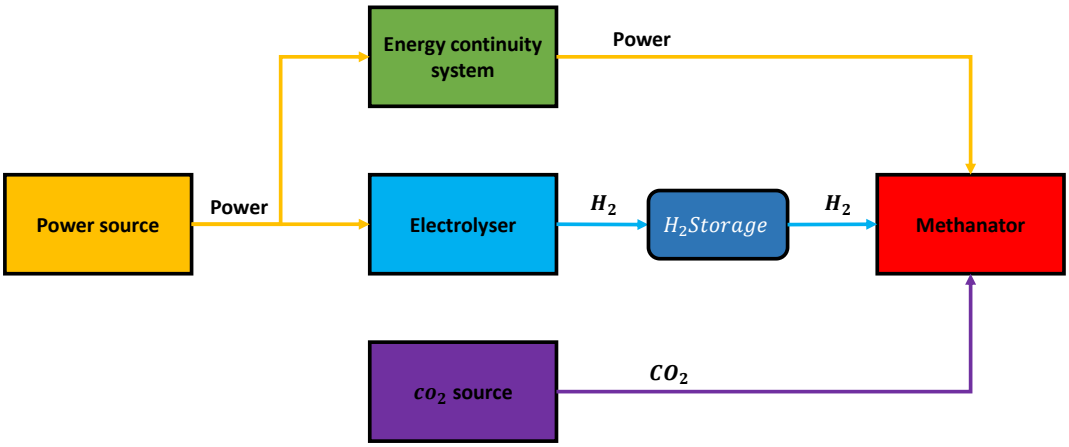

Figure 2.1 Schematic representation of a PtG plant

2.1 Technology review

Power generation

Some renewable technologies are appealing for a power to gas facility. In principle every RES could be used for this purpose, and the higher the reliability and predictability of the source the better it is. In terms of costs, the combination of PV and wind power production is most favourable since load factors of combined plants are substantially higher than for sites focused on single technologies. Locations that allow for a combination of PV and wind are therefore of particular interest as wind resources tend to complement solar resources.

Appealing locations for this integration are [7]:

- Mena region and western Sahara
- South of Latin America
- Some region in Australia

Nevertheless in this study it will be assessed a full PV based facility, because wind potential is difficult to be evaluated without onsite measurements and the same could be said for a new hydropower facility, while data on PV performances are reliable and open source and it is easier to evaluate by sketch the power plant. The vast majority of today's solar cells

are made from silicon and offer both reasonable prices and good efficiency. Another commonly used photovoltaic technology is known as thin-film solar cells because they are made from very thin layers of semiconductor material, such as cadmium telluride or copper indium gallium diselenide. A third type of photovoltaic technology is named after the elements that compose them. III-V solar cells are mainly constructed from elements in Group III. These solar cells are generally much more expensive to manufacture than other technologies. But they convert sunlight into electricity at much higher efficiencies.In this work will be used only the silicon solar cells [8].

Electrolysis

Electrolysis of water is the decomposition of water into molecular hydrogen and oxygen driven by the passage of current.

$$H_2O + \text{Electricity} \rightarrow H_2 + \frac{1}{2}O_2 \qquad \textit{Eq. 1}$$

This reaction Eq. 1 is highly endothermic and in the PtG is used to produce the molecular hydrogen that will react with CO_2 to synthetize syngas. For the electrolysis step there are mainly three technologies available: Alkaline, PEM, and SOEC cells. Each technology shows some advantages and weak points. Alkaline electrolyzers are those that shows the lowest specific costs ($/kW) in the present, PEM is the best technology for dynamic operations such as when it is coupled with very fluctuating load [7]. SOEC technology has the main difference of working at very high temperature respect of the two but shows very high efficiency. In future it is possible that PEM and SOEC will overcome the AEK, resulting in lower cost of hydrogen produced. In this study only the alkaline option will be considered because the other two technology are not mature enough.

CO_2 Capture

For the CO_2 capture two path can be followed: capturing CO_2 from exhaust of industrial plant (in this work this solution will be referred as CC) or capturing the carbon dioxide directly from the air (DAC, direct air capture). In both cases the physical principle for carbon capture is the same (adsorption), but the specific energy expenditure to extract CO_2 is

different due to the concentration. In particular CC from industrial plants is cheaper than DAC as the stream to be treated is enriched of CO_2, so less air needs to be moved by fans for the same amount of CO_2 collected. In the following figure are reported the companies working on DAC and are clustered by the technology used.

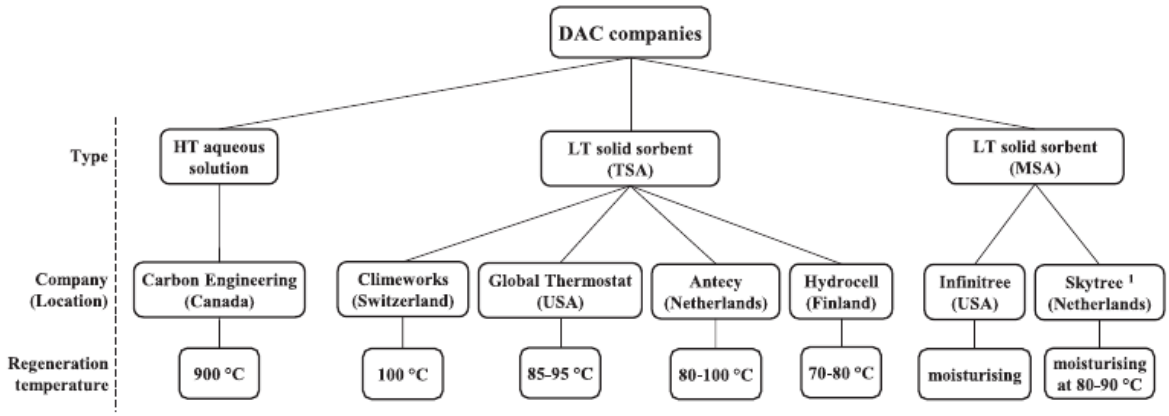

Figure 2.2 Different type of DAC technologies and producers [9]

Two groups of technologies can be identified for DAC carbon capture, the first uses a water solution containing hydroxide sorbent with a strong affinity to CO_2. The second relies on the use of amines bonded on a porous solid support. The big difference in operation condition is the temperature, the capture using liquid sorbent requires high operating temperature (T > 800°C) [3], this highly valuable heat can be provided by burning natural gas or other fossil fuels, then the CO_2 is capture as well to avoid additional emissions. The CO_2 capture using solid sorbent requires instead very low temperature heat that could come from waste heat of other processes or low-quality heat sources like heat pumps.

The extraction of CO_2 is made up with two steps, adsorbtion followed by desorbtion of the solid sorbent. In the first phase air is moved by fans to go through the solid sorbent. At ambient temperature, CO_2 chemically binds to the filter and CO_2 depleted air leaves the system. This step is completed when the sorbent is fully saturated with CO_2. In the next step, fans are switched off, the inlet valve is closed and the remaining air is optionally swept out through a pressure drop by vacuuming or injecting steam into the system. Then, regeneration happens by heating the system to a certain temperature, depending on the sorbent.

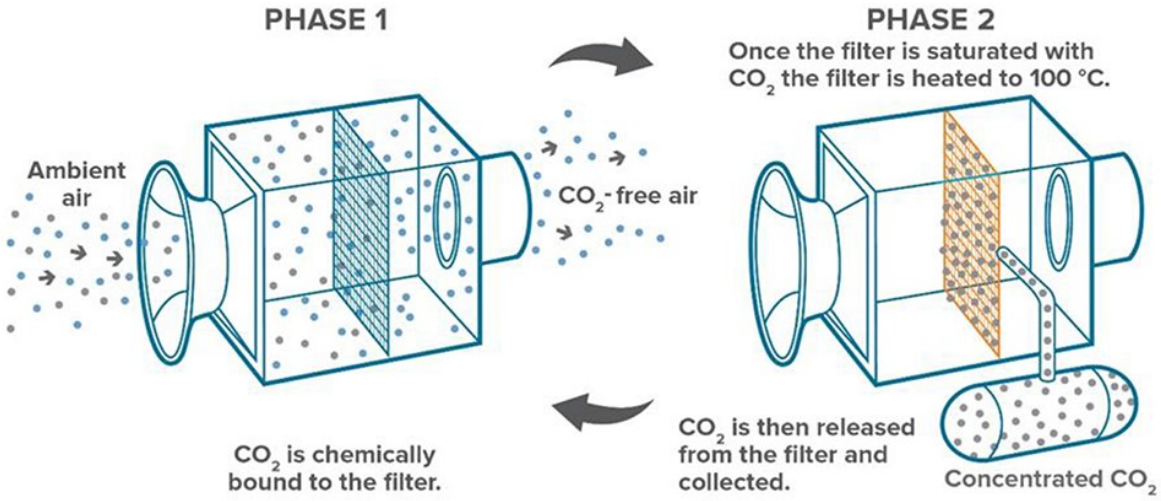

Figure 2.3- Adsorption and desorption cycle of DAC from Climeworks

Released CO_2 is collected and transported out of the system for purification, compression and utilisation/storage. In order to start another cycle, the system should be cooled down to ambient conditions. In this work only solid sorbent technology will be considered because the waste heat coming from other processes in the plant could be used as input for this technology [9].In this work both the two alternatives are explored (CC and DAC) in the different configurations.

Methanation

The final step for the fuel synthesis is the methanation process. Methanation could be done both with a catalytic reactor or throughout anaerobic digestion. The latter is more focused on biogas as a source for carbon, the reason why in this analysis only the catalytic methanation is considered [10]. The latter is also more established. The most conventional technology for chemical methanation reactors is represented by adiabatic fixed bed reactors, while other technologies such as fluidized bed reactors are less diffused mainly for difficulties in unsteady operation and catalyst abrasion.

The process is carried out by some reactions, but the most important are the metanation Eq. 3 and reverse water gas shift Eq. 2.

$$CO_{2(g)} + H_{2(g)} \rightleftarrows CO_{(g)} + H_2O_{(g)} \qquad \Delta H°_R = \pm 41.2\ kJ/mol \qquad \textit{Eq. 2}$$

$$CO_{(g)} + 3H_{2(g)} \rightleftarrows CH_{4(g)} + H_2O_{(g)} \qquad \Delta H°_R = \mp 206.2\ kJ/mol \qquad \textit{Eq. 3}$$

The resulting reaction Eq. 4 is still exothermic because the methanation reaction is widely more exothermic than the reverse water gas shift.

$$CO_{2_{(g)}} + 4H_{2(g)} \rightarrow CH_{4(g)} + 2H_2O_{(g)} \qquad \textit{Eq. 4}$$

For its exothermic nature, methanation process needs to be cooled down during operations to maintain the appropriate thermodynamic conditions. Lower temperatures result in higher equilibrium constants and better conversion rates. Nevertheless, low temperature also promotes unfavourable side reactions; for this reason selectivity of the catalyst is critical. Nickel catalysts are usually preferred in commercial applications, but other metals such as Rubidium, Rhodium, Platinum, Iron, and Cobalt may also be used [11]. Since in the global reaction Eq. 4 there is a reduction of the moles, high pressure promotes the conversion. The Fixed Bed Methanation reactor is by far the most established technology, and several processes have been developed using this reactor configuration, Lurgi, HICOM, and TREMP (Topsøe's Recycle Energy Efficient Methanation) processes among others. In order to avoid catalyst destruction by local temperature peaks in the bed (hot spots), temperature control is crucial. Most common configurations address this issue splitting the reaction in cascade of adiabatic reactors with gas inter-cooling and gas recycling. For this work it will be considered the configuration composed by three adiabatic reactors (TREMP).

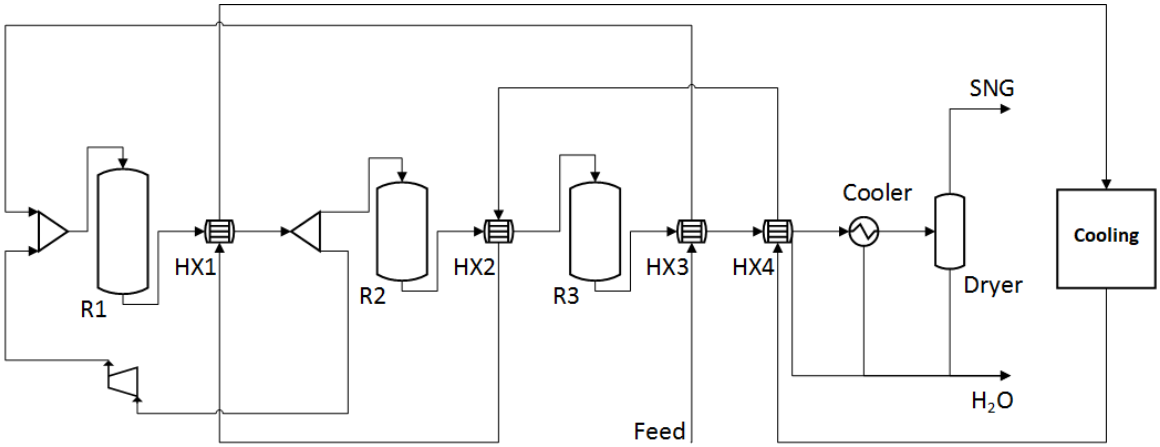

Figure 2.4- Process flowsheet for the methanation system with three adiabatic reactors [2]

Table 2.1- CO_2 methanation system with three adiabatic reactor (example of a methanator coupled with a 1 MW_{el} PtG electrolyzer) [2]

			Reactor 1		Reactor 2		Reactor 3		
Stream #	**1**	**2**	**3**	**4**	**5**	**6**	**7**	**8**	**9**
	CO_2 Feed	**H_2 Feed**	**Inlet**	**Outlet**	**Inlet**	**Outlet**	**Inlet**	**Outlet**	**SNG (Std.Cond)**
Temp. [°C]	130	50	255	665	255	511	195	323	15
Pres. [bar]	25.0	25.0	24.5	24.5	24.0	24.0	23.5	23.5	1.0
Total Flow [kg/h]	93.8	17.0	226.2	226.2	110.8	110.8	110.8	110.8	36.20
Total Flow [kmol/h]	2.15	8.43	18.47	15.47	7.58	6.82	6.82	6.44	2.29
Mol. Frac. [%]									
H_2	0	100.0	58.4	29.9	29.9	13.2	13.2	2.3	6.4
CO_2	99.0	0	14.1	6.0	6.0	3.4	3.4	0.8	2.3
CH_4	1.0	0	8.7	20.1	20.1	27.9	27.9	32.5	91.3
H_2O	0	0	17.9	41.8	41.8	55.3	55.3	64.4	0
CO	0	0	1.0	2.3	2.3	0.2	0.2	0	0
Reactor H_2 conversion			73.1 %		60.3%		16.4%		
Cumulative H_2 conversion	-	-	-	73.1%	-	89.3%	-	98.3%	-
HHV [MJ/Nm^3]	-	-	-	-	-	-	-	-	35.259

Figure 2.4 is the configuration of methanator used in this work. It will be not simulated in detail, but results from Figure 2.4 will be adopted.The flow rates will be proportionated with the size of the mathanator while temperature and pressures are assumed to remain the same of Table 2.1.

Others

For the plant operations some auxiliaries are needed such as lithium batteries, H2 compressors, CO_2 compressors as well as gas storage systems. Above all the ORC technology will be considered as it allows for a deep integration between components of the plant in order to increase the overall efficiency. More details will be provided in the section in which these components will be relevant.

2.2 Location selection

The selection of the location is a critical aspect of this work as it can rise both threats and opportunities. There are lots of locations worldwide that show an appealing solar potential. Nevertheless solar radiation is not the only indicator for the selection. The plant needs an economical and reliable source of water for the electrolyzers. In addition, the proximity to the distribution infrastructure of oil & gas is an asset because it reduces the costs for gas transport. Also the political situation of the region is a relevantaspect: a stable governance is an essential requirement to guarantee significant investment to be undertaken. Finally, in our configuration there is one case in which CO_2 is purchased from an industrial plant, so the presence of a nearby power plant or in general a source of cheap CO_2 is a strict condition.

Considering these requirements, Yanbu, Saudi Arabia appears to be a good location. Yanbu is an important petroleum shipping terminal and is home of three oil refineries, a plastics facility and several other petrochemical plants. It is the country's second port (after Jeddah) and serves as the main port for the holy city of Medina, 160 km to the east. In Figure 2.5, it can be seen that Yanbu hosts the terminal of the east-west pipe which is one of the most important distribution channel for oil & gas product in the country.

Figure 2.5 Position of Yanbu and connection with gas network pipelines [12]

Moreover, Yanbu shows an appealing photovoltaic potential as can be seen in Figure 2.6. This location satisfies at best all the conditions.

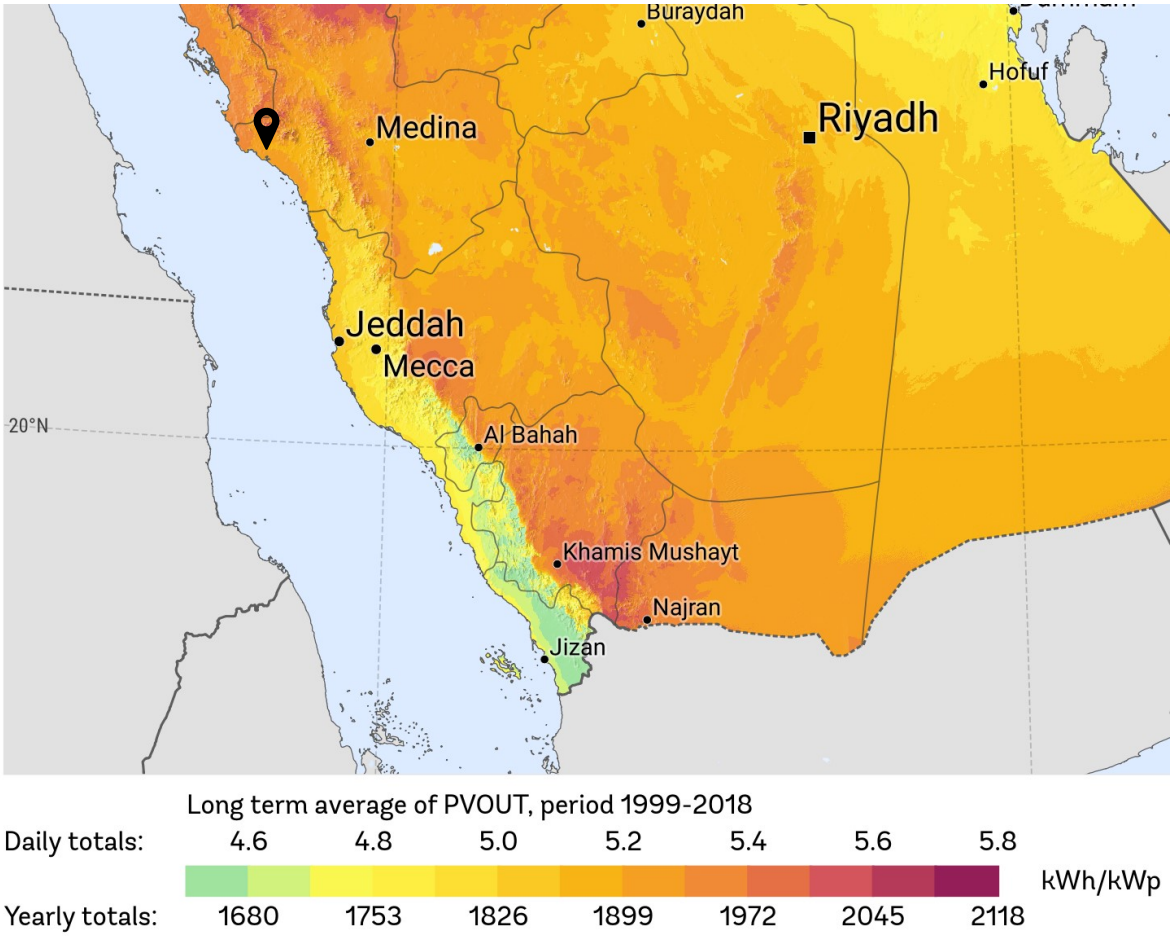

Figure 2.6 Photovoltaic power potential map in Saudi Arabia [13]

A final remarkable consideration is that the latitude of this location fits quite good because if we look at the monthly generation of electricity [kWh] from PV (Figure 2.7), it is quite stable. This feature is really appreciated because allows to exploit at best the energy available without requiring a seasonal storage.

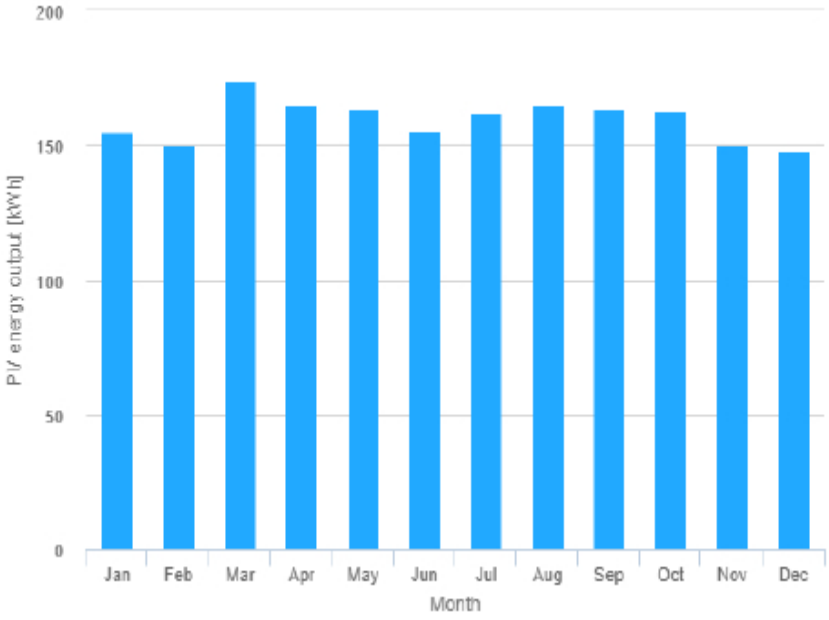

Figure 2.7 Monthly energy output of a fix-angle PV system in Yanbu'

2.3 Configurations

The main aim of this work is to design and evaluate the economic feasibility of a 100 MW_{LHV} off-grid power-to-gas plant. A power-to-gas plant needs a power block, an electrolyzer, a methanator and a system to ensure the carbon dioxide. There are also some other components that guarantee the correct operation of the plant such as batteries, storage systems and so on.

In this work, in order to explore some different combinations of technologies, three supply chains will be considered. These three configurations will be further evaluated in three different scenarios that allow to assess different strategies.

All cases are reported in Table 2.2.

Table 2.2 Supply chains configurations matrix

Full load	Batteries	DAC	CO_2 Provision	Gas Turbine	ORC	HX_m
PV-CC-BES	x		x			
PV-DAC-BES	x	x				
PV-DAC-GT		x		x		

Full load - Recovery	Batteries	DAC	CO_2 Provision	Gas Turbine	ORC	HX_m
PV-CC-BES	x		x		x	
PV-DAC-BES	x	x				x
PV-DAC-GT		x		x		x

Partial load - Recovery - Oversized	Batteries	DAC	CO_2 Provision	Gas Turbine	ORC	HX_m
PV-CC-BES	x		x		x	
PV-DAC-BES	x	x				x
PV-DAC-GT		x		x		x

Full load (FL)

The first and simplest case is the *Full load* in which there are only indispensable components. PV-CC-BES is the only supply chain that purchase carbon dioxide instead of capturing it from atmospheric air. PV-DAC-BES and PV-DAC-GT both use a DAC system but they differ in the way the plant stores energy. In the first case a massive amount of lithium-ion batteries is used to store electric energy during the day to power the plant during the night, while in PV-DAC-GT all electric energy form the solar field is used to produce hydrogen, and part of it is burned into a gas turbine to produce electric energy for the BOP's while exhaust is used to cover the heat demand of the DAC system.

Full load – Recovery (FLR)

This second case wants to exploit the useful heat out of the methanator. A 100 MW methanator discharge around 28 MW of high temperature heat, so from the thermodynamic perspective this stream worth some attention. For each supply chain it has been planned a specific way to exploit this energy.

PV-CC-BES has not appliances that use thermal energy, so heat recovered feeds a high efficiency ORC system to produce electric energy. This solution can provide a constant and reliable source of power to the plant as the methanator always run at full load.

PV-DAC-BES includes the low temperature DAC system, which in the FL case was powered by batteries. Batteries cover either the thermal (by electric resistances) or electrical needs of the DAC system. In this case a part of the thermal need is covered by the heat recovered from the methanator. So placing an heat exchanger (HX_m) it is possible to use the waste heat from the methanator to downsize the batteries capacity as well as the PV field size.

In PV-DAC-GT the heat from the methanator will be used to power the DAC as well as the PV-DAC-BES. In this case the thermal need of the DAC will be provided by the exhaust of the gas turbine and the waste heat of the methanator. This introduction is expected to lower the size of the turbine and the size of both AEK and PV plant.

Partial load – Recovery – Oversized (PLRO)

This final case does not introduce new components, layouts will be identical to the FLR case but the methanator block will be oversized. With the methanator block are intended all the BOP's (Balance of plant) that work in synergy with the methanator, such as the DAC system, H_2 compressor, CO_2 compressor and so on. Oversizing the methanator will result in a higher production even though the size of AEK and PV remain the same. Indeed to guarantee the continuous full load operation, the sizing procedure will be done on a "worst case" condition, meaning that in the "normal" condition some PV energy will not be used and gets wasted.

This oversizing protocol, however, raise the need to remove the condition to work always at full load, because otherwise the consumption of hydrogen of the methanator will overcome the production of hydrogen by the AEK, and the plant risk to shut down frequently.

2.4 General modelling approach

Throughout this work, some models are used to answer different tasks. There are four models as represented in Figure 2.8. *Days Clustering* is developed in order to define the profile of

energy input to simulate and the results will be used for all cases, this is why it is placed in the upper side of Figure 2.8.

Sizing on Worst day and *Hourly model* are used in all cases while the *daily model* only applies on the PLRO case. In PLRO case the sizing is not present as sizes of PV and AEK comes directly from the FLR case.

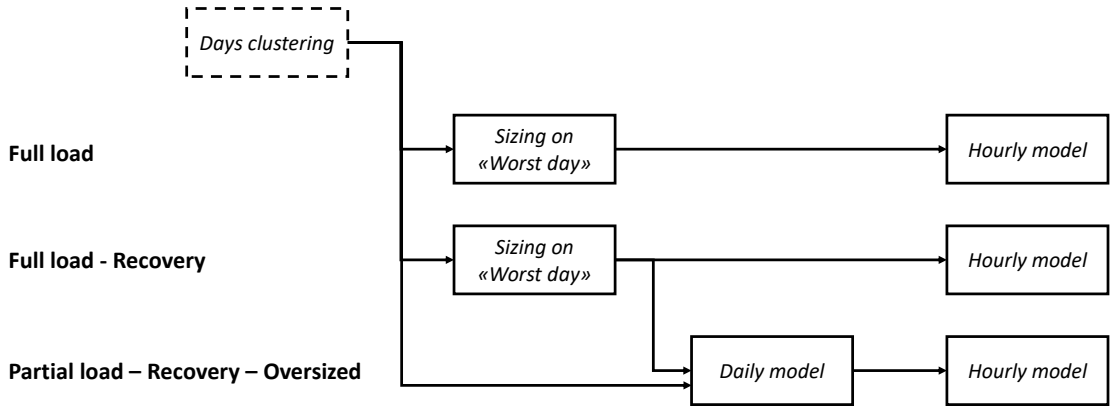

Figure 2.8 Resume picture of the models used in each case

Days clustering

This model is used to create prototypical days that are used to simulate the real conditions.

Three days will be created, "Best day", "Average day" and "Worst day". The "Worst day" is much important as it will be the reference in the sizing procedure. All prototypical days will be considered in the daily model instead. This model is explained carefully in 2.5.1.

Sizing on "Worst day"

In this model starts the sizing of the plant. To explain how the model works it is taken as example the PV-DAC-BES supply chain, but the logic is valid for all cases.

As Figure 2.9 suggests, the plant can be divided into two blocks. The first block includes the PV plant and the AEK because they work coupled. In the morning when the PV plant starts producing electric energy the electrolyzer starts working and it goes off when the power

stream from the PV plant ends. So these two components start and stop every day and follow the same operation profile.

The other block works instead in steady state conditions. It includes the methanator, the DAC system and the BOP's. The hydrogen storage and the batteries allow the intermittent block to produce enough resources to let the other block work without breaks.

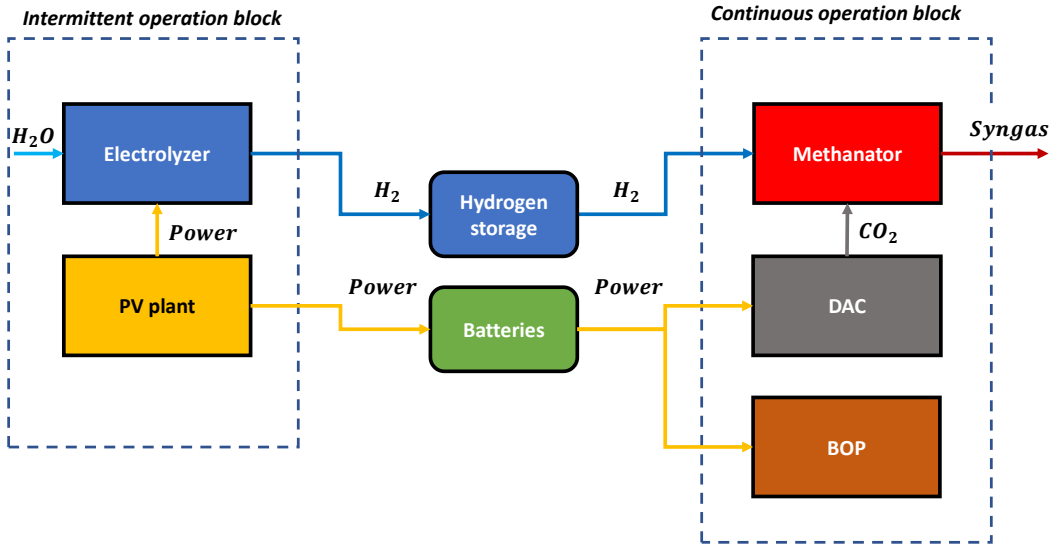

Figure 2.9 Simplified layout of the plant in PV-DAC-BES

The sizing of the continuous block is not difficult as they are sized with respect to a component, the methanator, that works always at full load (100 MW_{LHV} of methane output, taken as reference). So the fitting size can be uniquely assessed.

The same cannot be said for the Intermittent block. In fact to produce a certain amount of hydrogen on a daily basis, there are infinite combinations of size and operating hours that guarantee such amount of hydrogen. The analysis must take into account the curve of power coming from the PV plant. Figure 2.10 displays how a certain amount of hydrogen can be produced in different combination of PV size and AEK size. The green area represents a fixed amount of energy required to synthetize a certain amount of hydrogen, let's say that it is the fixed amount of hydrogen that is needed each day to run the 100 MW plant. In the figure as example the hourly production of a 1 kW and 3 kW PV are represented. It can be

noticed that the same amount of hydrogen (green area) can be produce with 1 kW of PV and 700 W of AEK, or with a 3 kW PV and 500 W of AEK.

In the first case the ratio between the nominal power of AEK and PV ($R_{AEK/PV}$) is 0.7, while in the second case it is 0.17.

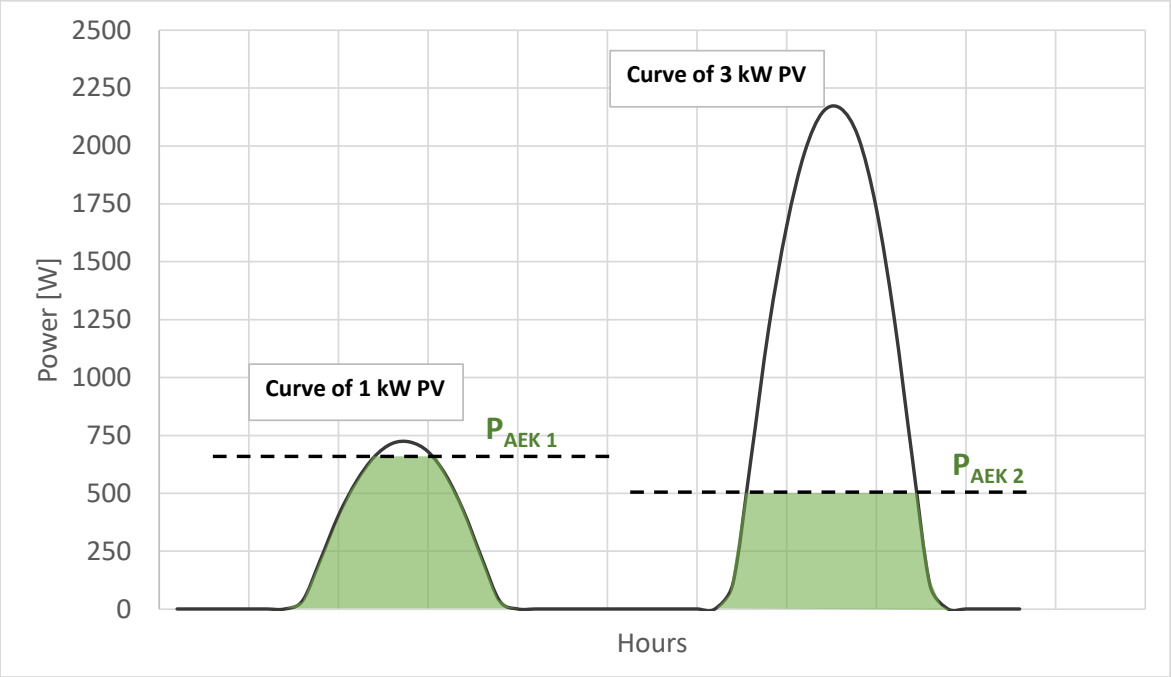

Figure 2.10 Matching PV production and AEK consumption.

Granted that there are infinite rates that ensure the energy need of the AEK, it must be assessed which rate is optimal. The second case is definitely less efficient than the first case, nevertheless if the cost of PV would be way lower than the cost of AEK it could result in a better choice.

It is evident that this analysis must take into consideration the economic perspective in order to assess the optimal rate. Another thing to be considered is the fact that some energy must be available to charge batteries (i.e. to power auxiliaries, DAC, …), that energy is taken from the white region between the peak power of PV and the maximum power of AEK. This limitation results in a upper bound to $R_{AEK/PV}$ which is specific to each supply chain. PV-DAC-GT does not include batteries, so no restriction takes place.

The economic view is considered adding the investment cost of PV,AEK and batteries in the analysis, so for each rate are unequivocally found the size of PV, AEK and the minimum capacity that let the batteries power the plant during the night.

The *Continuous operation block* calculates the amount of hydrogen needed on a daily basis, then dividing this value for the efficiency of the AEK it is possible to assess how much electric energy is required. Now that the amount of electric energy is fixed it is conducted a sensitivity analysis on $R_{AEK/PV}$ from 0 to 1 with a sensibility of 0.05. For each value it is calculated the investment cost of PV, AEK and Batteries. Then it is verified which

$R_{AEK/PV}$ complies with the bound. Then the $R_{AEK/PV}$ with the lower investment costs is picked so even the sizes of the *Intermittent operation block* are found.

This model is implemented on excel and it is solved by means of a macro. It must be pointed out that $R_{AEK/PV}$ found in this way depends on the assumptions of costs of AEK and PV.

The output of this model gives the size of all components except for the capacity of hydrogen storage. Hydrogen storage capacity will come from the output of the "hourly model", also in this model has been estimated the batteries capacity, but in the hourly model this value can be corrected, so the first guess value for the batteries behave as the starting point for the "hourly model".

Hourly model

This model has been developed to answer two tasks:

1. Verify and design the correct size of storages
2. Calculate the amount of syngas produced in one year

This model uses as input the nominal sizes calculated in the sizing on "Worst day" procedure. The model takes a vector of 8760 measurements that represent the hourly production of electric energy of the PV plant to simulate how the plant behaves in real conditions. For each hour the model takes the energy produced by the PV plant, then using a *Power flow logic* distributes electric energy to AEK, batteries or other consumers (BOP). The electric energy that goes to AEK is transformed into hydrogen and gets into the hydrogen storage. Meanwhile a certain amount of hydrogen comes from the storage to feed the methanator.

The difference between the inlet and outlet stream in the H_2 storage gives the net flow of hydrogen in the storage, after each hour the actual load of each storage (batteries and hydrogen tanks) is updated adding the net flow to the current load.

During the day when the PV plant is operative, the net flow of hydrogen (produced minus consumed) is almost always positive. Then during the night net flow of hydrogen storage and batteries is always negative.

In total the model performs 8760 steps and keeps records of the level of storages and syngas production after each step.

This tool is useful to verify if the plant shuts down, if it happens the model shows a production of 0 MW and starts working again as hydrogen stocks overcome a critical threshold. This analysis starts with capacity of batteries calculated in the sizing procedure and with a starting value of the hydrogen storage capacity, then the model is launched many times to find the lower values of capacity that avoid the shutdown of the plant. Even in this case the model is developed on excel using a macro, each supply chain takes around one hour and half of processing, and capacities are found using a trial and error approach, lowering step by step the capacities and checking if the plant avoid stops during the entire year.

Daily model

This last model only gets implemented in third scenario of Table 2.2, PLRO. This model is created to estimate how much to over-size the *Continuous operation block* in Figure 2.9. The model is called “daily” as it works on a daily basis. From the “Day clustering” model three prototypical days are built up, “Best day”, “average day” and “worst day” and for each of them it is associated the number of days. In this way it is obtained a prototypical year represented by the combination of three prototypical days.

The model takes the sizes of from the FLR case in Table 2.2, and oversize the *Continuous operation block* from a 0% to 50% using a step of 2%. In this way for each supply chain there are 25 cases. Then for each case it is calculated the yearly production using as input the prototypical year mentioned before. For each case of each supply chain is reported the cost of investment of the plant, as well as the yearly production.

After all it is plotted for each supply chain the specific cost of syngas in order to evaluate the breakeven point in which the oversizing effort pays back with an additional productivity. The expected result are three curves (one curve for each chain) that displays "U" curves with a minimum, plotted on a graph in which the horizontal axis represent the additional size (form 0 MW to 50 MW) and the specific cost of syngas in [$/MWh]. This specific cost is a simple calculation calculated as the fraction of the annual cost [$/y] divided by the annual production [MWh/y] calculated using the prototypical year. This cost does not take into account installation costs and only applies for this evaluation. In this way the sizes referring to the minimum will be used, and the sizing process of this scenario continue with the hourly model.

2.5 Design phase

2.5.1 Days clustering

In this section it will be defined how prototypical days are created for the sizing of the three supply chains (PV-CC-BES, PV-DAC-BES, PV-DAC-GT).

In order to simplify the model, the year will be represented by a combination of three different days: "best day", "worst day", "average day". The first step before defining these three cases is to decide which data to use. For this work PVGIS-CMSAF database will be used as a source of data [14]. PVGIS-CMSAF is a scientific tool powered by the European commission and provides a free and open web access to solar radiation and temperature data and to PV performance assessment tools for any location in Europe and Africa, as well as large part of Asia and America. The value that is more interesting for this study is the power output of the PV panels which is set to have a nominal power of 1 kW. Larger plants are simulated scaling up linearly the production.

A set of assumptions are considered for selecting the values in this database:

Table 2.3 Set of assumptions used in PVGIS-CMSAF database.

Latitude (decimal degrees):	24.131
Longitude (decimal degrees):	38.160
Elevation (m):	21
Slope:	24 deg.
Azimuth (optimum):	2 deg.
Nominal power of PV system (crystalline silicon) (kW_P):	1.0
System losses (%):	14.0

A timeframe of three years (2014 to 2016) will be considered, and a vector of 26256 values is extracted. This vector of hourly measurements is grouped in 24 measurements to be converted in days, turning into a vector of 1094 values (26256/24). Days are then classified for their total energy output. In order to cut off some extraordinary conditions a threshold at the 2.5th percentile is set to the vector of days classified by their energy content. The "worst day" reference will be exactly the day placed at the 2.5th percentile. The "best day" is found in the same way, setting the threshold at the 97.5th percentile. The average day is the day across the 50th percentile. With this selection, 56 days are excluded from the original pool of 1094 days. The following table shows the vector of hourly power output of a single 1 kW PV panel of the three prototypical days.

The following graphs show better the daily power curve of the PV panel in these prototypical days.

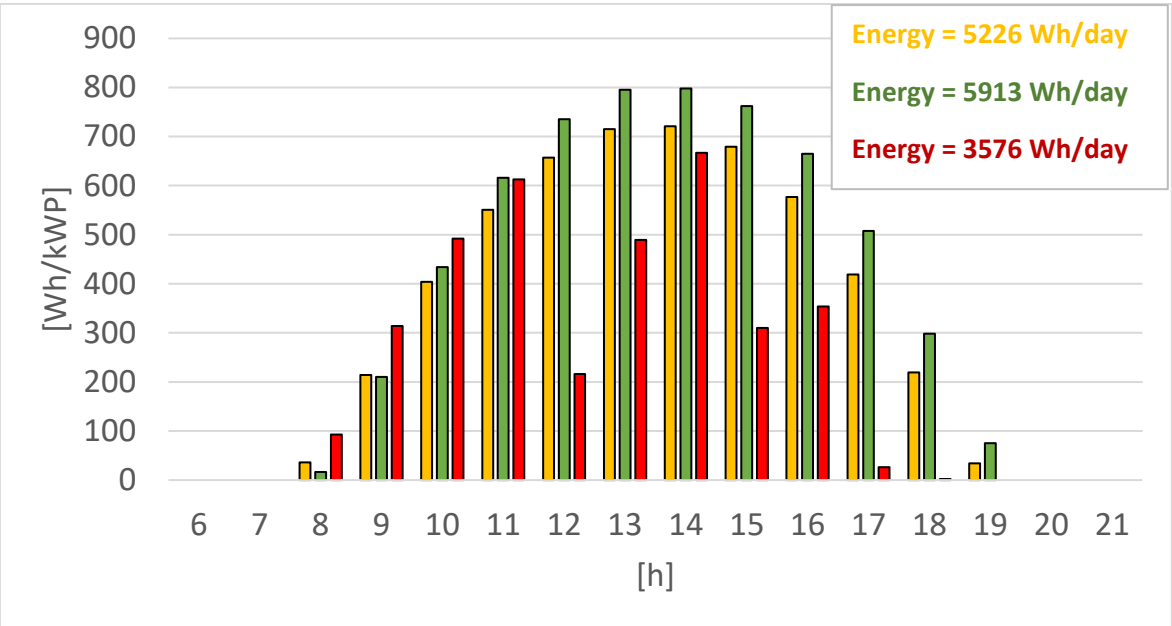

Figure 2.11 Power profile of 1 kWp PV system during the three sample days, "best day" (green), "average day" (orange), "worst day" (red).

The next step is to assess the right combination of these three prototype days to represent at best one year. This kind of evaluation is called clustering. There are several methods that can be used to cluster days. At first is useful to look at Figure 2.12 that shows the frequency of the days classified by the total energy.

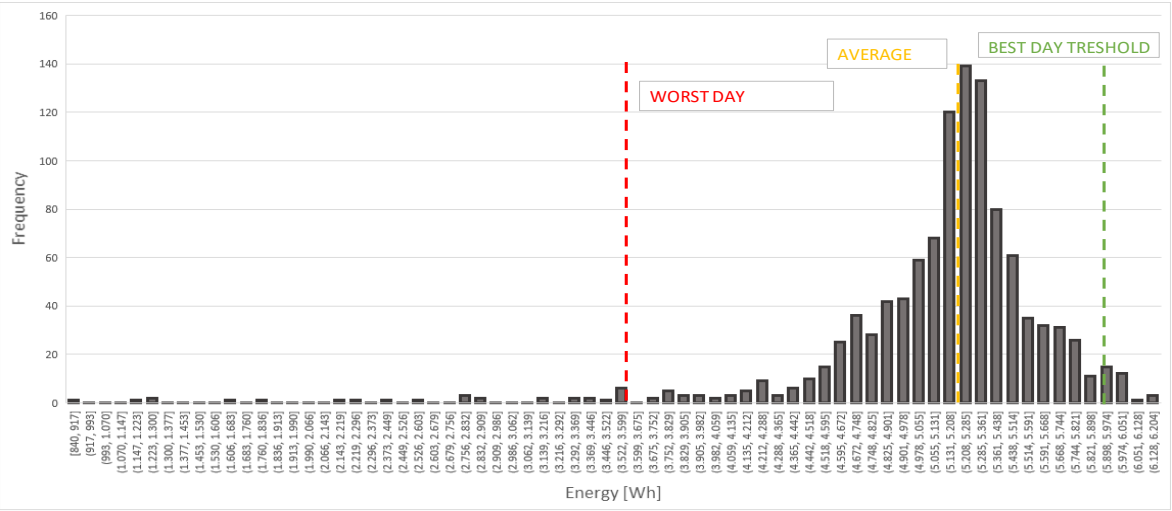

Figure 2.12 Histogram of days classified by the energy produced by a 1 kW PV system.

It is not surprising that there is a wide range of low energy days respect to the high energy days. This peculiarity comes from the effect of clouds that drive down the energy content of

some days. This aspect will be critical in the design of the storage system that guarantee consistency of operations.

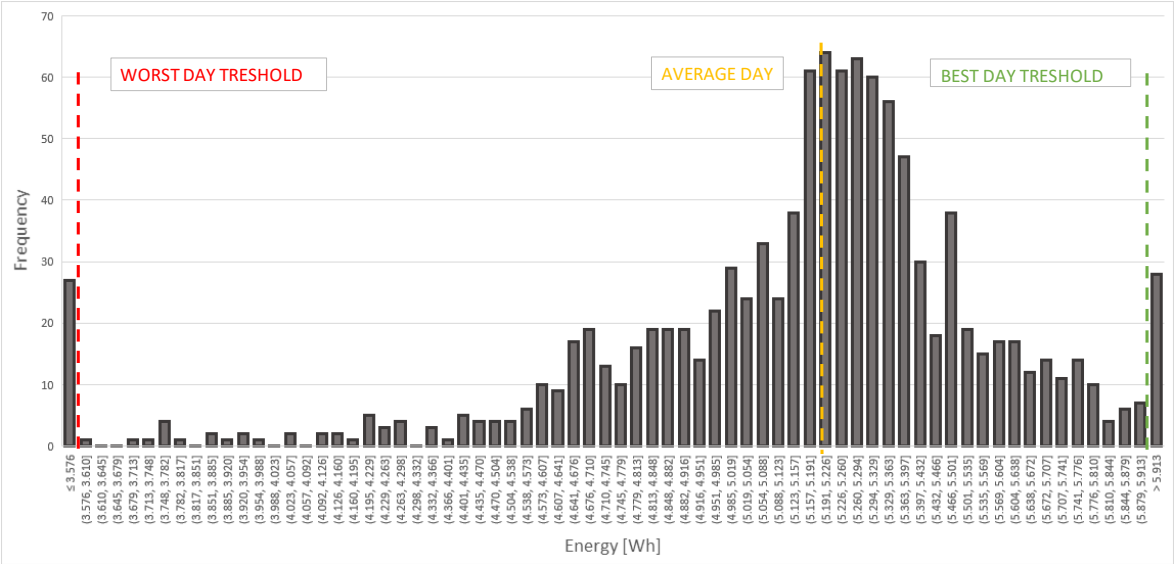

Figure 2.13 Histogram of days classified by energy after the thresholds

Once established the three cases, the next step is to evaluate the best combination to represent at best one year. Looking at Figure 2.13 one important aspect comes out, the mean doesn't align with the median. In specific left region has a wider range of values respect to the region at the right of the "average day" threshold. This aspect will drive the clustering method selection.

First, to cluster days it is necessary to introduce some parameters:

- E_{tot_left} is the total energy calculated as the sum of the energy of all days with energy lower than the average day (50th percentile) divided by 3 to make it annual (2014 to 2016 timeseries).
- E_{tot_right} is the total energy calculated as the sum of the energy of all days with energy greater than the average day (50th percentile) divided by 3 to make it annual.
- E_{tot} is the total energy of the 1094 days divided by 3 to make it annual.
- E_a, E_b, E_w are the total energy of average, best and worst day, respectively.

The difference in values of E_{tot_left} and E_{tot_right} is due to the fact that the average day is not the mean but the median. Nevertheless the difference is not that big but still remarkable.

Then, the following variables are introduced:

- -a_{left}, a_{right} are the number of average days that will be present in the left side and right side of the median.
- -w and b are the numbers of worst and best days.

The presence of a_{left}, a_{right} is justified to solve the system of equations but finally in the clustering these two terms concur both to create the number average days.

Finally we set a system of four equations, four as the number of variables.

$$wE_w + a_{left}E_a = E_{tot\_left} \quad \textit{Eq. 5}$$

$$bE_b + a_{right}E_a = E_{tot\_right} \quad \textit{Eq. 6}$$

$$wE_w + a_{left}E_a + a_{right}E_a + bE_b = E_{tot} \quad \textit{Eq. 7}$$

$$w + a_{left} + a_{right} + b = 365 \quad \textit{Eq. 8}$$

The system gives as output the values of b, w, a_{left} and a_{right}. As mentioned before the total values of average days is the sum of a_{left} and a_{right}. This system could be reduced in a three variable with three equation system using a single variable respect to a_{left} and a_{right}. The variables must be discrete numbers, so the result will not satisfy completely the set of equations. Anyway the rate between the difference of the number of days on the right and on the left is kept under ±0.2%, so can be considered widely acceptable. This result is displayed in Figure 2.14. The high prevalence of "average days" is justified by the latitude of the location, this distribution would have been different in a different location.

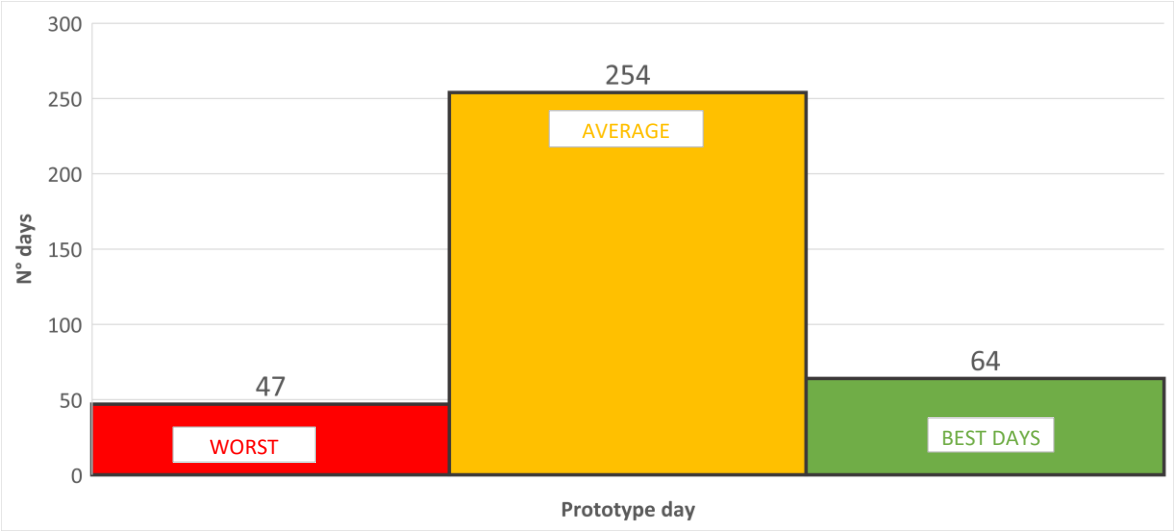

Figure 2.14 Histogram of days after clustering.

It can be noticed that the number of best days is higher than the number of worst days and this reflects the fact that $E_{tot\_right} > E_{tot\_left}$.

As mentioned before, the hourly model uses a vector of hourly measurements with the length of one year. Among the three years considered in this analysis it has been decided to use 2014 as the prototype year for the simulation. When the hourly model is used it takes values of the year 2014. The energy by day produced by 1 kW PV system in 2014 is represented in Figure 2.15. It can be noticed that the trend of the energy by day is quite stable along the year, as it was anticipated by Figure 2.7. One crucial aspect is the presence of extraordinary (but short) bad conditions in terms of irradiation and so in power production from the PV plant. In this specific case the valleys are caused by the presence of one or more days with lower total energy produced. Most of the negative inflections stands in the period of maximum irradiation per day, meaning that the period in which there is the highest irradiation is the same in which there is less stability of production. This aspect will have a strong influence on the seasonal storage of hydrogen.

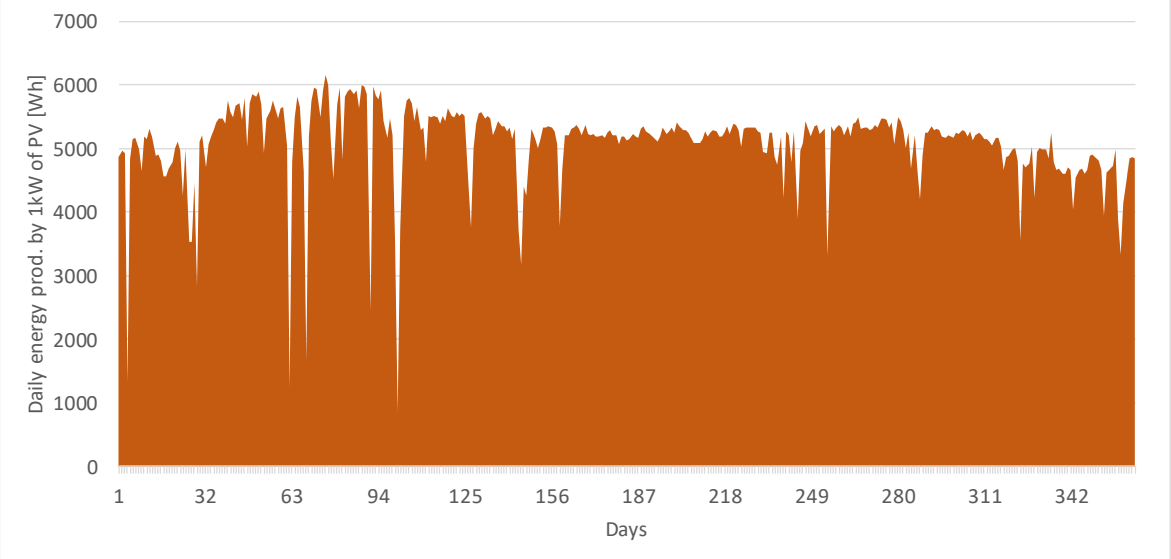

Figure 2.15 Total energy per day during 2014

2.5.2 Balance of plant sizing

This section gives a description of the BOP's (Balance of Plant). In addiction for the systems involved in calculations it is assessed how each system is modelled.

Desalting

Water is the source of elemental hydrogen for the syngas synthesis. For the electrolysis it must be used fresh water, which only sometimes is available in the territory. In dry regions such as Middle East, water must be obtained from seawater through a desalting process. In this work, since the idea is to design a self-sufficient plant the desalting process is included in the plant.

In order to evaluate the energy expenditure for fresh water purchase, it has been assumed 5 kWh to produce one ton of fresh water, [15]. This value turns out to be a marginal voice compared to other energy consumes, but it is still present in the design analysis because sometimes its presence weakly affects the batteries sizing.

From the economical point of view the cost related to desalting is such small that is not considered in most of the analysis of Power to Fuel, and even in this case it will be considered negligible, [16].

CO_2 storage

During operations DAC system works at full power in steady state conditions as well as the methanator. For this reason, in principle there is no need to have a CO_2 storage. In reality a CO_2 buffer is highly recommended for some reason such as to give the possibility to do maintenance on DAC system without switching off the whole plant, or to guarantee continuity if some DAC modules shut down for any reason. For the CC supply chain, it is the supplier that must guarantee continuity. Because in this work all backup systems are not sized, it not coherent to do that only for carbon dioxide, so the buffer will not be included in the sizing procedure.

H_2 storage

Hydrogen, out of the electrolyzer is stored in vessels that allow the methanator to work in steady state conditions even when the electrolyzer is off. In reality, hydrogen storage will be made by several pressurized vessels but in this work hydrogen storage will be considered as it was one single storage system. The hydrogen produced by the electrolyzer have a pressure around 30 bar, then as soon as it enters the H_2 storage it laminated to the pressure of the tanks. Storage pressure in this model can vary from a minimum of 3 bar to a maximum of 30 bar. The minimum level (3 bar) is arbitrary set to the 10% of the maximum operating pressure. Downstream the storage a compressor is placed, responsible to pressurize the hydrogen up to the operating pressure of the methanator (25 bar). If the H_2 storage is full, the pressure is 30 bar and there is no need of the compressor since the pressure of the tank is higher than the pressure in the methanator so hydrogen moves spontaneously. As the pressure of the tank fall below 25 bar then the compressor starts working as intensely as the emptiness of the storage.

A better solution should also include another bypass that goes directly from the AEK to the methanator, in this way the hydrogen produced is divided into two streams: one goes directly to the methanator and avoid the lamination and compression which would result in a loss of efficiency, the other stream goes laminated to the H_2 storage. In the model this solution is not implemented in order to simplify the model, nevertheless this solution will not impact considerably the final LCOM.

The capacity of the storage will be assessed in the hourly evaluation.

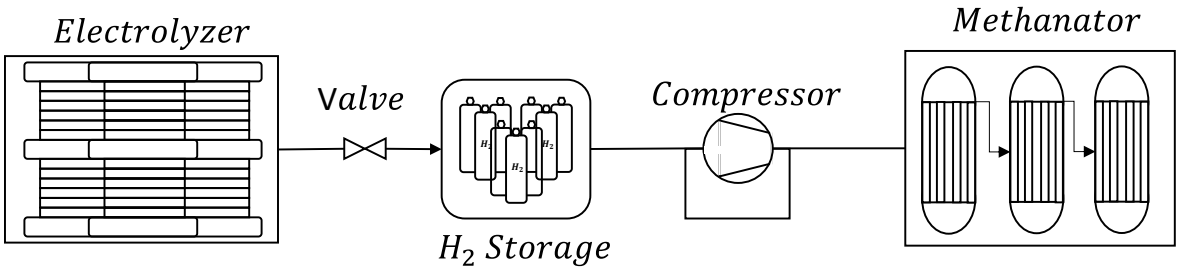

Figure 2.16 Schematic representation of the matching between AEK, H_2 systems and methanator

CO_2 compressor

Carbon dioxide, whether it comes from DAC system or from an external source must be brought at methanator pressure. This effort is done by a compressor, and in this case compressor will work always at full load with no load fluctuations. The initial pressure is 1 bar, and final pressure is 25 bar, using a prudential approach the sizing is done using a final pressure of 30 bar. The compression power requirement for each stage $W_{s,i}$ is given by the following equation [17]:

$$W_{s,i} = \left(\frac{\dot{m}\, Z_s R T_{in}}{M \eta_{is}}\right)\left(\frac{k_s}{k_s - 1}\right)\left[\beta^{\frac{k_s - 1}{k_s}} - 1\right] \qquad \textit{Eq. 9}$$

In general:

Z_s is the average CO_2 compressibility for each individual stage

k_s is the average ratio of specific heats of CO_2 for each individual stage

For all stages:

R = 8.314 [kJ/kmol K] is the gas constant

M = 44.01 [kg/kmol] is the molar mass of carbon dioxide

T_{in} = 313.15 [K] is the temperature at inlet of each stage

η_{is} = 0.8 is the isentropic efficiency

β = 2.34 is the compression ratio of each individual stage

$\dot{m}$ = 5.5 [kg/s] is the mass flow of carbon dioxide

The whole conversion is made up by four inter refrigerated stages. Each stage has its own Z_s and k_s.

Table 2.4 Compressibility (Z_s) and specific heats ration (k_s) for each stage [17]

	k_s	Z_s
Stage 1	1.277	0.995
Stage 2	1.286	0.985
Stage 3	1.309	0.970
Stage 4	1.379	0.935

The total power required of the four stages for a stream of 5.5 kg/s is 1.49 MW with a specific enthalpy per stage of 71.24 kJ/kg. Finally considering an organic electric efficiency of 95% the total power consumption is 1.57 MW.

H_2 compressor

This component is sized on the worst condition, which takes place when the hydrogen storage is at the minimum pressure, 3 bar. The final pressure should be 25 bar, because it is the operating pressure of the methanator but 30 bar will be used in order to overcome possible pressure drops. The flow is always steady state so the only variation in operation consists on the compression ratio. The equation used is the same of CO_2 compressor but in this case all stages have the same Z_s and k_s because in this range of pressure, for hydrogen Z_s and k_s don't change that much. Eight stages will be used because otherwise the enthalpy per stage would be too high.

These are the parameters used:

$$W_{s,i} = \left(\frac{\dot{m}\, Z_s R T_{in}}{M \eta_{is}}\right)\left(\frac{k_s}{k_s - 1}\right)\left[\beta^{\frac{k_s-1}{k_s}} - 1\right] \qquad \textit{Eq. 10}$$

R = 8.314 [kJ/kmol K]

$M = 2$ [kg/kmol]

$T_{in} = 313.15$ [K]

$\eta_{is} = 0.8$

$\beta = 1.334$

$\dot{m} = 0.904$ [kg/s]

$Z_s = 1.01$

$k_s = 1.4$

The electrical power consumed is 3.75 [MW], even in this case an organic-electric efficiency of 95% is used. The specific enthalpy for each of the eight stages is 493 [kJ/kg].

2.5.3 DAC & batteries sizing

Batteries

Several systems could be used for energy storage, for this size mainly of electrochemical kind. For energy storage some interesting results are coming from both flow batteries and fuel cells, but for this study the lithium ion batteries will be used because this solution is the most mature and economically viable at the moment.

In the model the charge-discharge efficiency is assumed to be 85% for each cycle. To evaluate the capacity of the batteries, it is calculated the total amount of energy by day that is required to power all the BOP's. Then this value will be adjusted or confirmed using the hourly model that verify if the size fits or not in the real operations.

DAC system

As mentioned before there are DAC systems that for the regeneration require high temperatures usually using aqueous solution as sorbents, and systems using solid sorbents that are able to perform regeneration at low temperatures. In this study only the solid sorbent system is investigated because the low regeneration temperature allows to use heat recovered to feed the regeneration process. In Table 2.1 there are some sorbents types with their

temperatures for the regeneration and the total energy required, either electrical and thermal. In general electric energy is used to power fans and pumps to create vacuum, while the thermal energy is used to heats up the sorbent and let regeneration takes place. For this study it will be used as a reference the case of Climeworks, using amine-based solid sorbent. On the official site of Climeworks it is specified that DAC system requires hot water around 100°C. In this work it is assumed that the hot pressurized water circuit ranges from 70°C to 120°C.

The energy requirements are 250 kWh/tCO_2 electrical, and 1750 kWh/tCO_2 thermal.

Table 2.5 Low thermal solid sorbent DAC specifications [9]

sorbent	CO_2 con.	adsorption	desorption		energy demand		
	ppm	T (°C)	T (°C)	P (bar)	kWh_{el}/t	kWh_{th}/t	
amine-based	400	ambient	100	0.2	200–300	1500–2000	Climeworks (2018b); Vogel (2017)
amino-polymer	400	ambient	85–95	0.5–0.9	150–260	1170–1410	Ping et al. (2018b) (Global Thermostat)
TRI-PE-MCM-41	400	ambient	110	1.4	218	1656	Kulkarni and Sholl (2012)
MOF (Cr)	400	ambient	135–480	1	1420		Sinha et al. (2017)
MOF (MG)	400	ambient	135–480	1	997		
K_2CO_3/Y_2O_3	400	ambient	150–250	–	–	–	Derevschikov et al. (2014)
K_2CO_3	–	ambient	80–100	–	694	2083	Roestenberg (2015); Antecy (2018)
-	**400**	**ambient**	**100**	–	**250**	**1750**	**final model (this study)**

In the PV-DAC-BES supply chain both electrical and thermal needs are covered by the batteries. In particular the thermal power is obtained using electrical resistances that heat up the water for the DAC system.

In the PV-DAC-GT case gas turbine feeds the DAC system, the electrical energy produced covers the electrical need of the DAC, while thermal energy is recovered from the exhausts using an heat recovery system that heats up the pressurized water.

DAC capacity is calculated in tons of CO_2 produced by year, in this case considering that the DAC must provide the carbon dioxide to feed a 100 MW methanator the resulting capacity is 173’448 tCO_2 per year.

2.6 Economic approach

2.6.4 General assumptions

The final goal of this work is to calculate the levelized cost of syngas produced by the plant. The yearly production of syngas is assumed to be constant during the lifetime of the plant. With this assumtion the LCOM is calculated with Eq. 11.

$$LCOM\left[\frac{\$}{MWh}\right] = \frac{Annual\ cost\left[\frac{\$}{y}\right]}{Annual\ prod\left[\frac{MWh}{y}\right]} \qquad Eq.\ 11$$

The Annual production is calculated with the sum of the annual cost related to the CAPEX and the annual OPEX, Eq. 12.

$$Annual\ cost\left[\frac{\$}{y}\right] = OPEX\left[\frac{\$}{y}\right] + CAPEX_a\left[\frac{\$}{y}\right] \qquad Eq.\ 12$$

$CAPEX_a$ is calculated in Eq. 14 using the CRF (Capital recovery factor) which is derived from WACC (Weighted average cost of capital) using Eq. 13.

$$CRF = \frac{WACC \cdot (1+WACC)^N}{(1+WACC)^N - 1} \qquad Eq.\ 13$$

$$CAPEX_a\left[\frac{\$}{y}\right] = \sum_i \{CAPEX_i[\$] \cdot (1+K_i)\} \cdot CRF\left[\frac{1}{y}\right] \qquad Eq.\ 14$$

K_i is a parameter, calculated as a percentage of the CAPEX and used to take into account additional installation costs. This item includes land, infrastructure and development cost of the plant as well as project management and consultancy. To evaluate this coefficient, it has been taken as a reference an economic evaluation of a 408 MW natural gas fuelled power plant in Singapore. From Table 2.6 it is calculated the proportion of item 3 with respect to item 2 multiplied by item 1. The proportion is 60%, so the parameter K_i will represent an additional sixty percent of the CAPEX. This coefficient will be applied to all capital costs except for the PV and AEK whose specific cost yet includes the installation costs.

Table 2.6 Summary of technical and economical parameters of a 408 MW natural gas power plant in Singapore [18].

ITEM	Value	Unit of measure
1. Size of the plant	408	MW
2. Capital cost of the plant	887	$US/kW
3. Land, infrastructure and development cost	157.7	$S million
3. Land, infrastructure and development cost $US	220.8	$US million
Exchange rate SGD/USD	1.4	

All the supply chains, to be comparable, uses the same values of WACC and lifetime. WACC is assumed to 8 %, and the lifetime is 20 years. The resulting CRF is 0.10185 [1/y].

The plant is intended to run all the time in the models but it must be considered a timeframe during the year in which the plant is under maintenance. To do so a coefficient called "Availability" is introduced. Its value is assumed to be 95%, so it means that the output of the hourly model must be multiplied by the availability to evaluate the annual production.

2.6.5 Components economic modelling

One of the most important items in the investment cost is covered by the PV plant.

In Figure 2.17 are reported some costs available from [4].

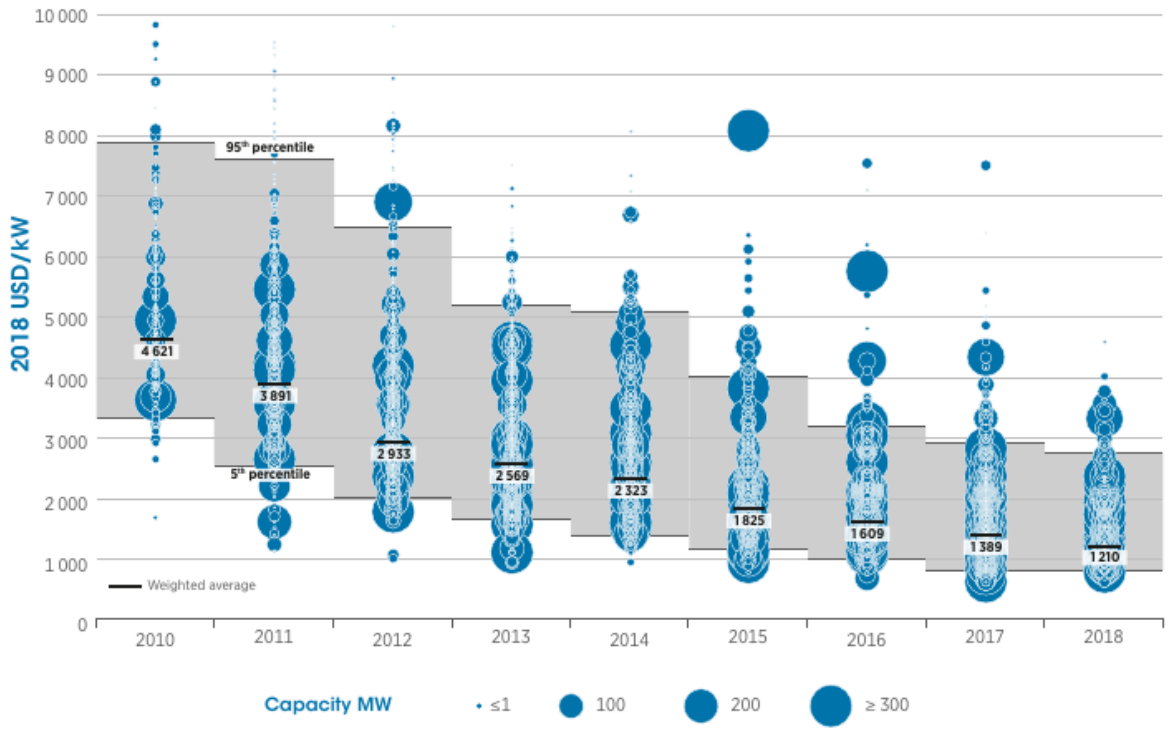

Figure 2.17 Total installed cost of utility-scale solar PV projects and the global weighted average 2010-2018 [4].

Latest projects achieved values around 700-800 $/kW. In this work as the expected size of the PV plant is over 1 GW it is assumed a specific installed cost of 700 $/kW.

For most of the components the total cost is evaluated multiplying the size with the specific costs reported in Table 2.7.

Table 2.7 Specific cost of components of the plant

Component	CAPEX	[Unit]	Ref.	Notes
PV plant	700	[$/kW]	[4]	Installed
AEK	900	[$/kW]	[19]	Installed
Methanator	270	[$/kW]	[20]	
H_2 Compressor	2100	[$/kW]	[21]	
Batteries	200 (300)	[$/kWh]	(see below)	
DAC system	664	[$/t$CO_2$ a]	[9]	
Gas turbine	400	[$/kW]	[22]	
ORC system	1500	[$/kW]	[23]	

Alkaline electrolyzer and batteries require some additional information.

AEK uses stacks whose lifetime depend of utilization. For this work, stacks are assumed to last 60000-90000 hours [6], and the results in terms of working hours per day suggest that AEK works for around 10 hours per day. For 20 years it means a total of 73000 hours, so with these assumptions a stacks replacement is not mandatory.

The specific cost of the methanation unit comes from a feasibility study of a 100 MW power to gas facility, [20]. The cost of methanation reactor and its auxiliary devices was estimated from the commercial Coal-to-SNG plant from literature [24]. The unnecessary devices such as coal gasifier and sulfur removal device in a Coal-to-SNG plant were removed from the calculation [24]. The unit cost was then scaled up by the plant capacity (100 MW) [20].

Batteries are assumed to have a lifetime that depends on the time and not on the number of cycles (Li-ion technologies). Lifetime is assumed to be 13 years [19], so it must be included a substitution of the non-electronic parts of the batteries. The cost of the substitution is assumed to be 50% of the initial battery CAPEX.

Replacement components are assumed to be purchased with all other components so finally the CAPEX of batteries becomes 300 $/kWh.

The Hydrogen storage is assumed to be an assemble of tanks with a maximum pressure of 30 bar and with a volume of 115 m^3 per single tank. The specific cost per unit of volume is 1350 $/$m^3$ [25], and the volume is calculated using the energy density of 96.1 kWh/m^3 which is the energy density of hydrogen at 30 bar and 20 C°.

For the CO_2 compressor the CAPEX is estimated through Eq. 15 [26].

$$\text{CAPEX}\,[\$] = 88 \cdot 10^3 \cdot P[kW]^{0.55} \qquad \textit{Eq. 15}$$

In this work it will be used a heat exchanger for flue gases heat recovery and its cost is calculated through Eq. 16.

$$\text{CAPEX}\,[\$] = 8500.71[\$] + 111.42\left[\frac{\$}{m^2}\right] \cdot S\,[m^2] \qquad \textit{Eq. 16}$$

DAC system CAPEX

About costs of DAC system there is lot of uncertainty because it is a new technology and so there are less case studies available. Table 2.8 reports two CAPEX for solid sorbent based technology, between these two values 730 [€/tCO_2 a] is assumed to fit best because the related capacity is more consistent with this study.

Table 2.8 Economics of DAC, [9]

technology	capacity	capex	opex	lifetime	indicated time of cost	reference
	t_{CO2}/a	€/t_{CO2}·a	%	years	year	
LT solid sorbent	3600	1220	-	25	2015	Roestenberg (2015)
	360 000	730	-	25	2015	(Antecy)
	-	-	-	-	first plant	Kintisch (2014); Ping et al. (2018a; 2018b)
	-	-	-	-	n/a	(Global Thermostat)
	300	-	-	20	2014	Climeworks (2018b)
	-	-	-	-	large-scale	

CAPEX is then calculated in dollars, 664 $/$tCO_2$ a. This value refers to the annual capacity of the system.

OPEX

Operational costs (OPEX), are on annual base and are reported for each component in Table 2.9.

Table 2.9 OPEX of components of the plant

Component	**OPEX**	**[Unit]**	**Ref.**
PV plant	1.0 %	[% of CAPEX]	[27]
Alkaline electrolyzer	1.5%	[% of CAPEX]	[19]
Methanator	4%	[% of CAPEX]	[19]
Turbine	5%	[% of CAPEX]	"assumption"
H_2 Compressor	5%	[% of CAPEX]	"assumption"
Batteries	5%	[% of CAPEX]	"assumption"
DAC system	4 %	[% of CAPEX]	[9]
Gas turbine	5%	[% of CAPEX]	"assumption"
ORC system	5%	[% of CAPEX]	"assumption"

PV-CC-BES supply chain does not include the DAC system, so the cost of CO_2 will be included in the operational annual cost. There are studies available on current and projected costs of CCS, but estimates are affected by lot of uncertainty and depend on a number of factors including the costs of energy. Available studies focus mostly on power generation. Therefore, even a larger uncertainty affects other industrial applications. The uncertainty also depends on the cost of the basic technologies. In Figure 2.18 are displayed some abatement cost, [28]. Abatement costs also include the cost of compression and transport. In general capture costs account for 70% of reported costs. For this work a value of 40 \$/tCO_2 will be used.

The most uncertain values are object of a sensibility analysis at the end of this work, to assess the impact of assumptions.

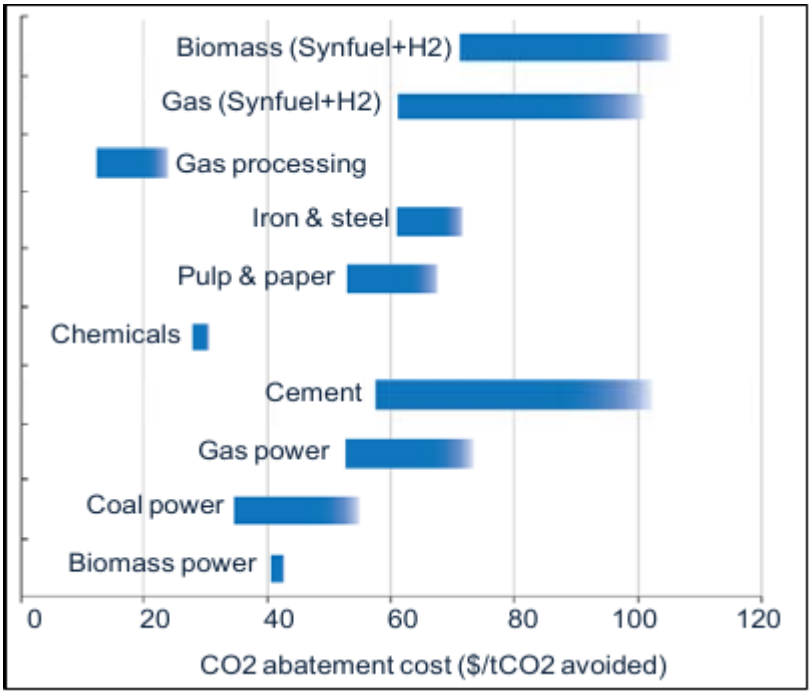

Figure 2.18 Abatement cost of carbon dioxide

Chapter 3 FL case: methanator operative always at full load

3.1 Plant layouts

In this section layouts of each supply chain are represented. The layout Figure 3.1 represents a general and simplified picture that includes the main components that such process must include.

For each layout are also represented the energy streams on a daily basis.

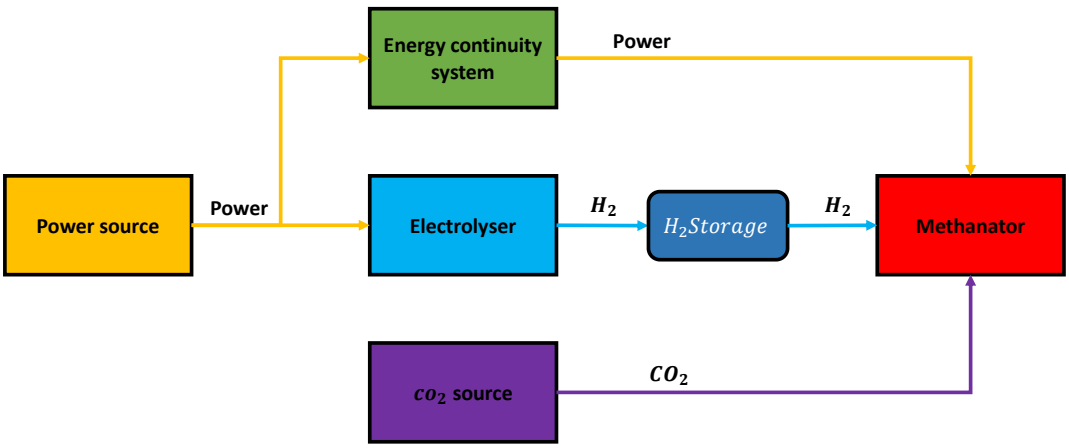

Figure 3.1 Simplified schematic representation of Power to gas process

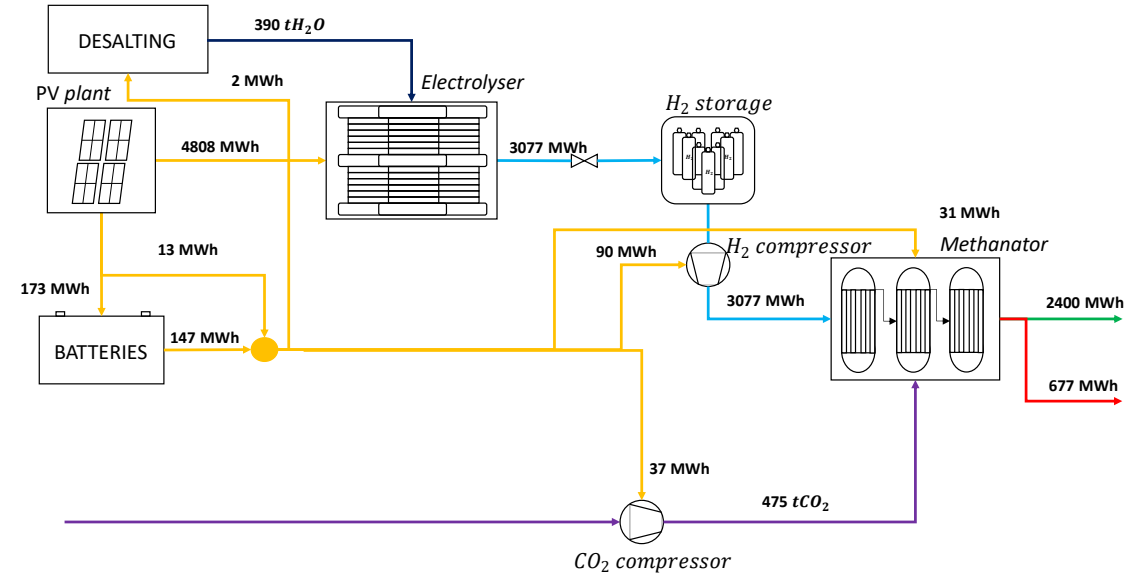

Figure 3.2 Process flow diagram on daily basis for PV-CC-BES

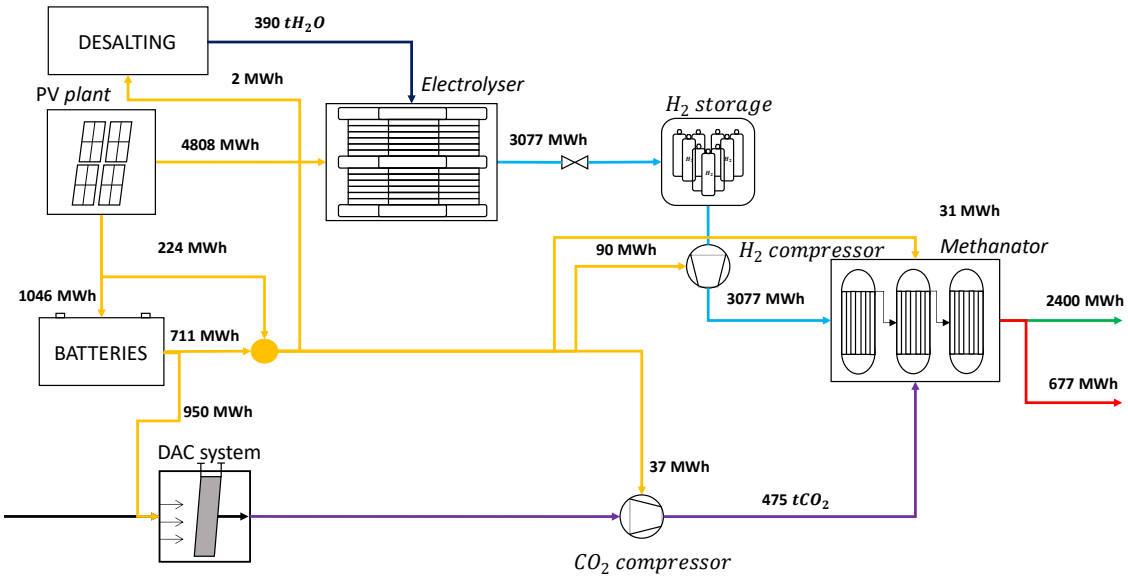

Figure 3.3 Process flow diagram on daily basis for PV-DAC-BES

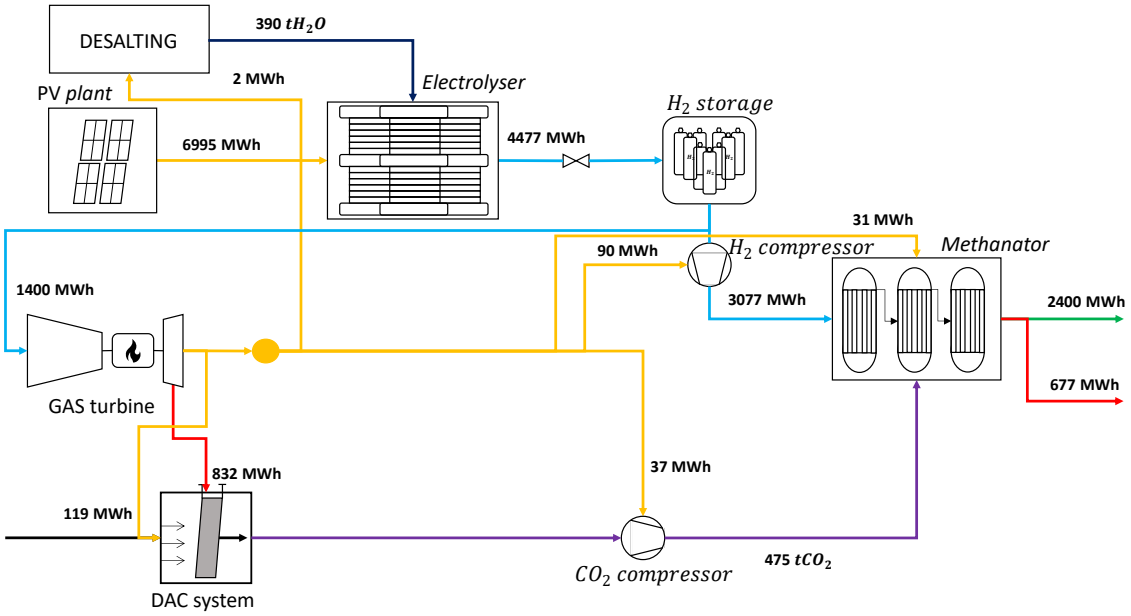

Figure 3.4 Process flow diagram on daily basis for PV-DAC-BES

3.2 Sizing

This section focuses on the sizing of the plant components. The starting point is the capacoity of the methanator which is set to 100 MW output. The methanator is intended to work continuosly in steady conditions at full load. In order to guarantee continuity, a hydrogen storage system is installed. The rest of the plant is designed accordingly. Table 3.1 resume the main assumptions used for calculations in this phase.

Table 3.1 General assumptions of components of the power to gas plant

Item	Value	Reference
Efficiency AEK 25 bar (LHV)	64%	[19]
Efficiency methanator (LHV)	78%	[19]
Turbine efficiency	20%	*Assumption*
LHV CH_4 [MJ/kg]	50	
Charge-discharge battery efficiency	85%	[29]
Methanator auxiliaries % of P_n	1,3%	[19]
DAC POWER [kWh_e/tCO_2]	250	[9]
DAC HEAT [kWh_t/tCO_2]	1750	[9]
Organic electric efficiency for Compressors & turbines	95%	*Assumption from current state-of-art*

The water for the electrolyzer is assumed to be obtained by desalting sea water. The energy expenditure is quite low but not negligible, so it is considered in the evaluations: 5 kWh_e/tH_2O [15].

The amount of water needed is calculated directly from the amount of hydrogen needed with the assumption that all water is converted into molecular oxygen and molecular hydrogen. The daily request of water is around 390 tons. The conversion of CO_2 is considered to be full, even if in reality it is typically slightly lower than 100%. The daily request to produce 100 MW of syngas leads to a CO2 demand of 475.2 tCO_2/d, equivalent of a steady state stream of 5.5 kg/s.

3.2.1 HX sizing for PV-DAC-GT

PV-DAC-GT supply chain uses a heat recovery system, so it also needs to be designed. For this evaluation the specific heat capacity of exhaust is considered to be constant in the heat transfer.

Table 3.2 Parameters and assumptions for heat recovery evaluation in PV-DAC-GT

Item	**Value**	**[Unit of measure]**
Exhaust temperature	500	[°C]
Heat available from exhaust	46.625	[MW]
Heat required by DAC	34.650	[MW]
Initial T of water	70	[°C]
Final T of water	120	[°C]

Table 3.3 Values for the T-Q diagram in heat recovery evaluation for PV-DAC-GT

EXHAUST			**WATER**		
T_{ie}	500	C°	T_{iw}	70	C°
T_{fe}	143	C°	T_{fw}	120	C°
$Q_{available}$	46625	kW	$Q_{exchanged}$	34650	kW
HX effectiveness	83%				

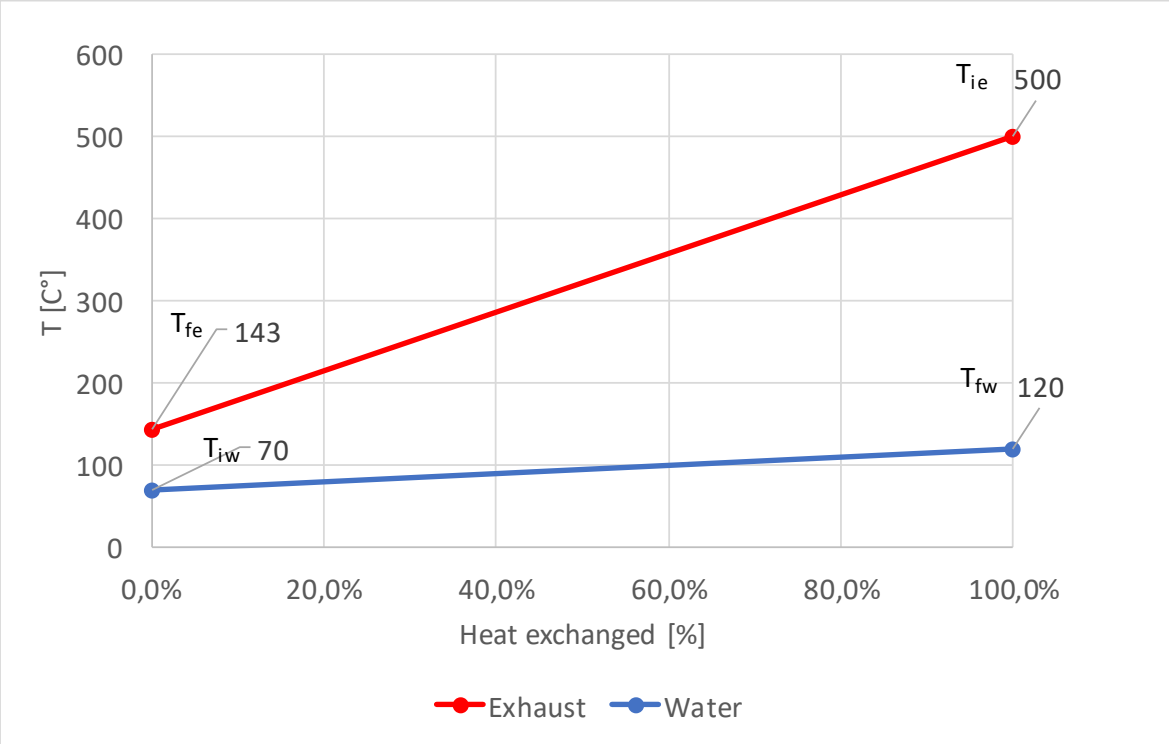

Figure 3.5 T-Q diagram of heat recovery in PV-DAC-GT

Using assumptions and parameters in Table 3.2 the T-Q diagram can be built up. A final temperature of the exhaust of 143 °C is reasonable, and it lead to an effectiveness of the heat exchanger of 83% and efficiency (calculated as the fraction of heat recovered over the heat available in the exhaust) of 74.3%.

In order to evaluate the surface of the heat exchanger Eq. 17 and Eq. 18 are used.

$$\mathrm{Q\ [W]} = U\left[\frac{W}{m^2 \cdot K}\right] \cdot A[m^2] \cdot \Delta T_{ml}[K] \qquad \textit{Eq. 17}$$

$$\Delta T_{ml}[K] = \frac{(\Delta T_1 - \Delta T_2)}{\ln(\Delta T_1 - \Delta T_2)} \qquad \textit{Eq. 18}$$

With ΔT_1 as the difference of temperature between the initial temperature of the hot fluid minus the initial temperature of the cold fluid, and ΔT_2 as the difference between final temperature of hot fluid minus cold one.

U is the heat exchange coefficient and it is assumed to be 70 [W/(m^{2}K)]. Area calculated from Eq. 17 is 7308 m^2.

3.2.2 PV and Electrolyzer sizing

The first step in this analysis is the rate between the P_n of the electrolyzer and the P_n of the PV power plant, which is $R_{AEK/PV}$. PV plant has to power both electric appliances (DAC system, methanator auxiliaries, H_2O desalting, H_2 compressor, CO_2 compressor) and the electrolyzer which is the main consumer. The $R_{AEK/PV}$ is very important to assess because a rate too low will result in a plant which waste too much power while a very high rate lead to higher costs for an electrolyzers that has a limited capacity factor. In the Figure 3.7 it can be seen the fraction of energy that goes directly to the electrolyzer and the rest which goes to the batteries and will be exploited during the night. The energy going to the BOP's is not always coming from the batteries, the logic is that electrolyzer has priority, then when the power output of the PV plant exceeds the nominal power of the electrolyzer the energy flows both to the batteries and to BOP's. It is preferable to power directly BOP's without going through the batteries in order to avoid losses occurring during the charge-discharge cycle of the batteries.

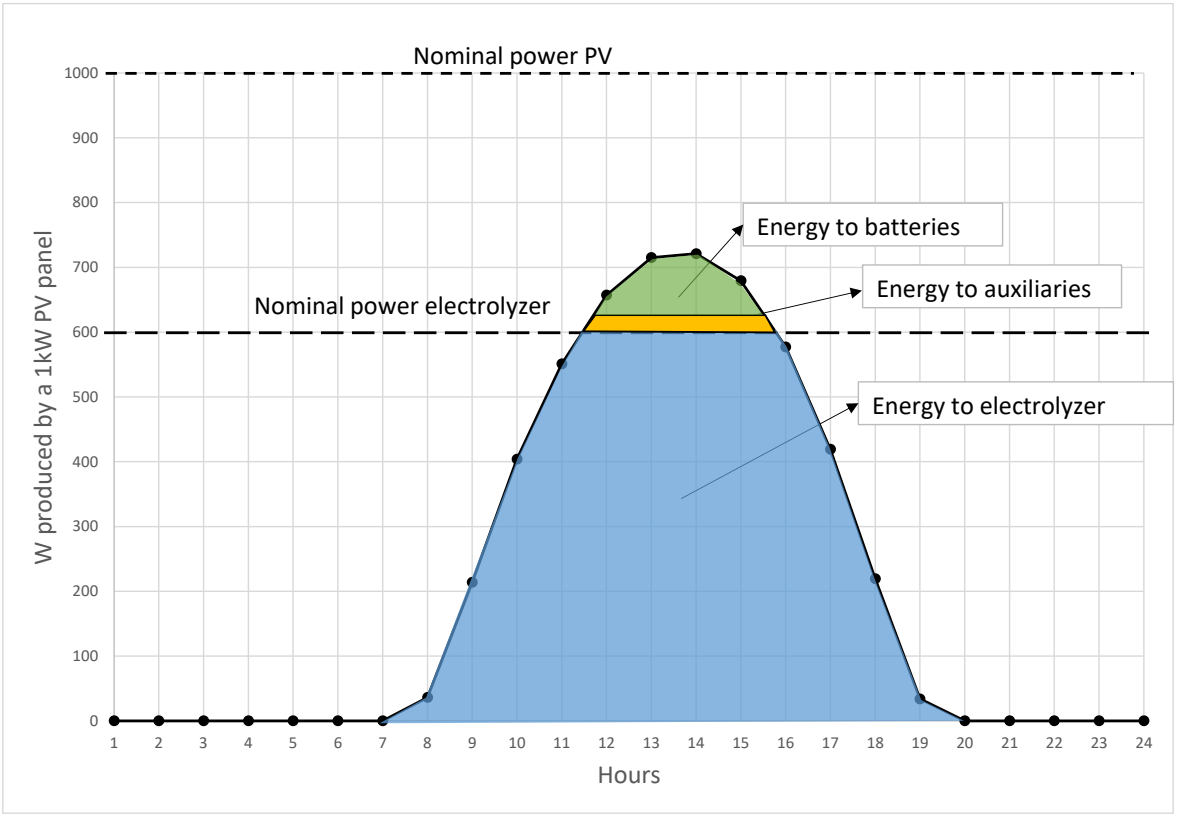

Figure 3.6 Energy stream out of the PV system

The optimal $R_{AEK/PV}$ must take into accounts the investment costs of PV, AEK and batteries. The higher the rate the higher the capacity of the batteries because the window in which the PV plant powers directly BOP's becomes shorter, so the amount of energy provided by the batteries during one day is larger. The Figure 3.8 below shows this aspect of the model for the PV-CC-BES case, the same could be done for the other supply chain but it is done just to show how the model works.

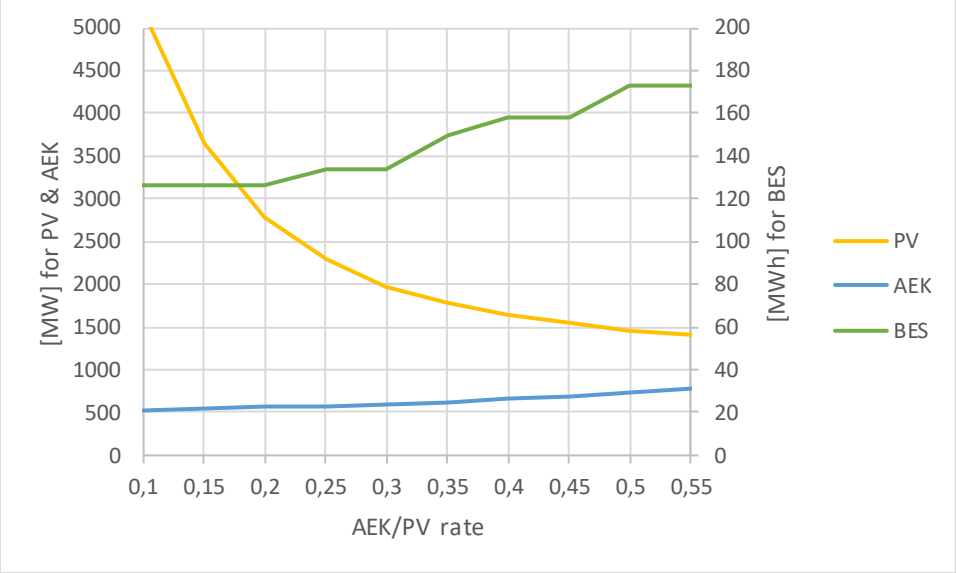

Figure 3.7 Size of components respect to $R_{AEK/PV}$ for PV-CC-BES

Figure 3.9Figure 3.8 Sensitivity analysis of the investment cost function of $RAEK_{/PV}$ considering cost of PV, electrolyzer and batteries shows instead the investment cost of PV, AEK and batteries along with $R_{AEK/PV}$ of each supply chain. This analysis is called sensitivity analysis and is used to find the best $R_{AEK/PV}$ plotting the results of the free variable (investment cost) and the independent variable $R_{AEK/PV}$.

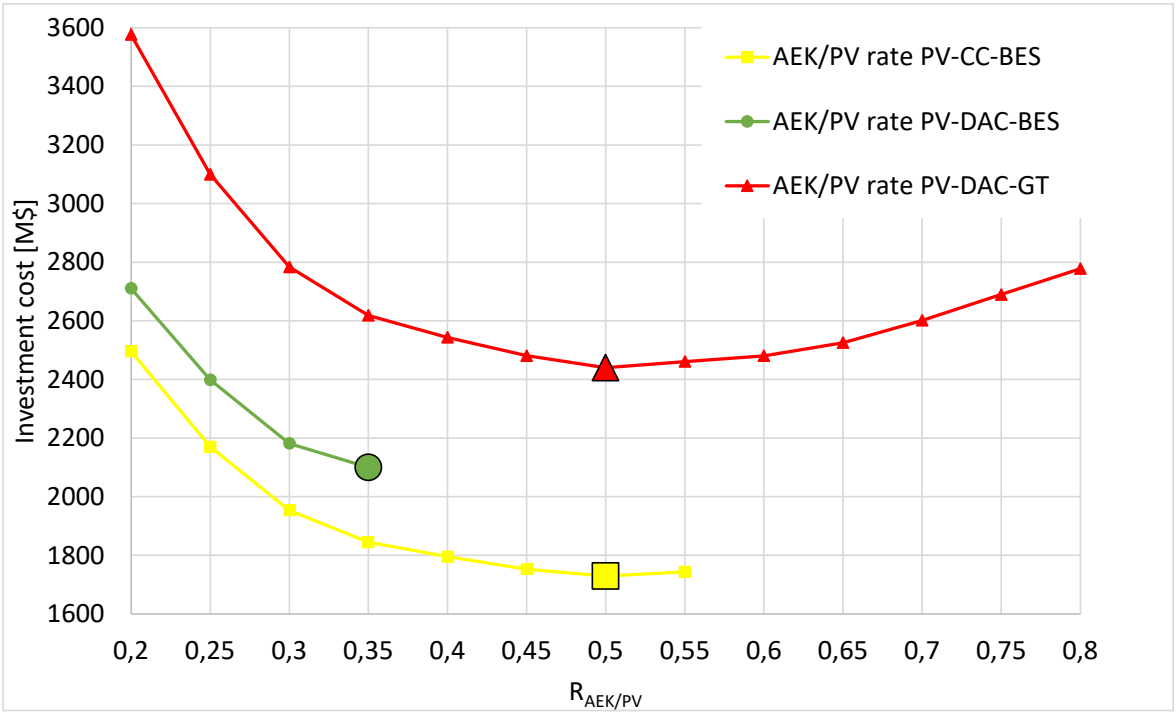

Figure 3.8 Sensitivity analysis of the investment cost function of $R_{AEK/PV}$ considering cost of PV, electrolyzer and batteries in FL case.

Two curves results interrupted. This happens because a part of the energy fm the electrolyzers, in particular the part that exceeds the P_n of the electrolyzer, must go to the batteries. So for PV-CC-BES case for example, for a $R_{AEK/PV}$ higher than 0.55 the amount of energy dedicated to the batteries becomes such narrow that can't hold during the night all the BOP's. This aspect is stressed in the PV-DAC-BES case as the battery pack is way higher. PV-DAC-GT is not affected by this aspect as the PV plant is completely dedicated to the electrolyzer. The oversized indicators in the figure are placed in the optimal point of each curve.

Throughout this analysis the sizing process is completed, in Table 3.4 are collected the results.

Table 3.4 Sizing resume table of the supply chains in FL case

		PV-CC-BES	PV-DAC-BES	PV-DAC-GT
PV	**[MW]**	1458	1649	2122
AEK	**[MW]**	729	660	1061
Methanator	**[MW]**	100	100	100
Gas turbine	**[MW]**			58
Batteries	**[MWh]**	173	1000	
HX	**[m^2]**			7308
H_2 compressor	**[MW]**	3.75	3.75	3.75
CO_2 compressor	**[MW]**	1.57	1.57	1.57
DAC system	**[tCO2/y]**		173448	173448

3.2.3 Power flow logic

In this section it is explained how the hourly model manage the power stream form the PV plant and which system has the priority. The algorithm is explained using the flow chart in Figure 3.9. In particular, the systems are put in order of priority, so for example in the case (PV->AEK-AUX-BAT) the energy goes at first to satisfy the AEK demand, then it goes to auxiliaries (DAC included) and finally the energy left goes to the Batteries.

Legend:

- P_{PV} : Power of the photovoltaic plant
- P_{AEK} : P_n of the alkaline electrolyzer
- HL : Hydrogen level of the storage
- BL : State of charge of the battery
- MIN : minimum level of the storages, for batteries is 0% while for hydrogen as previously described is 10%
- EL : Emergency level, for PV-CC-BES is 30% of the total batteries capacity, while for PV-DAC-BES it is 50%
- PV : Photovoltaic plant
- AEK : Alkaline electrolyzer

- BAT : Batteries
- AUX : Auxiliaries
- Φ : The plant is off

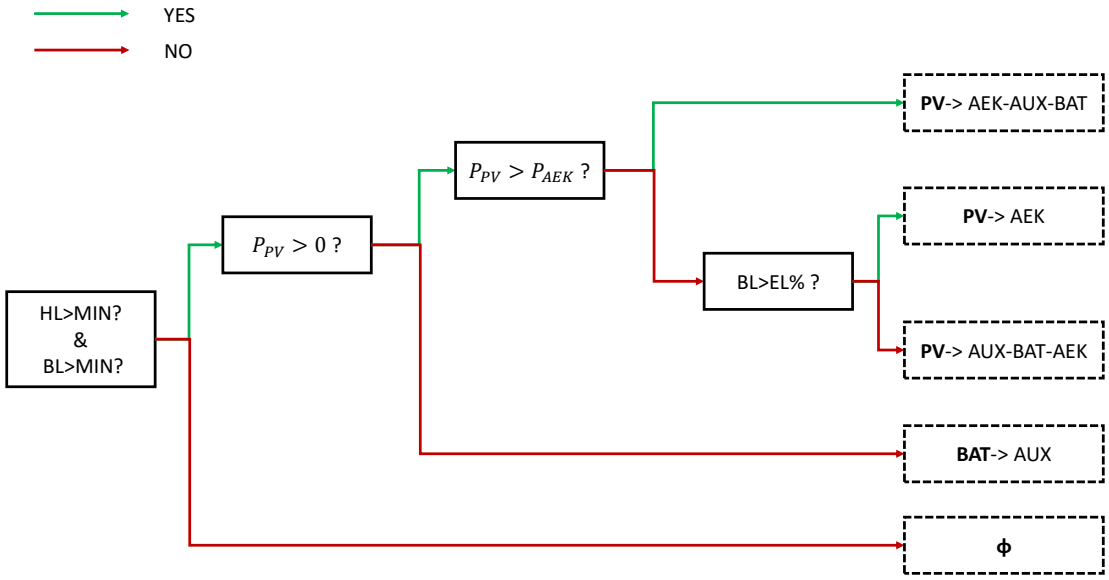

Figure 3.9 Power streams logic, FL case

3.2.4 Storages design results

In this section the results of the hourly model are reported. In particular, for each case it is reported the level in percentage of hydrogen level and the state of charge of the battery. The objective is to assess the correct capacity of both storages. In the case of the batteries, a rough estimation was yet made in the sizing on "worst day" and in this case that value can be confirmed or adjusted. The capacity found is the lower result that let the plant stand operative and never stop, so in other words it is the lower value that can avoid the shutdown.

The methodology is basically trial and error based, so the starting points were the values found in 47 and then some simulations were launched. Those values found are specific to the set of values belonging to year 2014. Anyway storages account for less than 10% of the costs, so even a variation of 20% of that value does not compromise the final result.

Since the sensibility of the analysis of the hourly model is 1 hour, for each hour it is traced the level of the storage in percentage. The total measurements for one year are 8760, so in

order to manage such high density of data it has been decided to use histograms. The first histogram in Figure 3.11 show the level of hydrogen in percentage to the maximum capacity. The same is done for the state of charge of the batteries (SOC). It is clear that for most of the time storages are full or in general over their half of capacity. This is not a good feature, because it means that the size of the storage is not needed for most of the time. This is caused by the fact that sometimes a series of bad days come over and the plant has to "survive" with the stocks of energy and hydrogen in the storages, so just for a few days the total capacity of the storages is over-sized. So the inefficient size of the storages is caused by the assumption of keeping the plant on whatever it costs.

The third graph is a focus of the levels during a series of "bad days". For a period of almost 40 hours both batteries and H_2 tanks are not supplied and they keep the plant on using the stocks. Then after the extraordinary conditions, batteries recover quickly the maximum capacity while the hydrogen recovery takes more time because its energy capacity is higher.

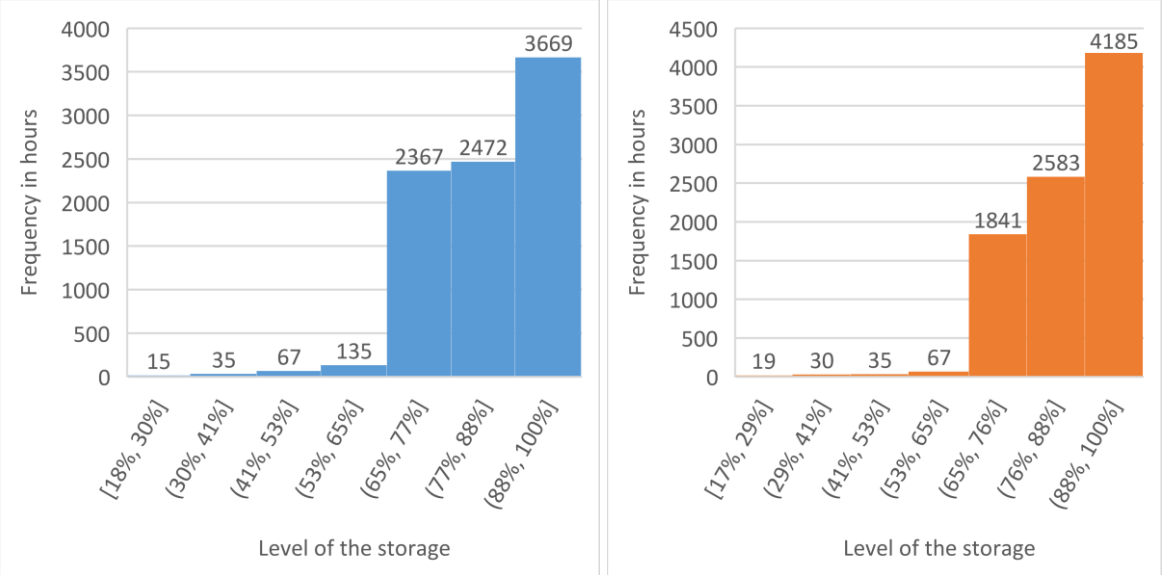

Figure 3.10 Storages level's frequencies PV-CC-BES in FL case, (hydrogen in "blue" and SOC in "orange").

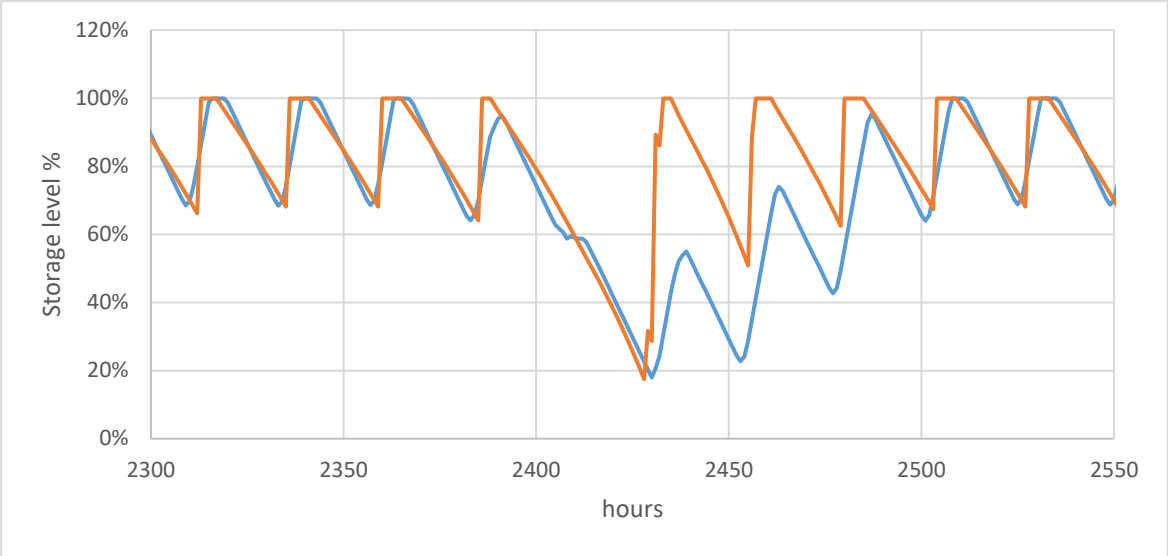

Figure 3.11 Focus of storages level in extraordinary conditions PV-CC-BES in FL case, (hydrogen in "blue" and SOC in "orange").

The same logic is applied for PV-DAC-BES supply chain. The results are almost identical with a small difference in the SOC histogram, in this case the distribution is weakly shifted towards lower SOC. The third graph in this case shows two differences. Firstly the use of electric energy is higher in percentage to the capacity respect to PV-CC-BES, in fact in 24h the SOC regularly goes at 50 %, while in the previous case it reached 70%. Then the extreme lower point in this case is deeper than the previous one. These two features are caused by the fact that in PV-DAC-BES the DAC system is the main energy consumer, and it is a component that works at steady state conditions all the time. This feature causes the total capacity of the batteries to be mainly driven to the ordinary conditions respect to extraordinary ones. In fact in PV-CC-BES case H_2 compressor is one of the most energy intensive components powered by the batteries and the more the H_2 storage empties the more the electrical power increase. This feature makes the capacity of the batteries to be oversized more. While in the PV-DAC-BES this variable part is widely reduced in proportions.

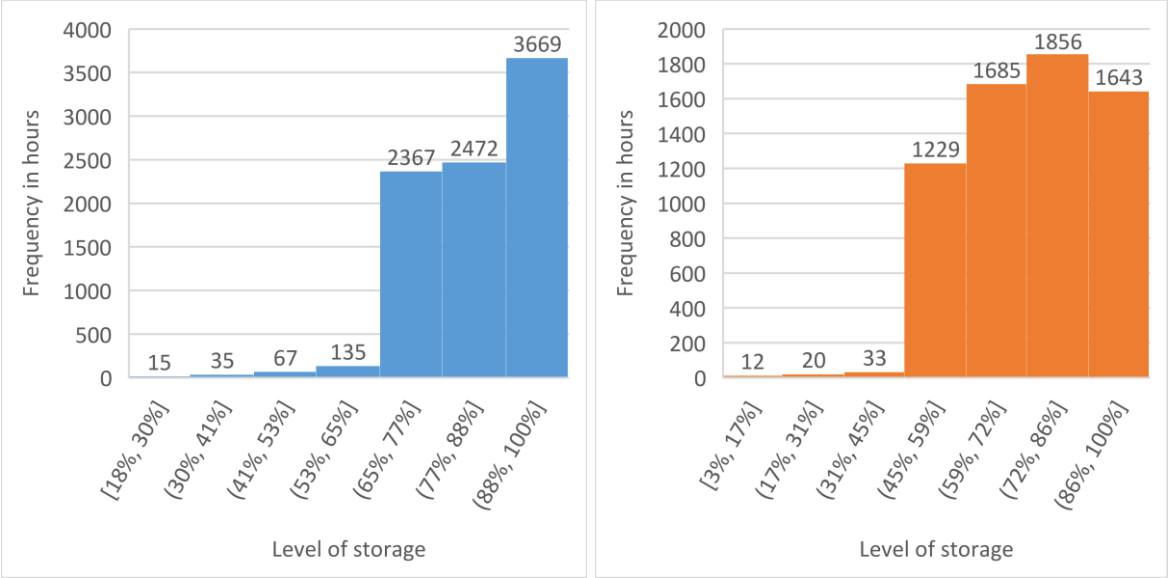

Figure 3.12 Storages level frequencies PV-DAC-BES in FL case, (hydrogen in "blue" and SOC in "orange").

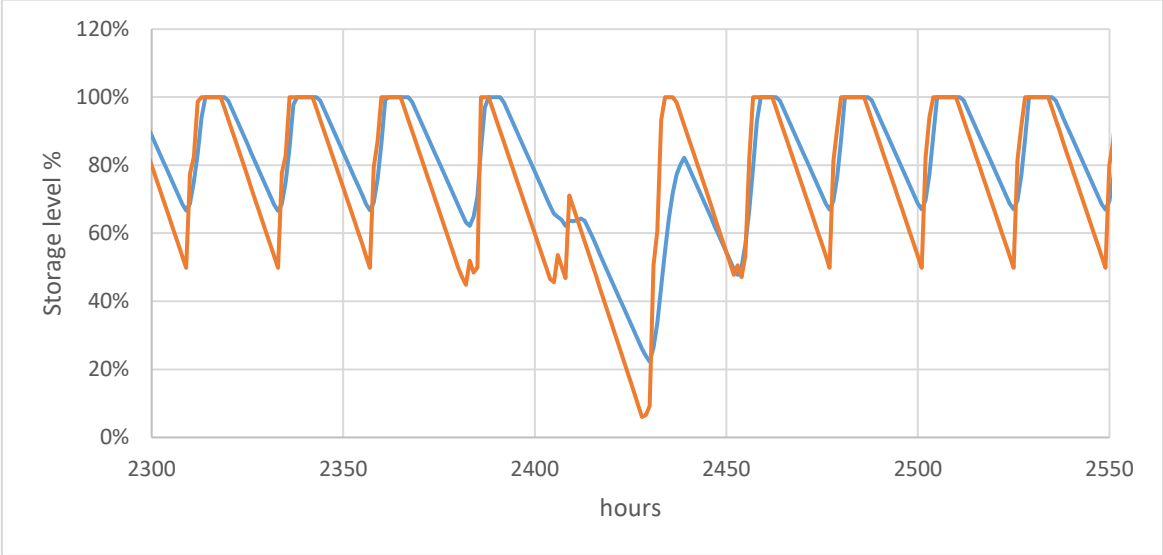

Figure 3.13 Focus of storages level in extraordinary conditions PV-DAC-BES in FL case, (hydrogen in "blue" and SOC in "orange").

Figure 3.13 represents the situation of PV-DAC-GT. In this case the only storage is the hydrogen obviously, and the behaviour is similar the other cases.

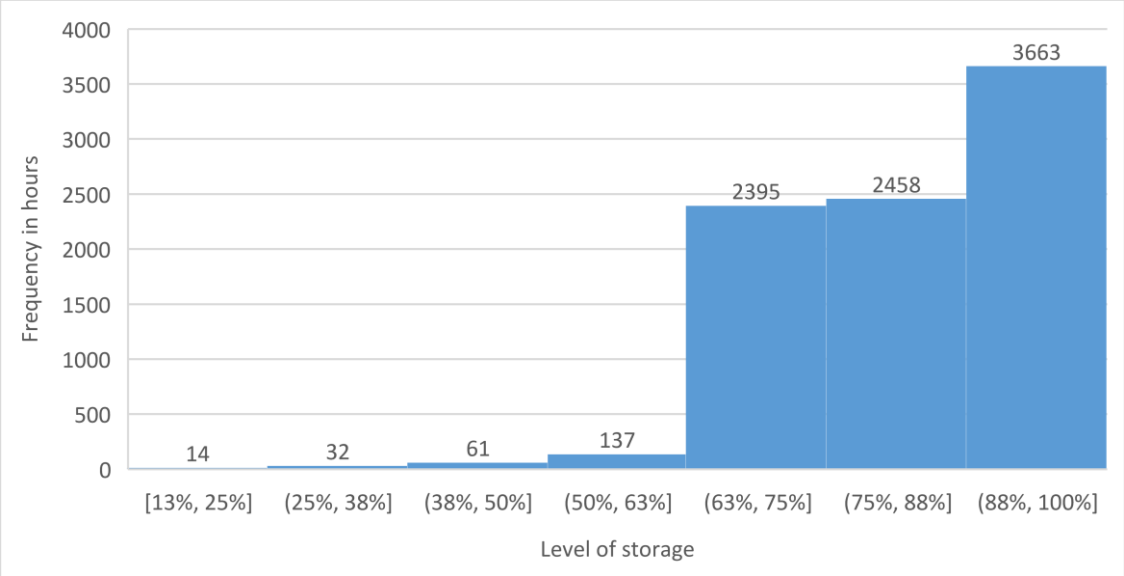

Figure 3.14 Hydrogen storage level frequency in PV-DAC-GT in FL case

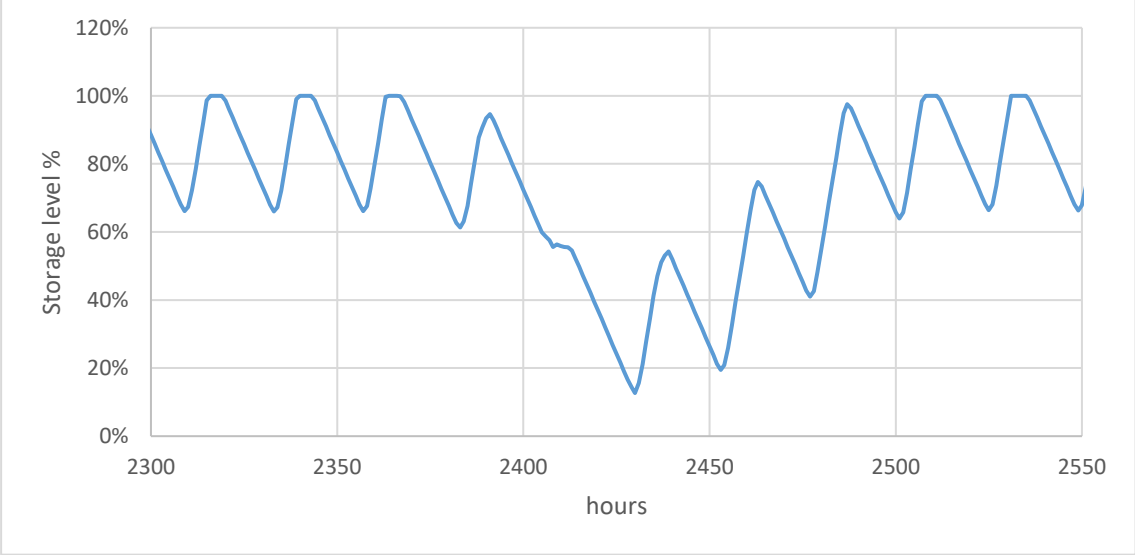

Figure 3.15 Focus of hydrogen storages level in extraordinary conditions PV-DAC-GT in FL case.

In the table Table 3.5 are reported the final capacities of the two storages as well as the maximum C_{rate} observed during the operations. Those values of C_{rate} are widely into a range of good operating conditions of batteries.

Table 3.5 Storages sizing after hourly model evaluation in FL case

	H_2 storage [MWh]	*Batteries [MWh]*	*Max C_{rate}*
PV-CC-BES	*5421*	*173*	*67%*
PV-DAC-BES	*5062*	*1000*	*50%*
PV-DAC-GT	*5421*	-	-

In addiction the hourly model provides the final level of hydrogen storage. This number is useful in order to take into account the difference compared to the initial situation. In all cases, storages starts 50 % full, but the final level depends on the specific case.

Table 3.6 Residual hydrogen at the end of the year, FL case

	Final level [%]	*Capacity [MWh]*	*Δ (final – initial) [MWh]*	*SNG [MWh]*
PV-CC-BES	*79 %*	*5421*	*1572*	*1226*
PV-DAC-BES	*77 %*	*5062*	*1367*	*1066*
PV-DAC-GT	*77 %*	*5421*	*1464*	*1142*

In Table 3.6 it is calculated the total amount of hydrogen left in the reservoir at the last hour of the year, this value is converted in syngas multiplying it for the methanator efficiency (78%). This value will be added in the yearly production before applying the availability. This value will appear as ΔE.

3.3 Economics

This section will focus on the economics of each supply chain. The final objective is to calculate the LCOM (Levelized cost of Methane).

Total CAPEX for each supply chain is reported in Figure 3.14. In these numbers are reported both cost of equipment and cost of installation.

PV-CC-BES is the cheapest in terms of CAPEX as there is no cost for CO_2 capture, in fact the cost for carbon dioxide purchase goes in the OPEX.

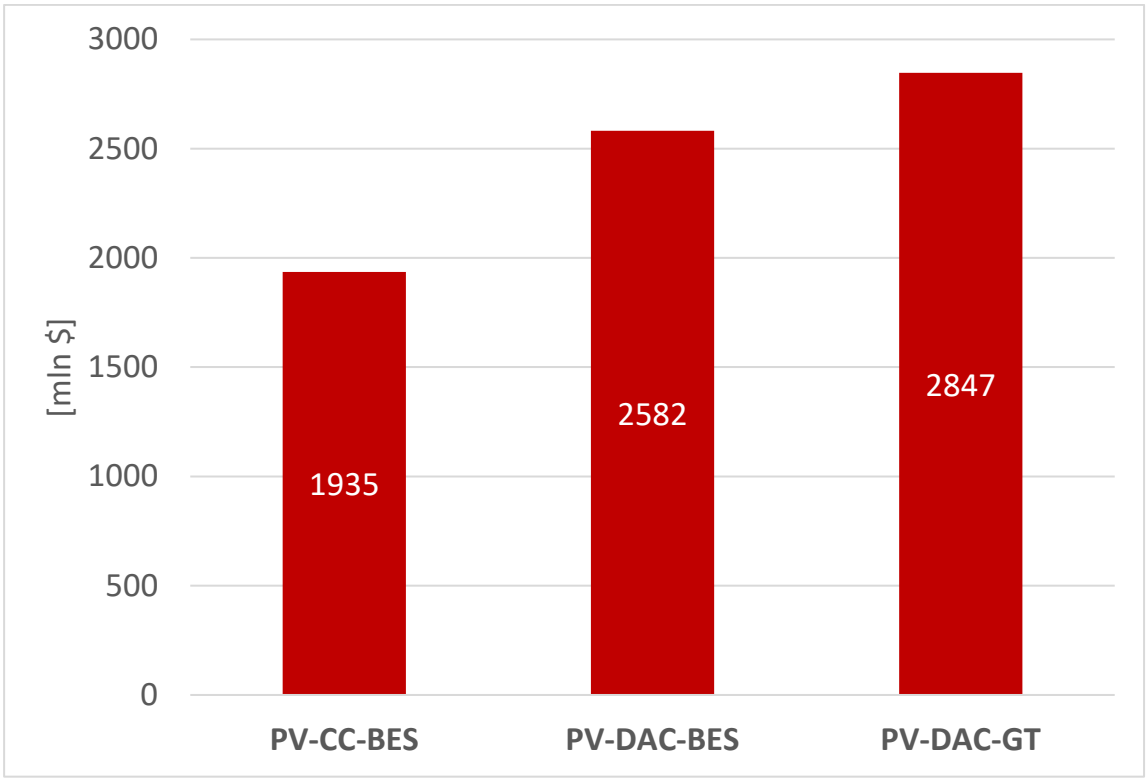

Figure 3.16 Total CAPEX for FL case

The annual cost in Eq. 12 is calculated with the annual CAPEX and the OPEX. Figure 3.15 represents the share of the $CAPEX_a$ and OPEX in the calculation of the Annual cost. It is clear that the OPEX represents a small part compared to the investment costs. PV-DAC-BES has the highest share of OPEX mainly driven by the maintenance costs of batteries.

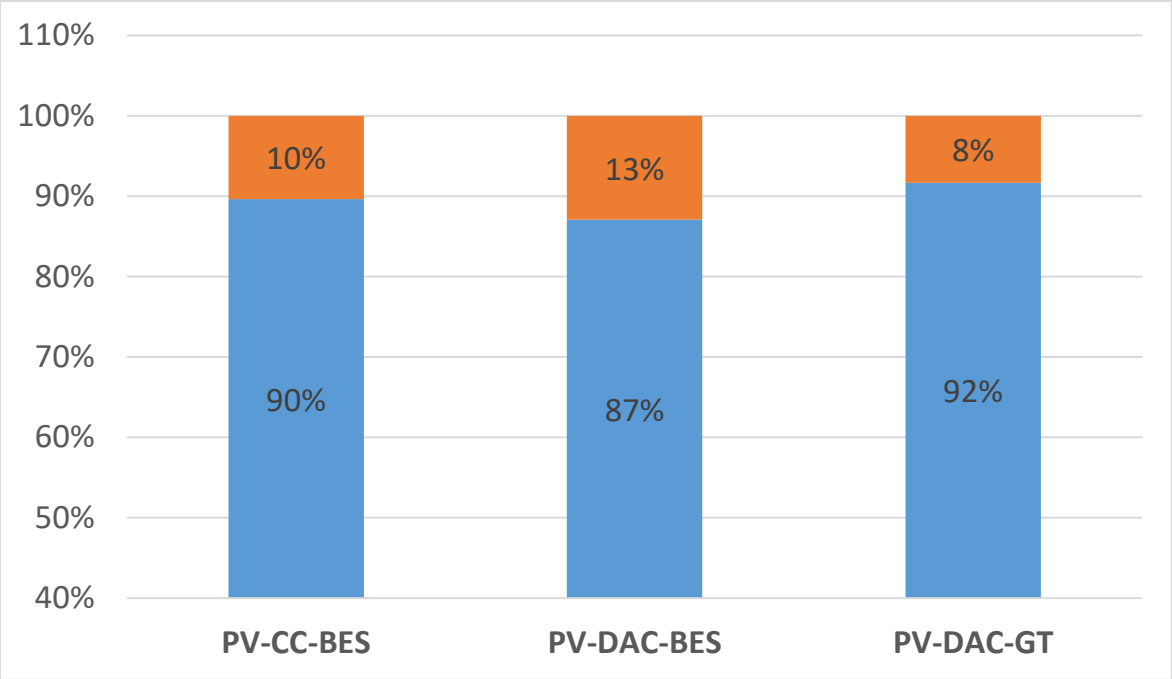

Figure 3.17 Share of Annual costs of CAPEX (blue) and OPEX (orange).

In the following graphs it has been evaluated the share of the annual cost for each supply chain. In the annual cost it included the total CAPEX of equipment, annualized using the CRF, and the OPEX. Costs of installation are not included in this analysis, because they are highly volatile parameters, and the results would be depending to much on uncertainties.

PV-CC-BES

The first voice in the investment costs is the cost of the photovoltaic field, it accounts for half of the costs. The second item is by far the cost of the electrolyzer. The first two items account for 87%. Other components have a marginal impact on the total cost.

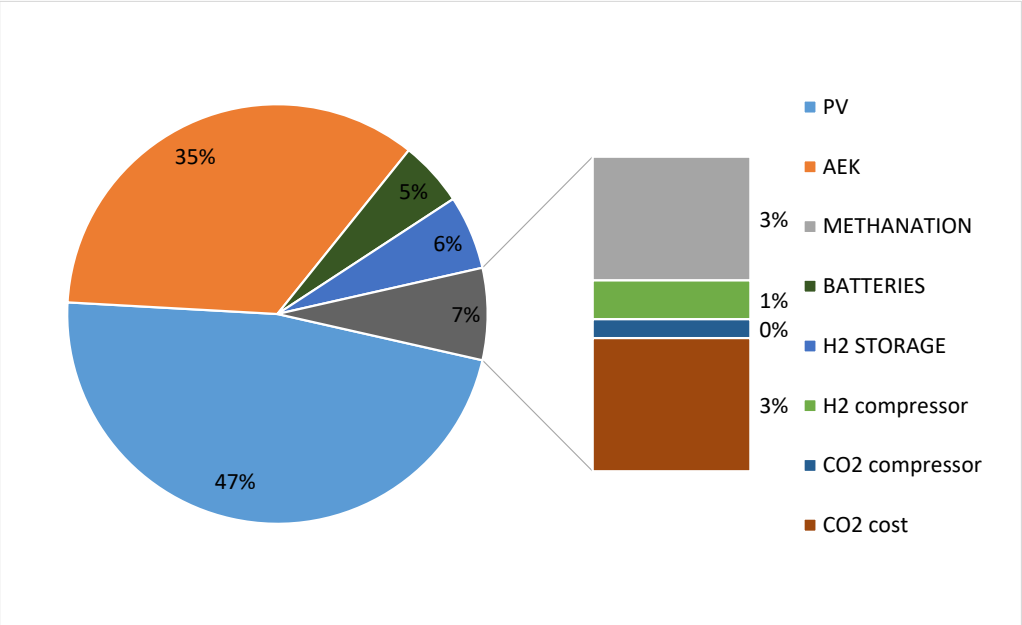

Figure 3.18 Shares of the CAPEX for PV-CC-BES in FL case

PV-CC-BES

In Figure 3.19 the first two voices are still PV and AEK, but the second leave some room for the cost of batteries that now is a significant part of the investment, 17% of total. It is not surprising as the total capacity of batteries is much larger than the PV-CC-BES case. In this case DAC system appear instead of the "CO_2 cost", and its contribution is larger. Even in this case the contribution of other components is marginal.

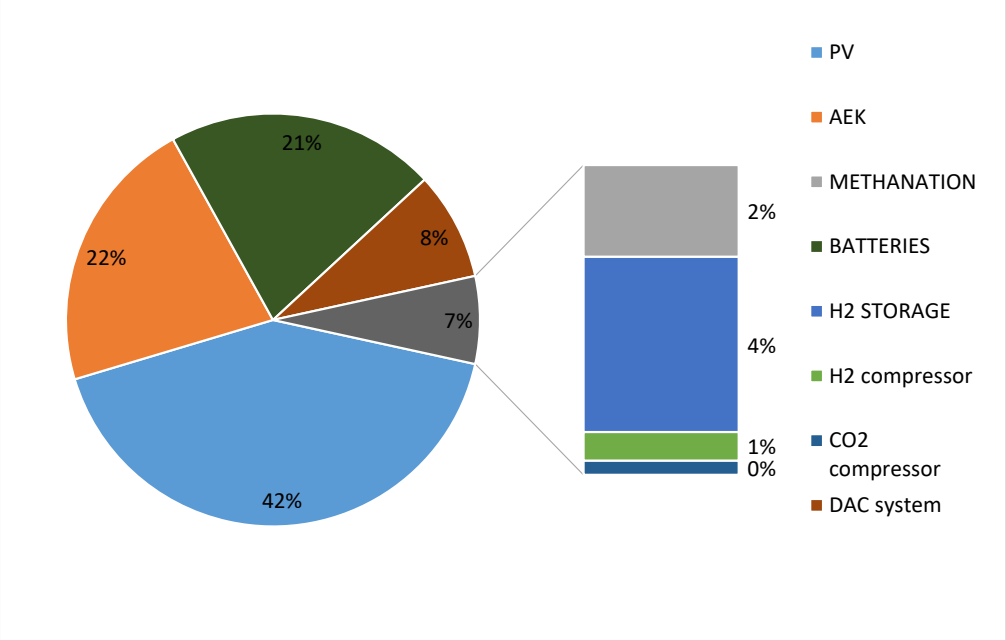

Figure 3.19 Shares of the CAPEX for PV-DAC-BES in FL case

PV-DAC-GT

The shares in Figure 3.20 is similar with Figure 3.16, but the total value is higher. It is important to notice that the cost of the heat exchanger for heat recovery does not appear in the pie, this is because the contribution is negligible.

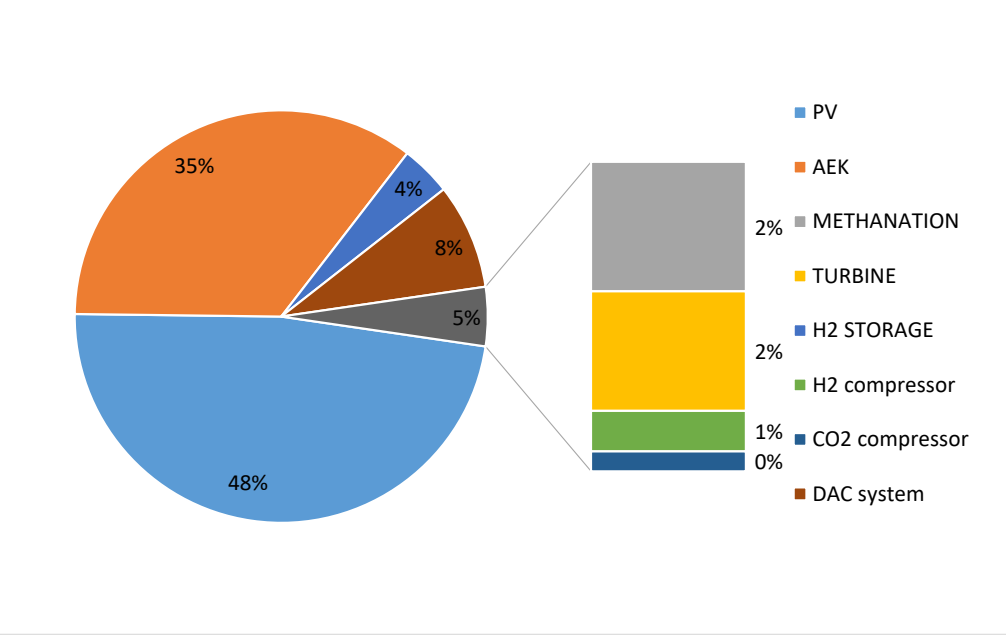

Figure 3.20 Shares of the CAPEX for PV-DAC-GT in FL case

LCOM Evaluation

Combining the Annual cost, and the yearly production it can be calculated the levelized cost of methane. In this case since the plant is designed to work always at full load the amount of syngas produced can be easily calculated with Eq. 19.

$$E_y \left[\frac{MWh}{y}\right] = \left(100[MW] \cdot 8760 \left[\frac{h}{y}\right] + \Delta E\right) \cdot Availability \qquad \textit{Eq. 19}$$

Availability is 95% as mentioned before.

Finally the LCOM is calculated using the annual cost that takes into account both CAPEX (equipment and installation costs) and OPEX. Since the production is considered constant for all years there is no need to make this calculation specifically on each year.

$$\text{LCOM} \left[\frac{\$}{MWh}\right] = \frac{\text{Annual cost} \left[\frac{\$}{y}\right]}{E_y \left[\frac{MWh}{y}\right]} \qquad \textit{Eq. 20}$$

In Table 3.7 are reported the LCOM for each supply chain. The most economical is by far the PV-CC-BES and takes advantage of the small battery capacity and the fact that purchasing carbon dioxide is cheaper than collecting it from the air.

Table 3.7 LCOM FL case

	Annual cost [mln $]	E_y [MWh]	LCOM [$/MWh]
PV-CC-BES	220	833365	267
PV-DAC-BES	302	833213	362
PV-DAC-GT	316	833285	379

Chapter 4 FLR case: additional heat recovery of methanator waste heat

In this chapter it is assessed the possibility to introduce a component that exploit the waste heat of the methanator. The methanator in this model has an efficiency of 78%, which means that the remaining 22% of energy is taken away by the cooling circuit. The heat is removed by means of a series of heat exchanger as can be seen in Figure 2.4. Powers and temperatures of each heat exchanger are reported in Table 4.1. HX_3 is not reported in this table because it is used to preheat the feed, so there is not available heat for recovery. These heat exchangers operate at very different temperature, for instance HX_2 and HX_1 work at higher temperature compared to HX_4 and cooler. Such high temperatures are very good for heat recovery as they open the possibility to use waste heat to produce electric energy by means of an ORC system. ORC system can be used to exploit either low or high temperature waste heat, but high temperatures ensure a higher electrical efficiency. Looking at the thermal powers, the sum of HX_1 and HX_2 represents 65 % of the total heat available for recovery, so the "hot" energy is even more abundant respect to the "cold" energy available. Heat could also be used to cover part of the thermal need of the DAC system, which is one the most important energy consumer in the plant with exception for the electrolyzer.

Table 4.1 Available heat for recovery for the methanator [2]

SIZE 2,65 [MW]	HEAT [KW]	T [C°]	T [C°]
HX4	192.0	135	192
HX1	360.5	255	665
HX2	126.0	195	511
Cooler	66.0	135	45
TOT for recovery	**744.5**		

Table 4.2 Available heat for recovery for the methanator scaled to 100 MW

SIZE 100 [MW]	HEAT [KW]	T [C°]	T [C°]
HX4	7245	135	192
HX1	13603	255	665
HX2	4754	195	511
Cooler	2490	135	45
TOT for recovery	**28094**		

Table 4.2 is obtained with the assumption that temperatures remain the same and the proportions of heat available for each circuit are the same. Then each power is multiplied by a factor of 100 divided by 2.65 getting to Table 4.2.

The available heat of the methanator will be used for the PC-CC-BES to power an ORC system entirely dedicated to electric production. Only HX_1 and HX_2 will be exploited by the ORC because of their higher operating temperatures, other heat exchangers will operate as usual. This integration aims to decrease the total capacity of the batteries, because part of the electric demand of BOP's will be covered by the ORC. For the PV-DAC-BES and PV-DAC-GT waste heat from the methanator will be used to feed the DAC system, in this case even HX_4 will be included because the low regeneration temperature of the solid sorbent make it possible. The idea is that in the supply chains using DAC, electric and thermal energy has the same value, because in the PV-DAC-BES case heat is obtained dissipating electric energy stored in batteries and in PV-DAC-GT hydrogen is burned in the turbine. So the goal in that case is to recover as much as possible energy, no metter if it is thermal or electrical energy, and recovering heat is more energy-efficient than producing electrical energy.

4.1 Sizing

All the components of the plant that have been previously described are sized at the same way. So this section will focus the sizing of the ORC systems as well as the HX.

4.1.1 PV-CC-BES

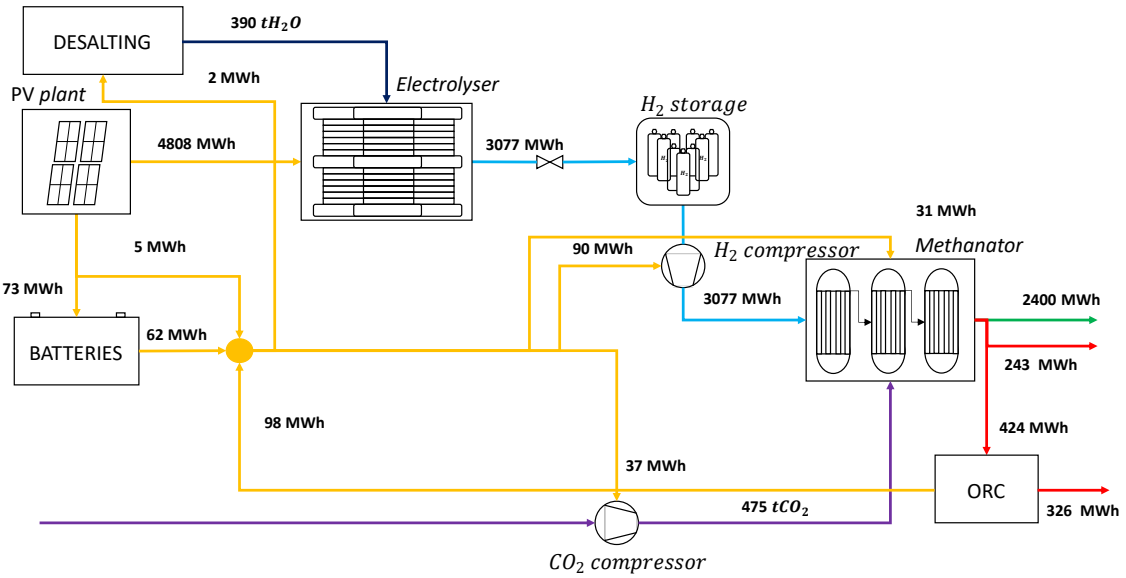

Figure 4.1 Process flow diagram on daily basis for PV-CC-BES (FLR)

For the ORC sizing, a sheet from Turboden is used as model. Table 4.3 reports the characteristics of an ORC of similar size to what is required for this study. From this table only the efficiency and the temperature of the oil circuit will be used because the size is not exactly fitting.

Table 4.3Typical performance characteristics of Turboden high efficiency units (HRS), model TD24HRS

Input - Thermal Oil		
Nominal Temperature (In/Out)	**C°**	**300 / 211**
Thermal Power	kW	9634
Output - Cooling Water		
Cooling Water Temperature (In/Out)	C°	81 / 99
Thermal Power	kW	7143
Performance		
Gross Electric Power	kW	2342
Gross Electric Efficiency	%	24.3
Net electric efficiency	**%**	**23.0**

Table 4.4Assumptions and parameters for the ORC integration

Assumptions		
$\Delta T_{o\text{-}gas}$ min	30	C°
C_{oil}	1.841	kJ/kg
Calculated		
$\dot{m}_{oil}$	107.8	kg/s

Table 4.2 shows the integration of the ORC with the model of the methanator, which in this study is a three reactors kind. In this integration only the HX_1 and HX_2 are exploited by the ORC because of their higher temperature. In particular, HX_1 is fully exploited while only a part of the heat available by HX_2 can be used because of the lower minimum temperature and the $\Delta T_{o\text{-}gas}$ min.

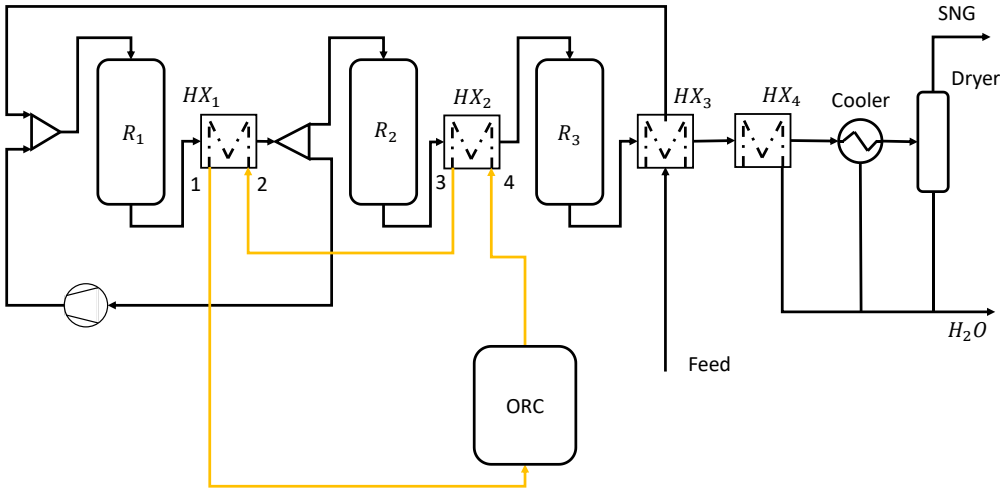

Figure 4.2 Layout of methanator with integration of ORC

With the assumptions and parameters in Table 4.4 are calculated both temperature and heat exchanged at each HX, also the the effectiveness calculated with the NTU (Number of Transfer Units) method.

Table 4.5 Data for the T-Q diagram of the PV-CC-BES, FLR case

HX2	OIL			METH GAS HX_2		
	T_{o4}	211	C°	T_{g3}	511	C°
	T_{o3}	231	C°	T_{g4}	241	C°
				Q	4063	kW
				η_{HX}	90%	
HX1	OIL			METH GAS HX_1		
	T_{o2}	231	C°	T_{g1}	665	C°
	T_{o1}	300	C°	T_{g2}	255	C°
				Q	13604	kW
				η_{HX}	95%	

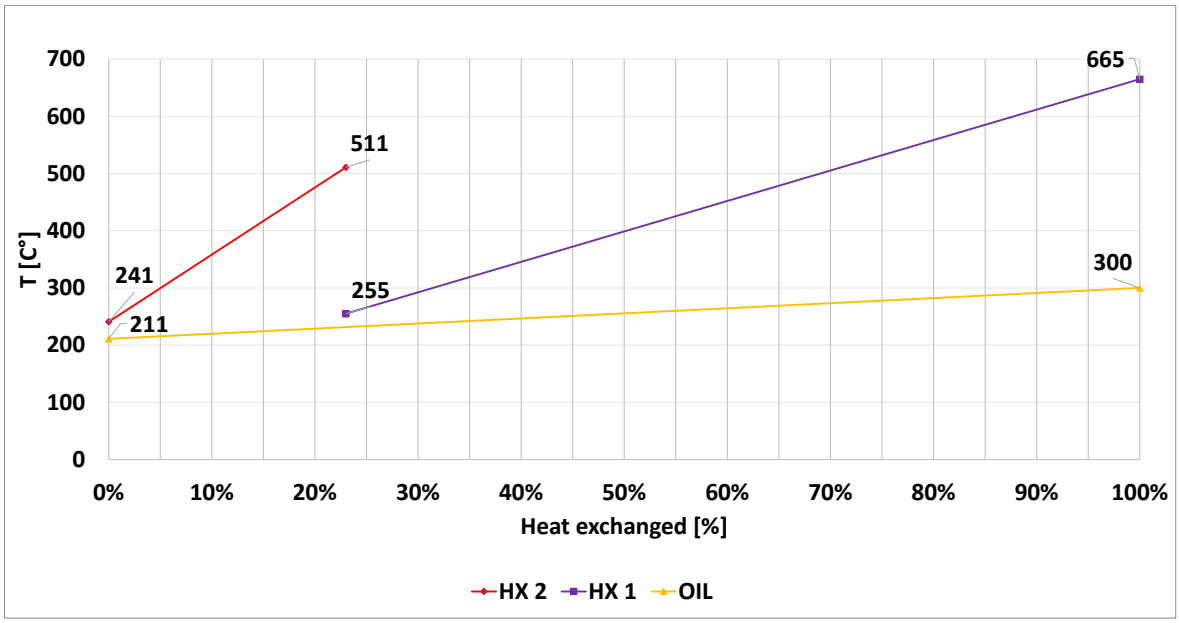

Figure 4.3 T-Q diagram of PV-CC-BES supply chain with integration of ORC, FLR case

Finally the result is that 4.063 MW of electric energy are delivered from the ORC to the electric appliances of the plant.

Table 4.6 Resume table of ORC integration, FLR case

Resume table ORC side	
Q_{in}	17.67 MW
P_e	4.06 MW
Q_{out}	13.60 MW

4.1.2 PV-DAC-BES

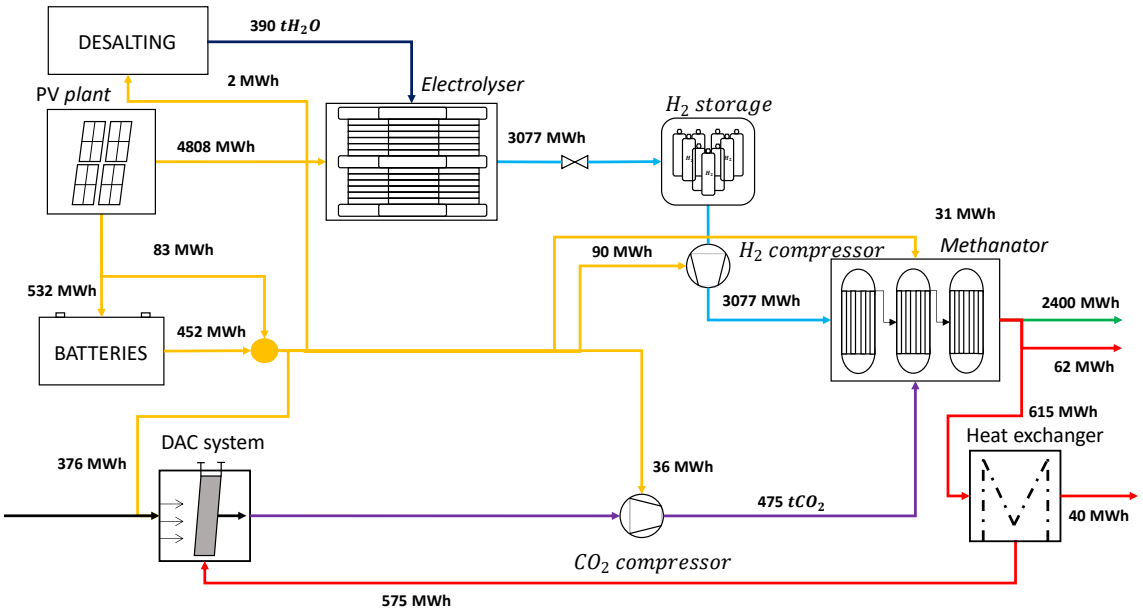

Figure 4.4 Process flow diagram on daily basis for PV-DAC-BES (FLR)

For the next two supply chains as it was mentioned, the heat available will be used to feed the DAC. Solid sorbent technology needs a temperature in the range between 70 C° - 100 C° for the sorbent regeneration. For this reason it has been assumed for this evaluation an inlet temperature in the DAC of 120 C° and an exit temperature of 70 C°, in this way the heat in the water circuit will be fully used for the regeneration.

In this case HX_1, HX_2, HX_4 can be fully dedicated for heat recovery. The lower quality of the heat demand of the DAC allows for an extremely efficient heat recovery, higher than the ORC case in the PV-CC-BES case.

Table 4.7 Assumptions and parameters for PV-DAC-BES with integration of HX

Assumptions		
$\Delta T_{w\text{-}o}$ min	25	C°
$\Delta T_{o\text{-}gas}$ min	30	C°
$\dot{m}_{oil}$	150	kg/s
T_9 water	70	C°
T_8 water	120	C°
C_{oil}	1.841	kJ/kg
C_w	4.18	kJ/kg
Calculated		
$\dot{m}_{water}$	165.8	kg/s

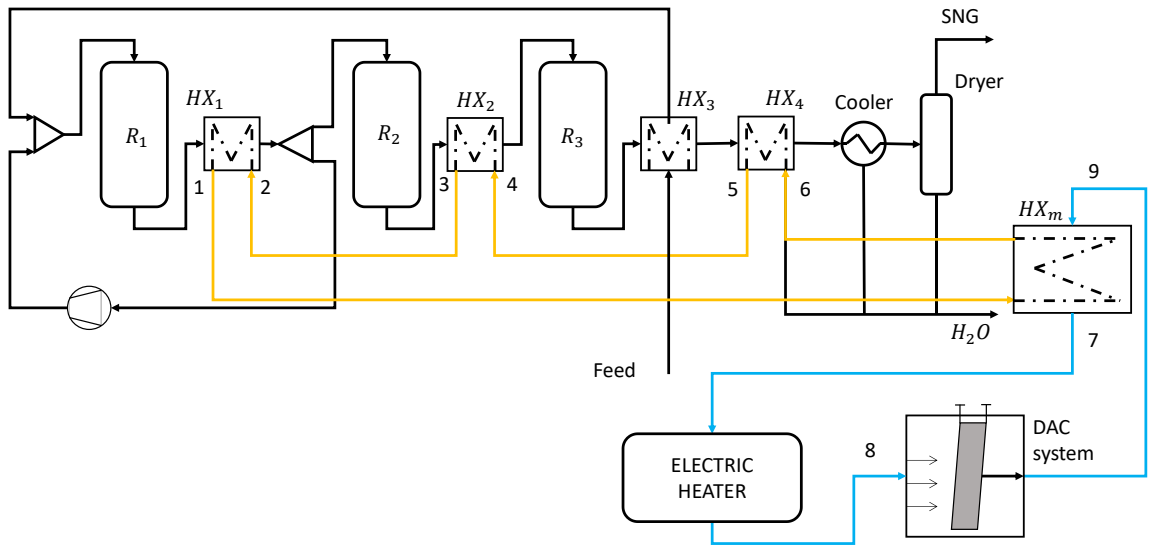

Figure 4.5 Layout of PV-DAC-BES with integration of HX with focus on the methanator

Table 4.8 Calculations for the T-Q diagram of the PV-DAC-BES with integration of HX

HX4	OIL			METH GAS HX_4		
	T_{o6}	75	C°	T_{g5}	192	C°
	T_{o5}	101	C°	T_{g6}	135	C°
				Q	7245	kW
				η_{HX}	59%	
HX2	OIL			METH GAS HX_2		
	T_{o4}	101	C°	T_{g3}	511	C°
	T_{o3}	118	C°	T_{g4}	195	C°
				Q	4755	kW
				η_{HX}	81%	
HX1	OIL			METH GAS HX_1		
	T_{o2}	118	C°	T_{g1}	665	C°
	T_{o1}	168	C°	T_{g2}	255	C°
				Q	13604	kW
				η_{HX}	78%	

HXm	OIL			WATER		
	To4	168	C°	T1	70	C°
	To1	75	C°	T2	107	C°
	Q	25604	kW			
	η_{HX}	79%				

As Table 4.8 shows, the average effectiveness of the heat exchanger is lower than the PV-CC-BES case, so the design of the heat exchanger is less critical and more feasible. The final part of the heating is not present in Table 4.8 as there is not a specific temperature of the heat coming from the electric resistances.

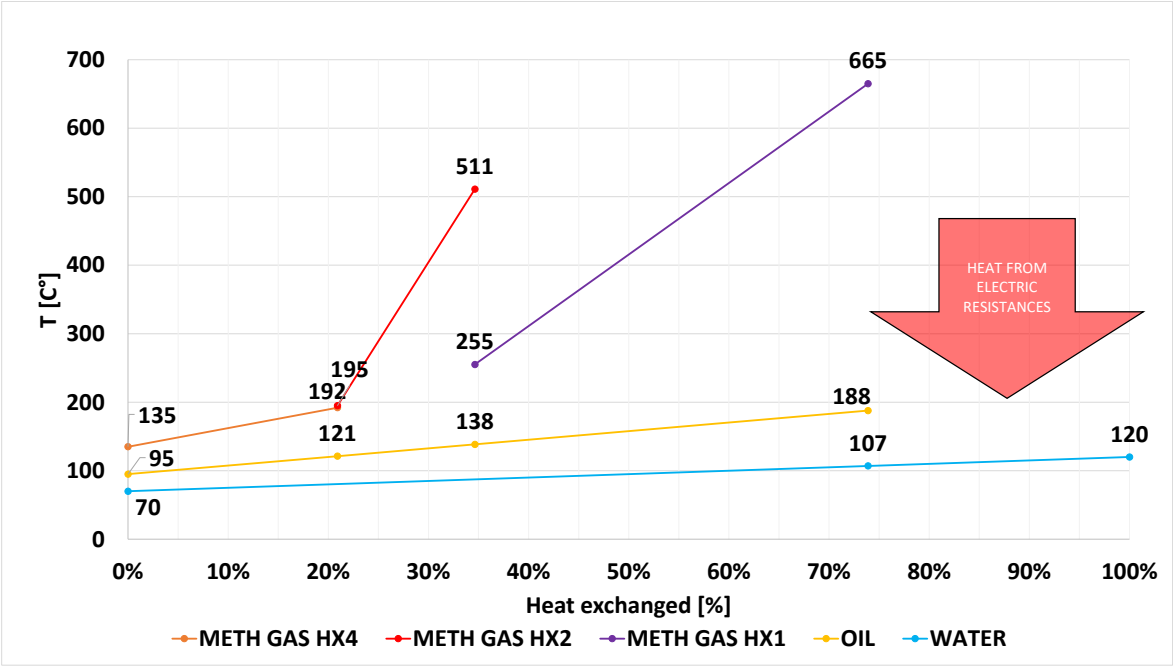

Figure 4.6 T-Q diagram for PV-DAC-BES case with integration of HX

In order to take into account possible thermal losses along the circuits the final heat going to DAC is 93,3% of the total heat transferred in the HX_m.

Table 4.9 Resume table for PV-DAC-BES with integration of HX

Resume table HX_m side	
Q_{in}	25.60 MW
$Q_{to\ DAC}$	23.81 MW
Q_{loss}	1.79 MW

4.1.3 PV-DAC-GT

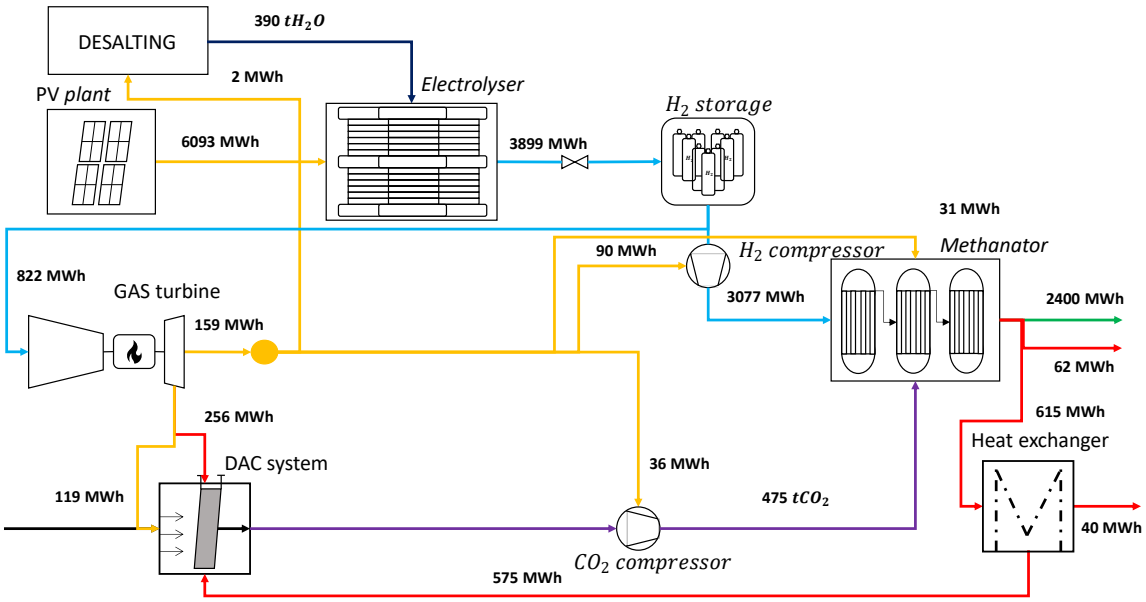

Figure 4.7 Process flow diagram on daily basis for PV-DAC-GT (FLR)

This final case is identical with the PV-DAC-BES case with the only exception that the final part of the water heating is carried out with the heat recovery in the gas turbine instead of using electric resistances.

Instead with respect to PV-DAC-GT, FL case, now with the introduction of HX_m, the amount of heat required from the turbine is lower. Since that, the rate between the electric power produced and the useful heat from the exhaust increase. To take advantage of that the efficiency of turbine could be increased. In fact in the case of integration with HX the nominal net electric efficiency of the turbine passes from 20% (previous case) to 34%. In addiction the size of the turbine is expected to decrease compared to the FL case.

Table 4.10 Assumptions for HX evaluation and sizing in PV-DAC-GT

Assumptions		
$\Delta T_{w\text{-}o}$ min	25	C°
$\Delta T_{o\text{-}gas}$ min	30	C°
$\dot{m}_{oil}$	150	kg/s
T_9 water	70	C°
T_8 water	120	C°
T_i exhaust	500	C°
C_{oil}	1.841	kJ/kg
C_w	4.18	kJ/kg
Calculated		
$\dot{m}_{water}$	165.8	kg/s

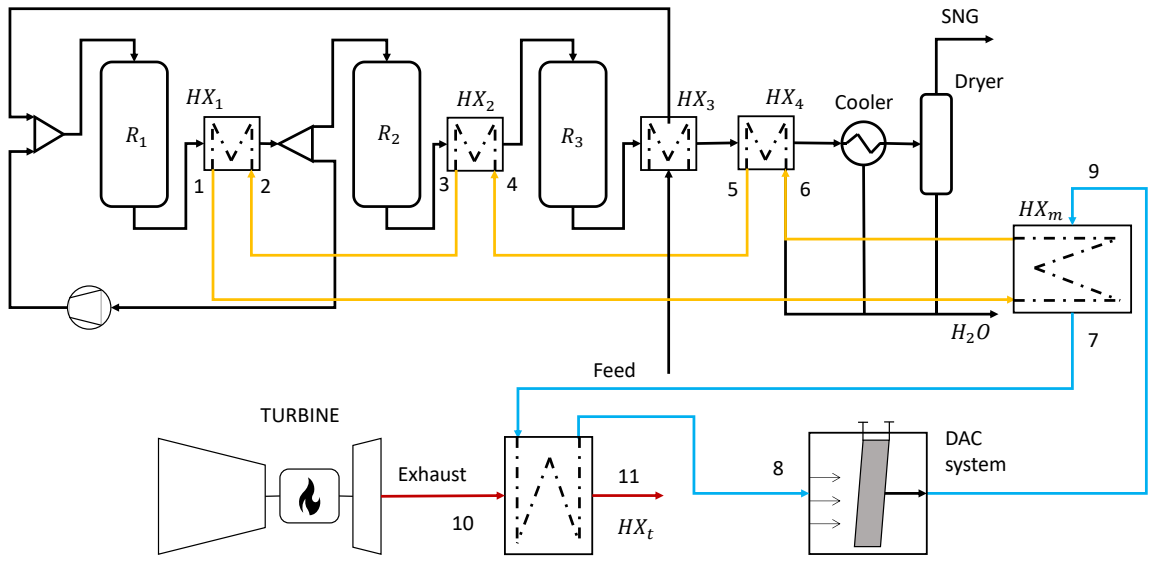

Figure 4.8 Layout of PV-DAC-GT after HX integration with focus on the methanator

The T-Q diagram is identical of the one in PV-DAC-BES, with the only difference that in this case the final heating comes from the exhaust of the turbine.

Table 4.11 Calculations for the T-Q diagram of PV-DAC-GT case after integration of HX

HX4

OIL			METH GAS HX_4		
T_{O6}	75	C°	T_{g5}	192	C°
T_{O5}	101	C°	T_{g6}	135	C°
			Q	7245	kW
			η_{HX}	59%	

HX2

OIL			METH GAS HX_2		
T_{O4}	101	C°	T_{g3}	511	C°
T_{O3}	118	C°	T_{g4}	195	C°
			Q	4755	kW
			η_{HX}	81%	

HX1

OIL			METH GAS HX_1		
T_{O2}	118	C°	T_{g1}	665	C°
T_{O1}	168	C°	T_{g2}	255	C°
			Q	13604	kW
			η_{HX}	78%	

HX_m

OIL			WATER		
T_{O6}	168	C°	T_{w9}	70	C°
T_{O1}	75	C°	T_{w7}	107	C°
Q	25604	kW			
η_{HX}	79%				

HX_t

EXHAUST			WATER		
T1	500	C°	T_{w7}	107	C°
T2	308	C°	T_{w8}	120	C°
$Q_{available}$	22619	kW	$Q_{exchanged}$	9046	kW
η_{HX}	49%				

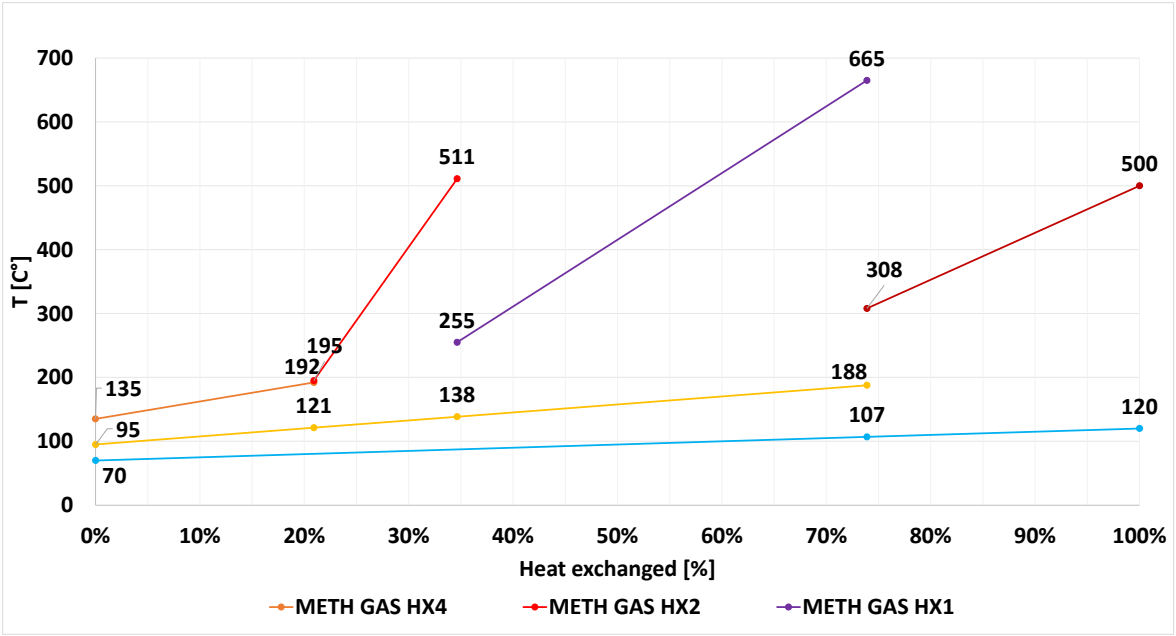

Figure 4.9 T-Q diagram for PV-DAC-GT case after integration of HX

Even in this case it has been assumed a loss of heat of 93.3%.

Table 4.12 Resume table of HX_m in PV-DAC-GT

Resume table HX_m side	
Q_{in}	25.60 MW
$Q_{to\ DAC}$	23.81 MW
Q_{loss}	1.79 MW

The size of the heat exchanger HX_m is calculated in the same way of the design of the heat exchanger of the turbine in PV-DAC-GT, the only difference is in the global heat transfer coefficient (U). Since in this case the fluids involved are diathermic oil and water, and oil is way much denser than gas, the heat transfer coefficient is expected to be higher. In this case U is assumed to be 300 [W/m^2K]. Using Eq. 17 it can be calculated the surface of both HX_m and HX_t with values reported in Table 4.13.

Table 4.13 Sizing values for HX's sizing

HX_m	Value	Unit of measure
U	300	$W/(m^2K)$

ΔT_1	118	C°
ΔT_2	-12	C°
ΔT_{ml}	27	C°
Q	23.97	MW
A	2992	m^2
HX_t	Value	Unit of measure
U	70	$W/(m^2K)$
ΔT_1	415	C°
ΔT_2	164	C°
ΔT_{ml}	45	C°
Q	10.67	MW
A	3359	m^2

Finally the sizing procedure is the same of the previous chapter. Looking at Table 4.14 the only rate that change compared to the FL case is in PV-DAC-BES. It passes from 0.35 to 0.45, and the justification for this increase lies on the decrease of the batteries capacity required, in fact the introduction of the heat exchanger lowers the amount of energy required to power the DAC, so more energy is available to feed the AEK. Also the introduction of heat exchanger causes a reduction of 7.5% of the size of the PV plant, while an increase of 5% of the size of AEK.

In PV-CC-BES $R_{AEK/PV}$ doesn't change as well as the size of PV and AEK, the use of the ORC only causes a reduction of the batteries capacity. Probably the fact that $R_{AEK/PV}$ doesn't change is due to the low sensibility of this analysis, in fact if the change is lower than 0.05 the model does not feel any difference.

Indeed in PV-DAC-GT the rate doesn't change, but there is a reduction in the size of both PV and AEK. The reduction in absolute terms is 13% of the FL case.

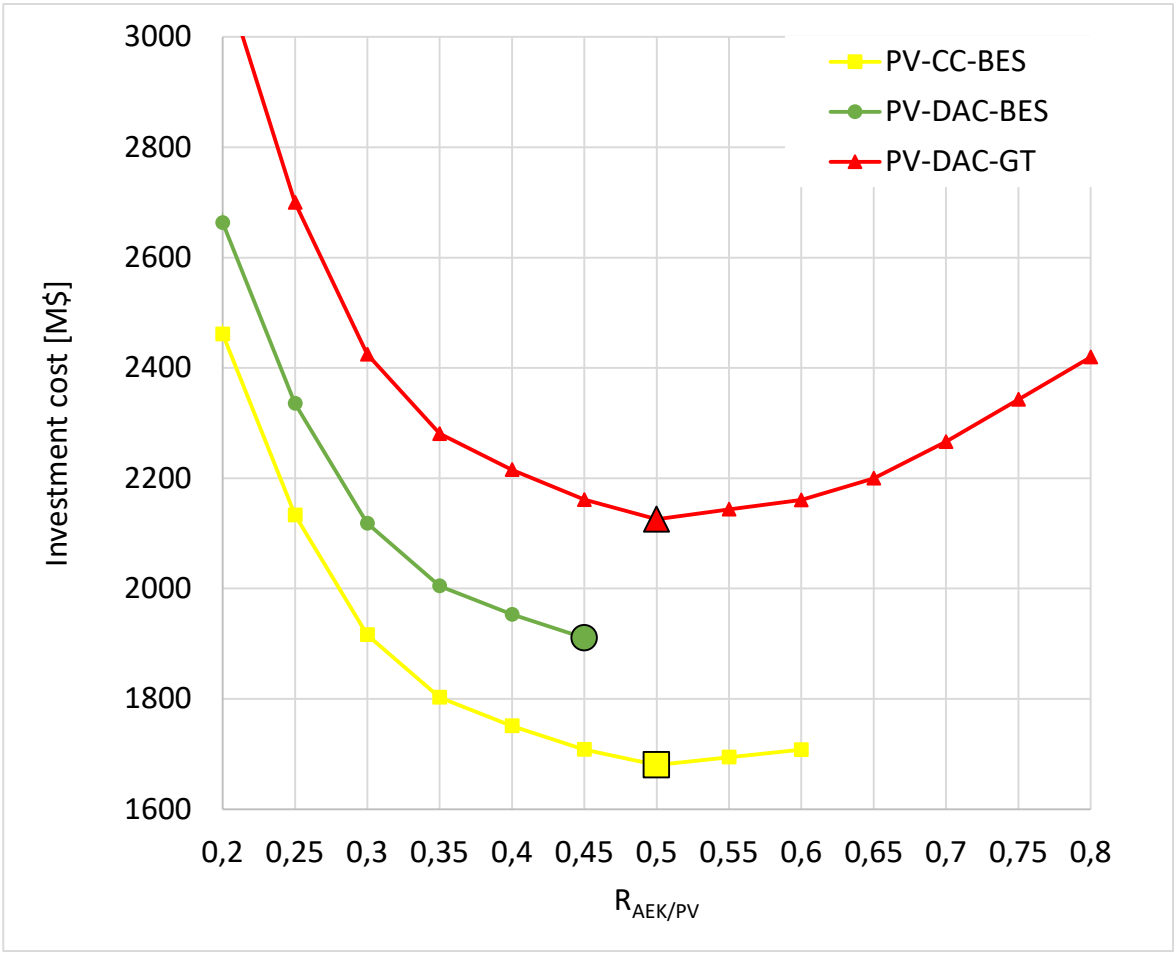

Figure 4.10 Sensitivity analysis of the investment cost function of $R_{AEK/PV}$ considering cost of PV, electrolyzer and batteries in FLR case.

Table 4.14 Sizing resume table in FLR case

			PV-CC-BAT	PV-DAC-BAT	PV-DAC-HX
PV	**[MW]**		1458	1543	1848
AEK	**[MW]**		729	694	924
METHANATION	**[MW]**		100	100	100
TURBINE or ORC	**[MW]**		4	-	34
HX_m	**[m^2]**		-	2992	2992
HX_t	**[m^2]**		-	-	6351
BATTERIES	**[MWh]**		68	488	-
H_2 compressor	**[MW]**		3.754	3.754	3.754
CO_2 compressor	**[MW]**		1.567	1.567	1.567
DAC system	**[tCO_2/y]**		-	173448	173448

4.1.4 Storages design logic and sizing

The logic that manages power streams is the same as the FL case. Nothing has changed respect to the FL case analysed earlier.

In the following graph are shown the frequencies of the level in percentage of storages.

In PV-CC-BES appears an important difference in comparison with the FL case. In this case the histogram of SOC is highly shifted on the right, meaning that most of the time batteries are full charged. After the introduction of the ORC the batteries capacity passed from 173 MWh to 6.8 MWh, so the role of the batteries appears to change. In the FL case they charge and discharge each day playing a role in ordinary conditions. Now batteries behave like a backup system that comes into operation only when the power consumption increase a lot. In particular this occur when the H_2 level is low, and the hydrogen compressor absorbs more power to cover the higher pressure gap. In

Figure 4.11 , in the third diagram it is visible this behaviour.

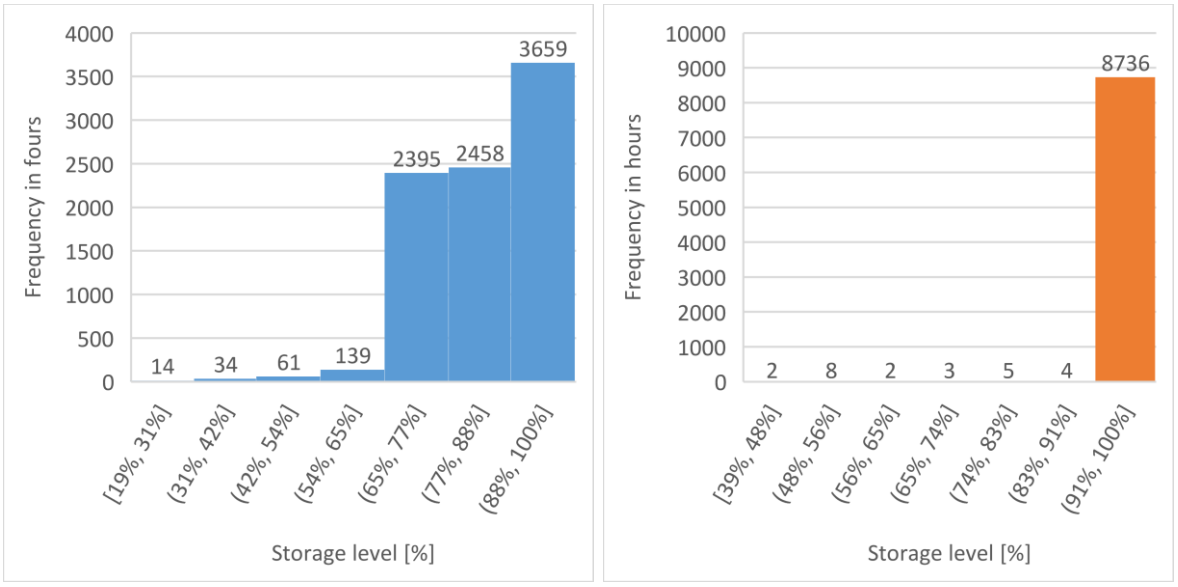

Figure 4.11 Storages level's frequencies PV-CC-BES in FLR case, (hydrogen in "blue" and SOC in "orange").

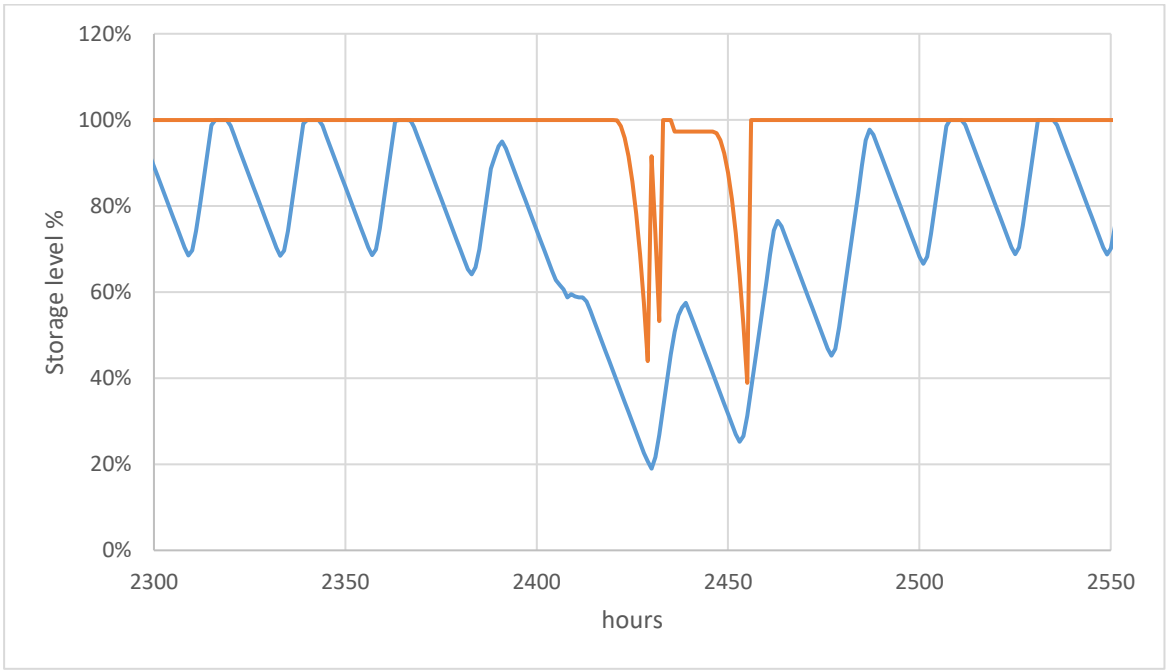

Figure 4.12 Focus of storages level in extraordinary conditions PV-CC-BES in FLR case, (hydrogen in "blue" and SOC in "orange").

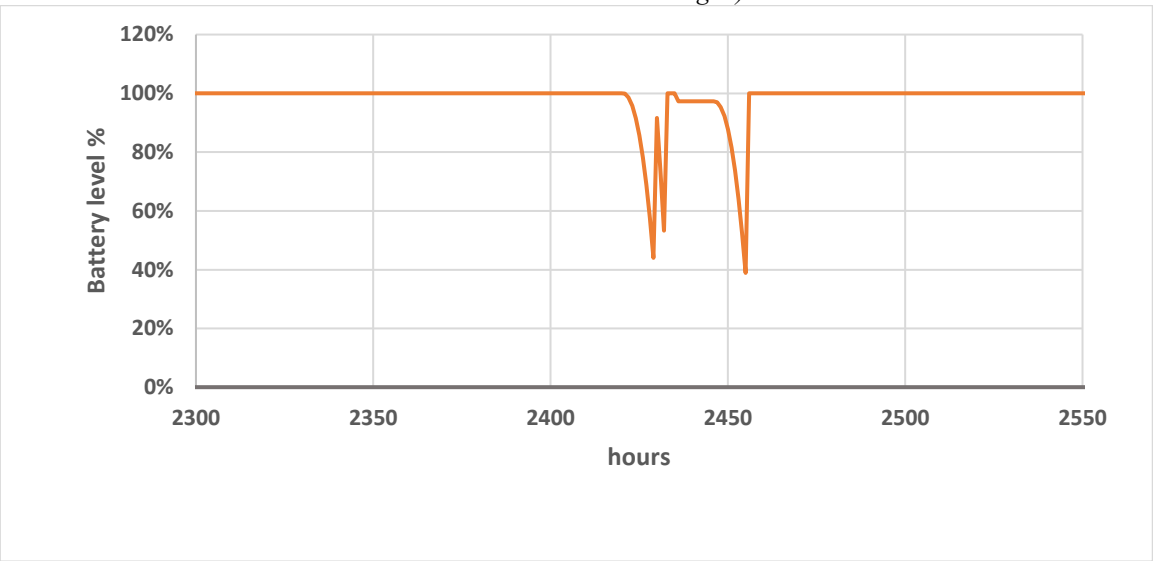

Figure 4.13 Comparison of SOC in PV-CC-BES FL case (Grey) and in PV-CC-BES FLR case (Orange).

In Figure 4.12 are represented the level of SOC in FLR case compared to the FL case. It is appreciable the un-stationary role of the batteries in this case respect to the dynamic and periodical trend of in the FL case.

In PV-DAC-BES graph Figure 4.13 is really similar to one in FL case. The only difference is in the depth of the SOC in ordinary operation, which in this case result higher. Even in PV-DAC-GT there are no such differences with respect to the FL case.

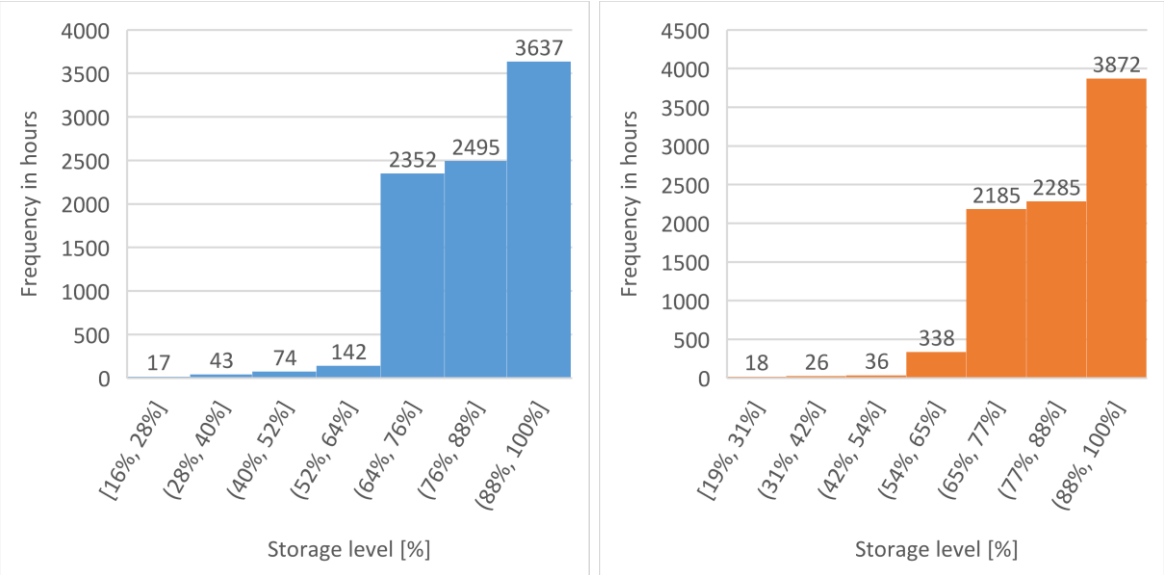

Figure 4.14 Storages level's frequencies PV-DAC-BES in FLR case, (hydrogen in "blue" and SOC in "orange").

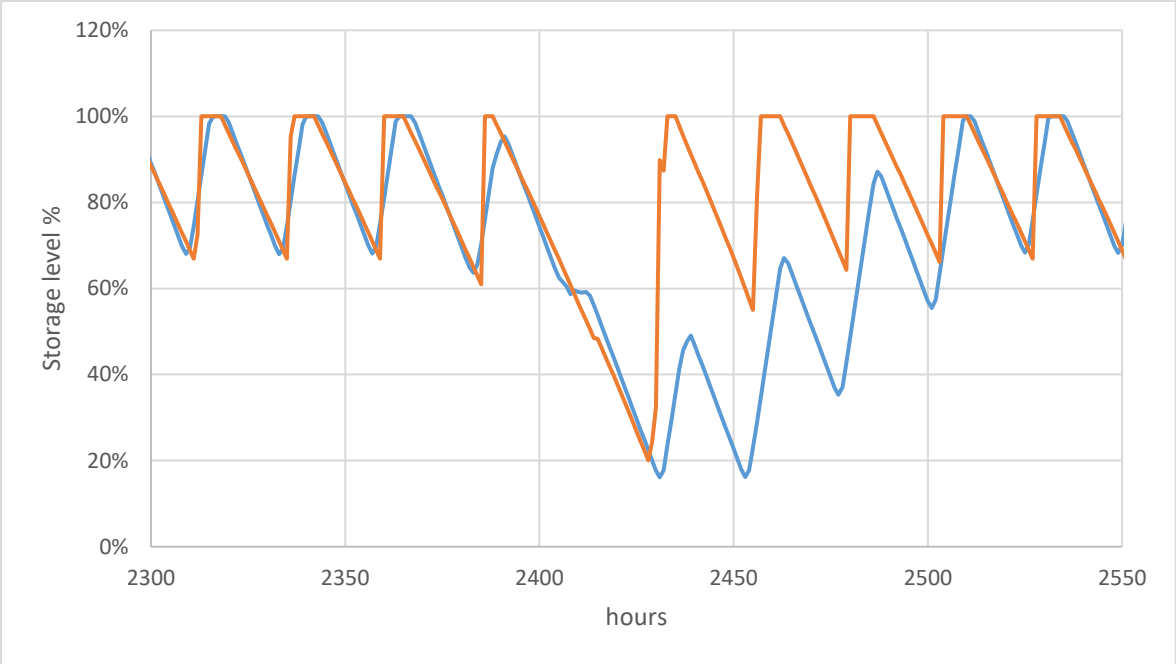

Figure 4.15 Focus of storages level in extraordinary conditions PV-DAC-BES in FLR case, (hydrogen in "blue" and SOC in "orange").

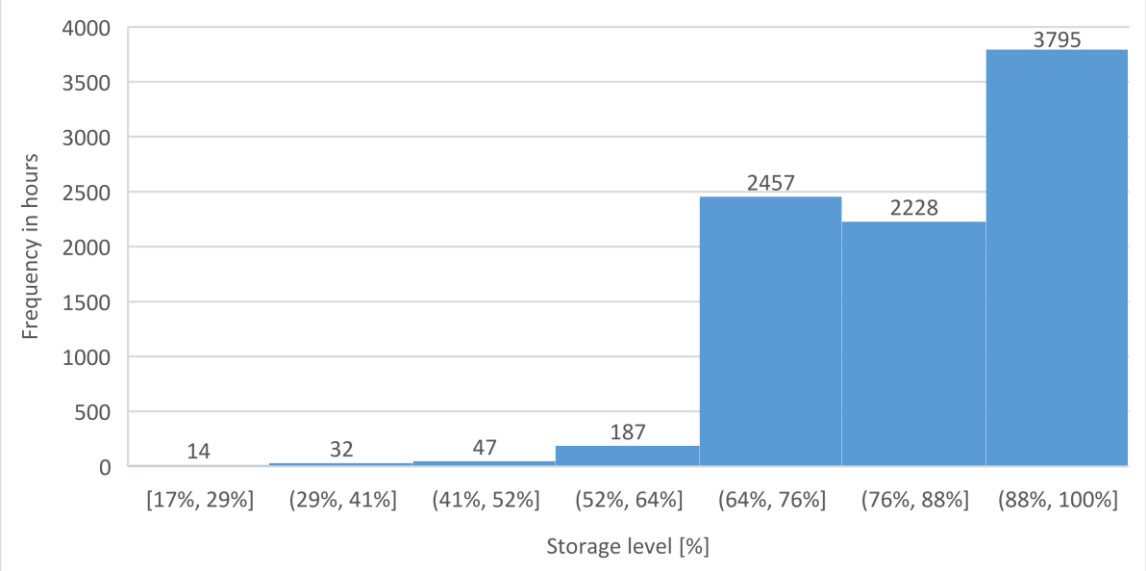

Figure 4.16 Hydrogen level in PV-DAC-GT, FLR case

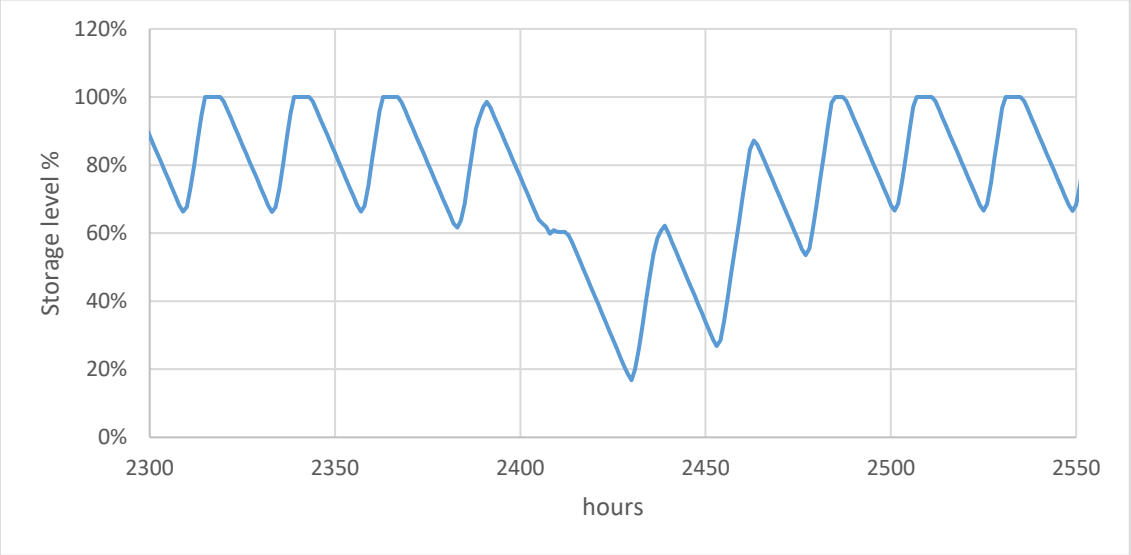

Figure 4.17 Focus of hydrogen storage level in extraordinary conditions PV-DAC-GT in FLR case.

Table 4.15 Storages sizing in ORC/HX integration mode after hourly model evaluation

	H_2 storage [MWh]	*Batteries [MWh]*	*Max C_{rate}*
PV-CC-BES	*5421*	*6.8*	*61%*
PV-DAC-BES	*5318*	*488.5*	*57%*
PV-DAC-GT	*5963*	-	-

Even in this case it is calculated the amount of hydrogen left in the storage to adjust the yearly production.

Table 4.16 Residual hydrogen at the end of the year, FLR case

	Final level [%]	*Capacity [MWh]*	*ΔE (final – initial) [MWh]*	*SNG [MWh]*
PV-CC-BES	*79 %*	*5421*	*1572*	*1226*
PV-DAC-BES	*78 %*	*5318*	*1489*	*1161*
PV-DAC-GT	*77 %*	*5963*	*1610*	*1256*

4.2 Economics

The economic evaluation follows the same approach of Chapter 2.

The shares of the investment with the installation contribution are calculated in the same way and the are no such differences compared to FL case.

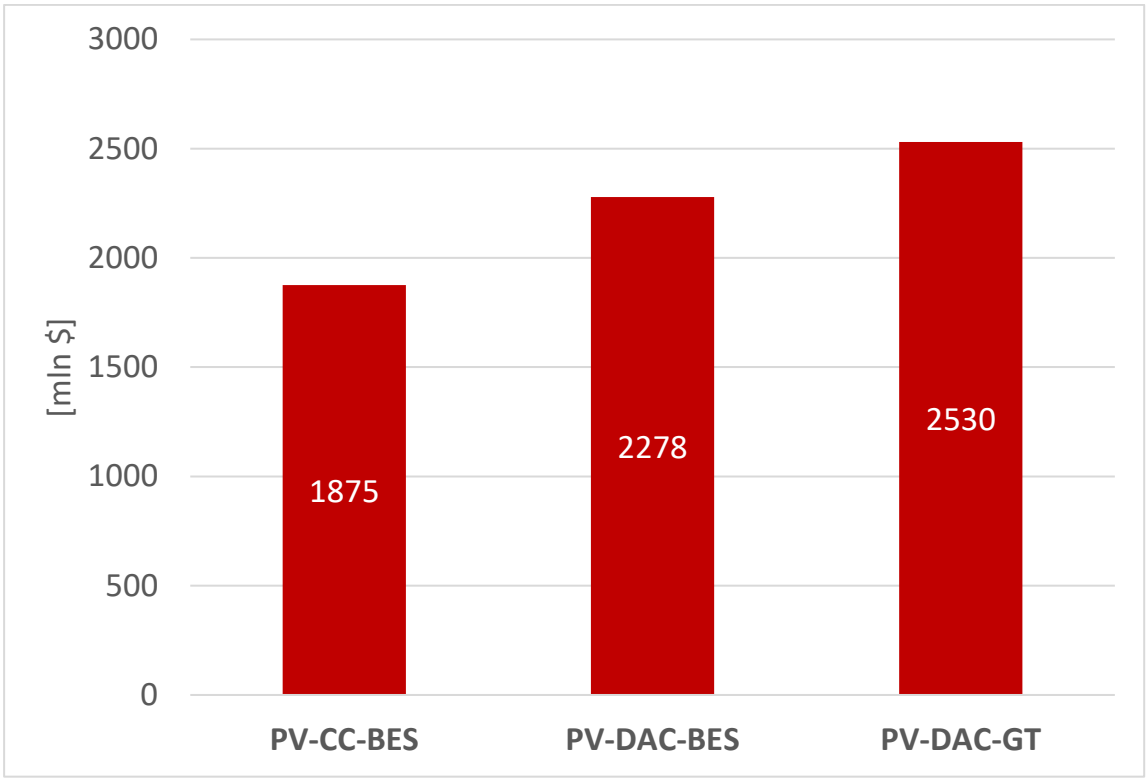

Figure 4.18 CAPEX of equipment and cost of installation for supply chains, FLR case

Even though the share is almost the same, in this case total cost of investment decrease. The TCI (Total cost of investment) decreases more in supply chains that use the heat exchanger (HX_m) instead of ORC because it results in a great advantage from the energetic aspect, with a negligible additional cost. Nevertheless also in PV-CC-BES case the introduction of the ORC instead of a larger battery capacity results in a lower total cost.

This lower TCI definitely results in a lower LCOM since the yearly production will be almost the same.

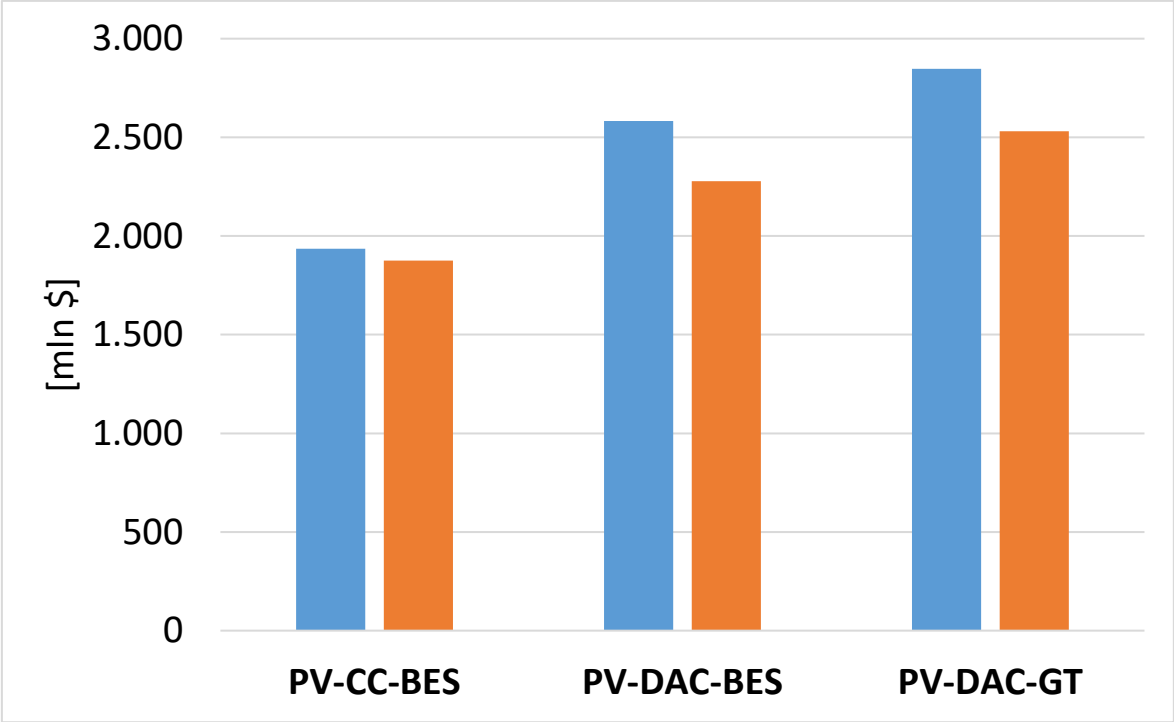

Figure 4.19 Total cost of investment in FL (blue) case compared to FLR (orange).

In this case the share of equipment cost are not shows because the differences are not that marked. As previously most of the CAPEX is driven by the PV and AEK.

LCOM

The levelized cost of syngas is calculated in the same way of Chapter 2. The only appreciable difference lies on the annual cost which in this case is lower for all cases.

Table 4.17 LCOM FLR case

	Annual cost [mln $]	**E_y [MWh]**	**LCOM [$/MWh]**
PV-CC-BES	211	833365	253
PV-DAC-BES	262	833303	314
PV-DAC-GT	282	833393	338

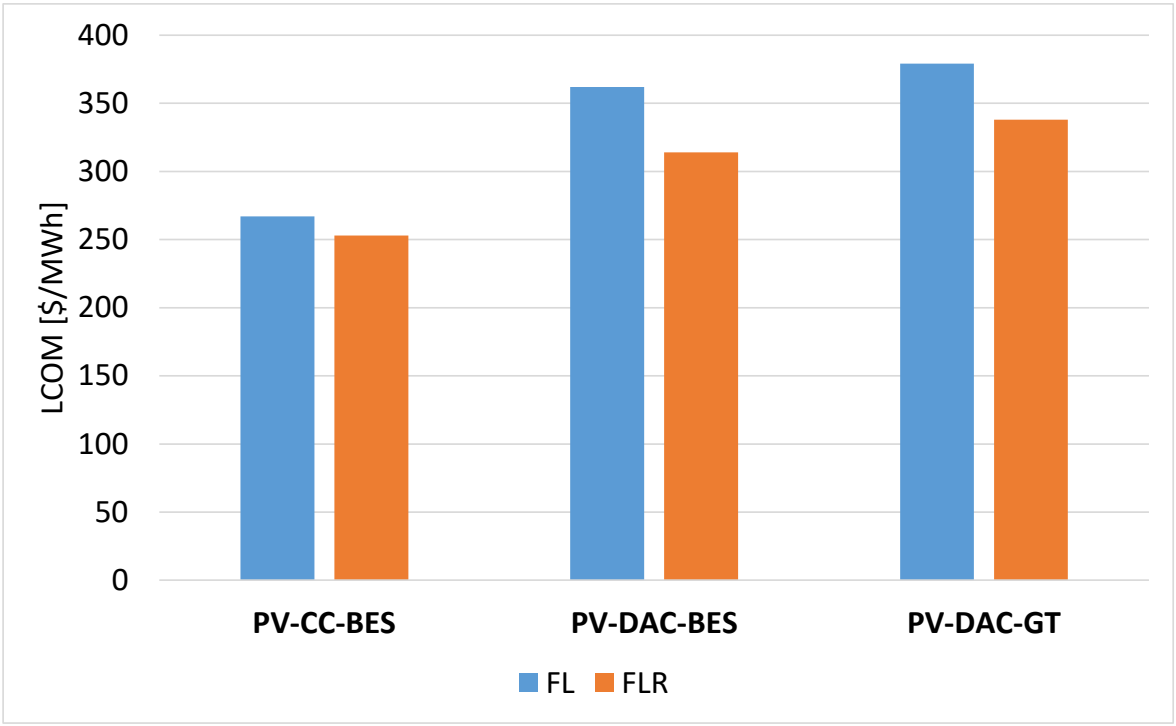

Figure 4.20 LCOM in FLR case

globally it results that the introduction of a heat recovery system is economically profitable for all cases, with particular advantage for supply chains that use the heat exchanger.

Chapter 5 PLRO case: oversized methanator unit and partial load operation

5.1 Partial load rational

The purpose of this chapter is to investigate if it is possible to achieve a lower levelized cost of methane adding flexibility to the plant. This analysis will be done for all the supply chains, and the case FLR will be the starting point because it has been proven more economical. The starting point of this work was a 100 MW plant working always at full load, and to guarantee so it has been sized on the worst prototypical day. The worst day was the day on the 2,5% percentile in the pool of days classified by their potential electric energy content. This means that during all the other days a certain amount of energy gets wasted, to be precise on 97.5% of days there is useful electric energy left back. The idea is to try to use a part of the unexploited energy. The power block of the PV plant remains the same, as well as the AEK, because the rate between the two components was already optimized with all the three prototypical days. The other block, which comprises all the other components will be oversized respect to the FLR case. Oversizing the methanator, plant storages (batteries and H_2 storage) are under risk of emptying because with a greater methanator the stream of hydrogen is greater so the tanks tend to empty much faster. This aspect lead to the second feature of this new case, the possibility to run the plant at partial load. With this possibility the plant can sometimes run at partial load to lower the production and save the stocks of hydrogen and power in case the plant is under risk of shutdown. Operations up to 30% of full load are possible for the methanation system, thanks to the reflow fraction on first reactor, which can be increased to compensate for the conversion efficiency losses due to the higher outlet temperatures resulting from the heat exchangers operating at partial loads

[2]. In this work since there are also some integrations such as ORC system or heat exchanger designed on working at full load, the partial load operation in this analysis will be considered at 50% of full nominal power and not lower. The oversized block needs to be well sized because the incremental advantage of sizing is compensated by the additional cost. A trade off must be found. This is way the daily model has been used. This specific task would have required a program able to run simulations for each size applied to the real pool of days and not to three prototypical days as it is in the daily model. In this work such tool was not available so the result is less accurate but still useful to understand if the oversizing process is convenient.

During partial load operation methanator is assumed to maintain the nominal efficiency since the load is not lower than 30% [2]. For gas turbines and ORC system instead, the net electrical efficiency at partial loads is decreased of 10% respect to the nominal conditions. The heat exchangers are assumed to work in the same way, so all temperatures are assumed not to vary in partial load conditions.

Whether the plant will run at partial or full load, will be handled in the Power flow logic.

5.2 Power flow logic

The power flow logic is a similar kind presented in Chapter 2, but with some new features.

The first great difference is that now the model is able to switch from full to partial load.

Figure 5.1 shows the algorithm that is used to select which load to run. Looking at the figure there are two new elements: Forecasts and H_2A & BA.

Considering the first new element, forecasts. The hourly model in previous case was a myopic model, which means that the model reacts only respect the current situation. In this case, since the model can switch from full to partial load, it is added the possibility for the model to “look forward” to the next 24 hours and include this aspect in the algorithm that rules the power flows within the plant. This tool wants to simulate the fact that in reality the plant management has access to forecasts so then the operators decide to run the plant in partial load if the next day is going to be cloudy.

Basically the model makes the sum of the total energy expected from the PV field, and if this amount is less than an arbitrary threshold the model goes preventively in partial mode

regardless of the other parameters. The threshold used is the same that in Chapter 2 was used to identify the "worst day" prototype. The positive outcome of this tool is to avoid over sizing of the storage systems caused by extraordinary bad conditions along the year. In fact the plant can be found ready in case of a series of "bad days".

The second element is the introduction of "alarms" for both battery and H_2 storage. This control system is used to work along with the forecasts to allow the model to be prepared in case of incoming bad weather conditions. Forecasts logic works with a threshold, so days are classified only in "normal" days and "bad days". Nevertheless could happen that a series of days is not bad enough to be detected by the forecasts algorithm but has an average energy which is lower than the average. In this case the plant could fall even in quite ordinary conditions. To avoid such eventuality, the two alarms control the level of storage of the two storage systems and when at least one of them falls below a threshold, the plant run at partial load. So using these two new control variables the plant can decide when to go full load considering the future conditions and the ongoing situation in terms of energy stocks.

Forecasts use as a threshold the 120% of the energy of worst prototype day, 4291 Wh (always related to the generation of 1 kW of PV panel).

Legend:

- P_{PV} : Power of the photovoltaic plant
- P_{AEK} : P_n of the alkaline electrolyzer
- HL : Hydrogen level of the storage
- BL : State of charge of the battery
- MIN : minimum level of the storages, for batteries is 0% while for hydrogen as previously described is 10%
- EL : Emergency level, for PV-CC-BES is 50% of the total batteries capacity, while for PV-DAC-BES it is 50%
- PV : Photovoltaic plant
- AEK : Alkaline electrolyzer

- BAT : Batteries
- AUX : Auxiliaries
- Φ : The plant is off

In Table 5.1 there are the thresholds used for each supply chian.

- H_2A: Hydrogen Alarm
- BA: Battery Alarm

Table 5.1 Alarms for the partial mode case

	H_2 A	*BA*
PV-CC-BES	*20% of TOT. capacity*	*20% of TOT. capacity*
PV-DAC-BES	*30% of TOT. capacity*	*30% of TOT. capacity*
PV-DAC-GT	*20% of TOT. capacity*	-

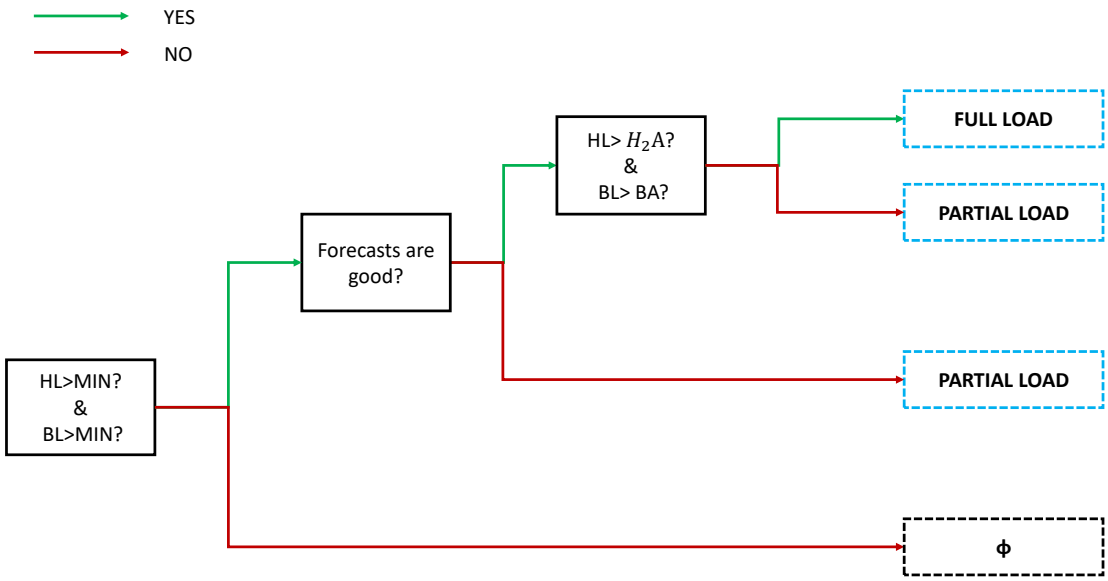

Figure 5.1 Mode selection in PLRO case

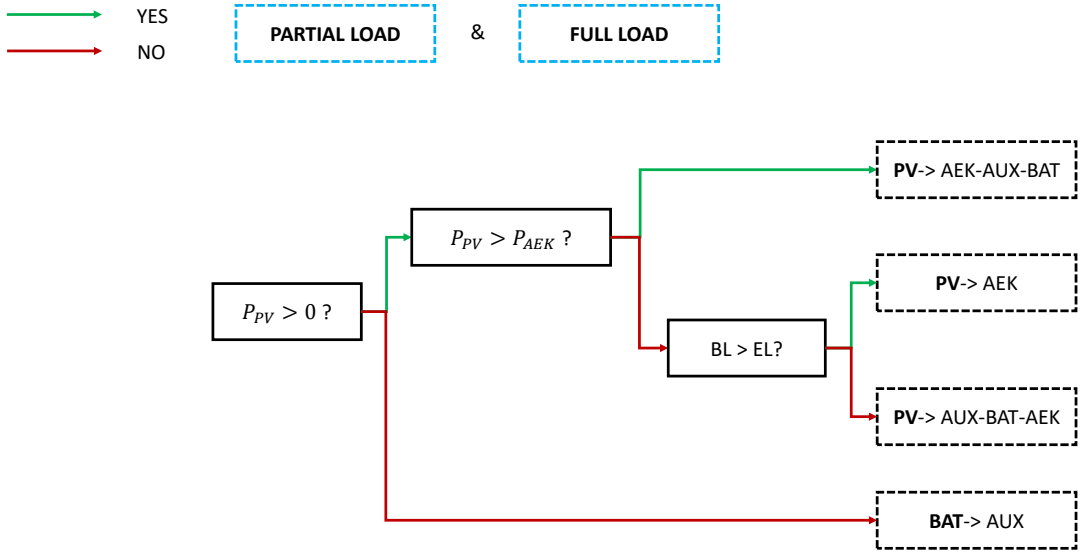

Figure 5.2 Power streams logic, PLRO case

5.3 Sizing

In this case the size of PV and AEK is the same of FLR case while methanator and system that work in synergy with it are over-sized.

Nevertheless it must be assessed if the integrated components (ORC and the HX_m) can still work in partial load conditions ensuring the correct operation.

Table 5.2 Temperatures and powers available for recovery in partial load compared to full load [2]

SIZE 0.53 [MW]	HEAT [KW]	T [C°]	T [C°]
Full load (100%)			
HX4	38.8	135	192
HX1	72.1	255	665
HX2	25.2	195	511
Cooler	13.2	135	45
Preheater	17.5	N/A	
Partial load (45%)			
HX4	16.9	143	194
HX1	35.3	288	573
HX2	8.0	204	435
Cooler	7.8	143	45
Preheater	5.1	N/A	

Table 5.2 reports temperatures and heat available for each heat exchanger. The first part of the table was yet used in FLR case to design the introduction of HX_m/ORC, while the second part of the table is used for the same evaluation but in partial load.

Looking at the differences it can be noticed that power of HX_2 is less than proportional while for HX_1 it is higher than proportional, while the range of temperatures for both HX_1 and HX_2 shrinks, leading to lower maximum temperatures and higher lower temperatures.

In the case of the table the partial load condition is at 45% of nominal, but in the analysis of this work the partial load condition is 50%, so the numbers must be adjusted. The idea is to keep the same temperatures as the difference is not that high, and to adjust powers making a simple proportion.

Finally the size needs to be referred to 100 MW, so another proportion is done. Table 5.3 summaries the results.

All data are reported to 100 MW size and the evaluation at partial load conditions will be carried out at this size. If the analysis confirms that heat exchangers and ORC can operate normally at half of power it is not necessary to make the analysis for each size of the methanator because all components are proportionally over-sized.

Table 5.3 Temperatures and heat available in partial load condition for a 100 MW methanator

SIZE 100 [MW]	HEAT [KW]	T [C°]	T [C°]
Partial load (50%)			
HX4	3543	143	194
HX1	7400	288	573
HX2	1677	204	435
Cooler	1635	143	45
Preheater	1069	N/A	

PV-CC-BES

In ORC systems off-design conditions can be managed with active regulation systems. Those can be:

- Sliding pressure
- Partial admission

In sliding pressure, the inlet turbine pressure decreases proportionally to the reduction of turbine inlet mass flow rate.

In partial admission the pressure is kept constant and the turbine inlet area is reduced using inlet guide vanes on the first stage stator.

For this work it will be assumed that an active regulation will be in place to guarantee the same delta temperatures of the oil circuit, then using an off-design efficiency curve it will calculated the off-design efficiency. For a partial load of 50 % the net electrical efficiency is assumed to suffer a 10% decrease [30].

For this analysis it has been made the same analysis of FLR case with the same assumptions. The only differences are mass flow rate of oil and water that of course decreases. As

mentioned before the oil temperatures are kept constant compared to nominal case, so the only difference is in mass flow rate.

In Figure 5.3 it can be noticed that the contribution of HX_2 is lower than the full load case, it passed from 23% to 16%. Even in this case a part of the available heat is not recovered as temperatures are not enough high.

Globally the amount of heat recovered is 8809 kW, which compared to 17666 kW is 50%, so the lower heat form HX_2 is successfully covered by the larger amount of heat from HX_1.

The net electricity produced in partial load condition is 1823 kW, which is only 45% of the full load case because of the drop of the efficiency.

In conclusion it can be said that it is possible for the ORC to continue working in synergy with the methanator even in partial load conditions.

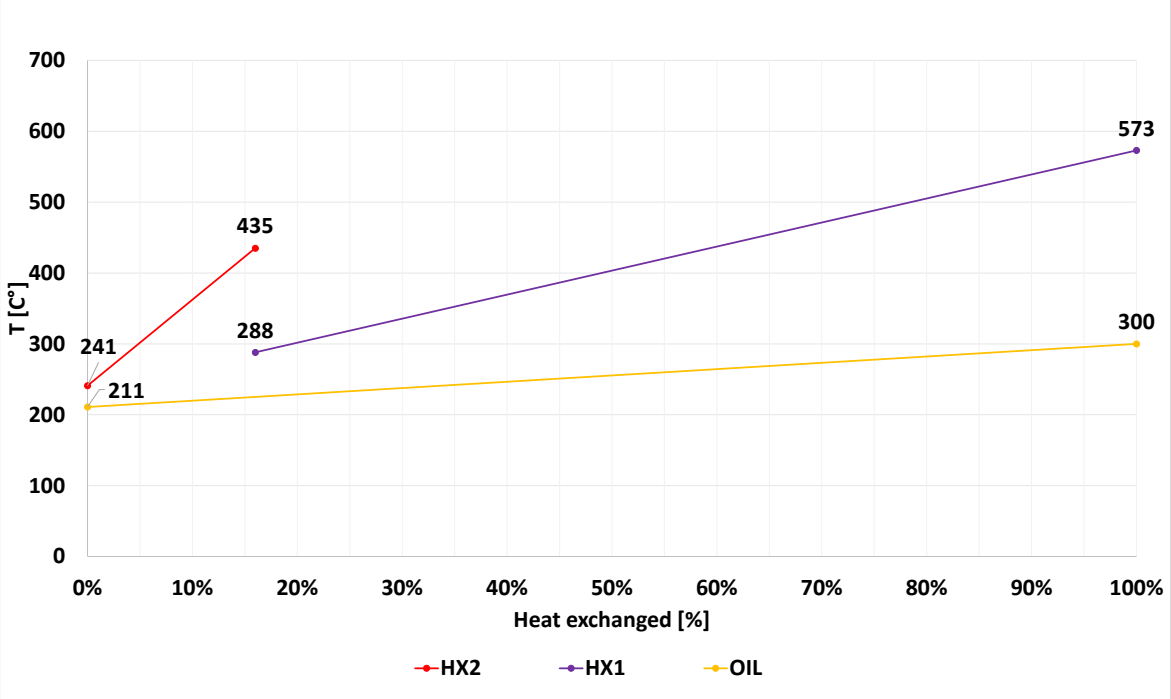

Figure 5.3 T-Q diagram for ORC in off-design condition

PV-DAC-BES & PV-DAC-GT

The same approach is being used for the other two supply chains, in this case the analysis is focused on HX_m. As well as the previous case HX_1 covers the loss of heat available from HX_2 and finally HX_m provides 73% of total energy required by DAC, while in the case of

full load the rate was 74%, the small difference will be covered by batteries in PV-DAC-BES and from exhaust in PV-DAC-GT.

Even in this case the integration results possible at half of load.

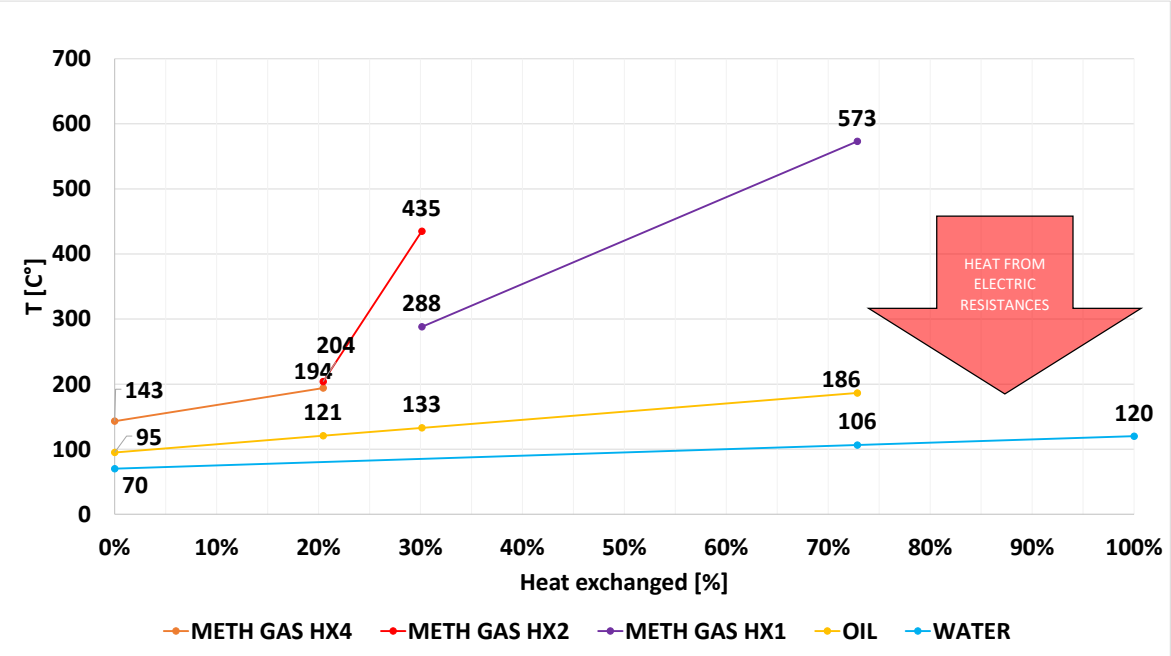

Figure 5.4 T-Q diagram of HX_m in off-design condition, PV-DAC-BES

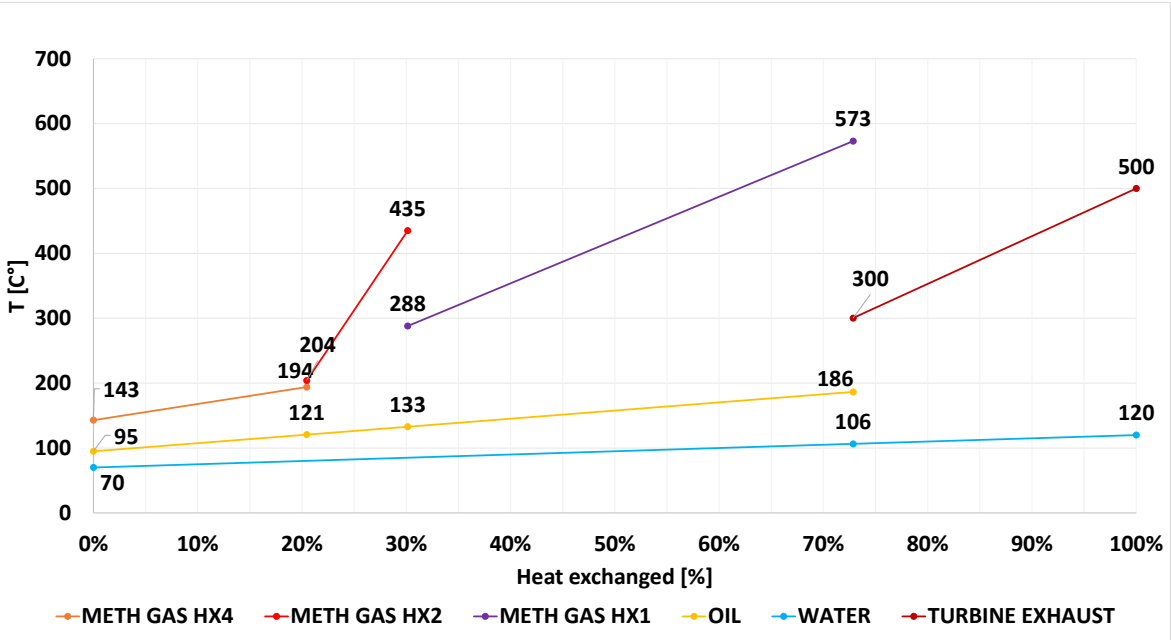

Figure 5.5 T-Q diagram of HX_m in off-design condition, PV-DAC-GT

5.3.1 Daily model

The daily model as mentioned before is used to assess the optimal size of the methanator. This optimal size coincides with the maximum size in which the additional cost for the over-sized systems is payed back by the additional productivity of the plant.

The graph Figure 5.6 shows the trend of the specific cost of syngas for each size of the methanator. This specific cost of syngas does not take into account the installation costs and it is calculated dividing the annual cost for the expected production in MWh. This model has not the purpose of giving the exact cost of syngas but to assess the best fitting size of the methanator.

Looking at the three curves, it is clear that each curve shows two different trends marked by a minimum. This behaviour is justified by how the model is structured. The steeper trend of the curves occurs when each additional size of the methanator allows to exploit better both the “average day” and “best day”. Then after the point of minimum the marginal increase in size also permits to take advantage on the “best day” and the economical expenditure does not pay back the additional investment.

From this evaluation turns out that for PV-CC-BES the best size is 132 MW, for PV-DAC-BES it is 130 MW and finally for the case with gas turbine the value is 136 MW.

These values will be used for the sizing process in the next paragraph.

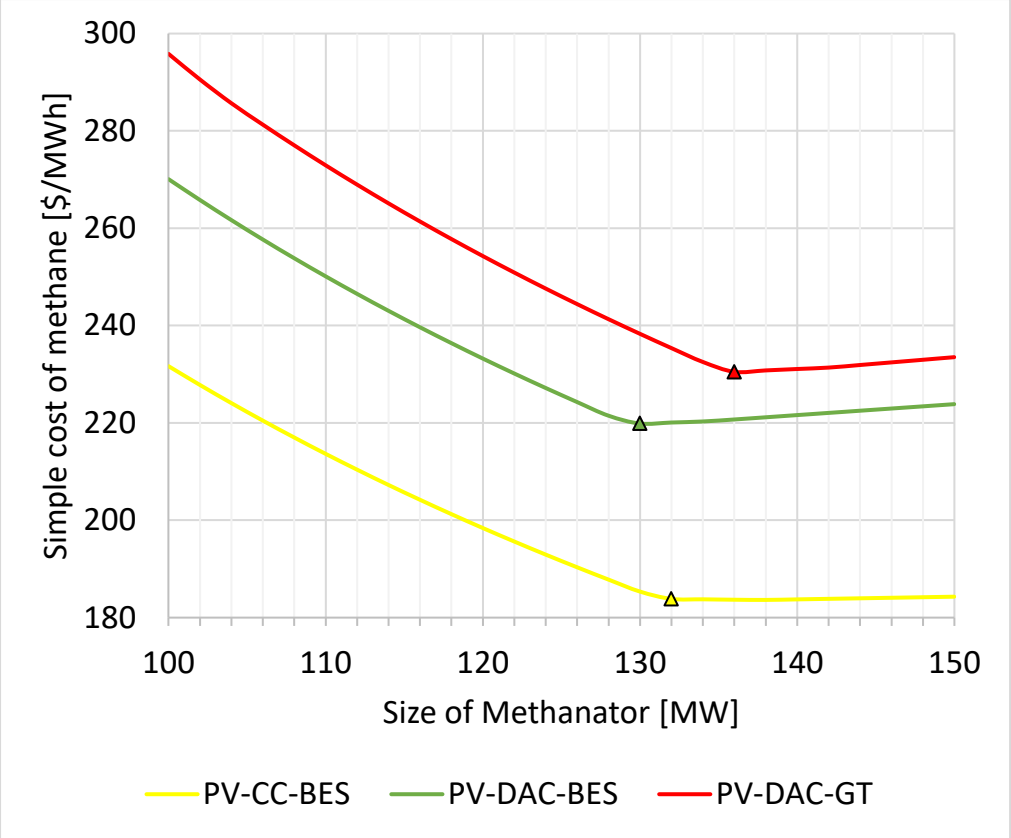

Figure 5.6 Daily model output for PLRO case

5.3.2 Systems sizing

The sizing phase starts from the values calculated in Table 4.14, while the methanator and all the equipment that work in synergy with it are oversized as the Table 5.4 shows.

Table 5.4 Oversizing factors for each component in each supply chain

	Methanator	*DAC System*	*Gas turbine*	*ORC*	*HX*	*Compressors*
PV-CC-BES	*32 %*	-	-	*32 %*	-	*32 %*
PV-DAC-BES	*30 %*	*30 %*	-	-	*30 %*	*30 %*
PV-DAC-GT	*36 %*	*36 %*	*36 %*	-	*36 %*	*36 %*

Table 5.5 shows the sizing table adjusted with the oversizing factors of Table 5.4.

Table 5.5 Sizing resume table for PLRO

			PV-CC-BAT	PV-DAC-BAT	PV-DAC-HX
PV	**[MW]**		1458	1543	1848
AEK	**[MW]**		729	694	924
METHANATION	**[MW]**		132	130	136
TURBINE or ORC	**[MW]**		5.38	-	46.61
HX_m	**[m^2]**		-	3890	4069
HX_t	**[m^2]**		-	-	8637
H_2 compressor	**[MW]**		4.95	4.88	5.10
CO_2 compressor	**[MW]**		2.07	2.04	2.13
DAC system	**[tCO_2/y]**		-	225482	235889

5.3.3 Sizing Storages

This analysis in conducted in the same way of the other cases. PV-CC-BES situation represented in Figure 5.7 displays a more distributed trend, meaning that the level of hydrogen is placed in the half of the level. This result is attributed to the oversized methanator that consumes faster the stored hydrogen. So often the level come across the threshold level and the plant start running at partial load to let the hydrogen level raise again above the emergency level.

On the contrary the state of charge shows the same trend of the previous case.

The third diagram in Figure 5.7 reveals exactly how the model reacts against an incoming extraordinary bad condition. Starting from the day before the plant decides to run at half of load even though the level of hydrogen and SOC were far above the alarms. The half load operations lead to a flatter curve and the depth of discharge of the storage is halved. The day after, the plant has not enough energy to fill the storage but keeping the load halved the plant avoid the shutdown.

Another aspect which is different to previous case is the daily depth of the level of hydrogen, which in this case is greater. To be more precise in the previous cases, in ordinary conditions the level of hydrogen in percentage reached 70%, now it gets below 50%. This is because the size of the hydrogen storage has not increased as much as the size of the methanator.

The same features can be observed in the other two supply chains. In addiction in PV-DAC-BES also SOC shows the same trend of the hydrogen, passing to a more uniform distribution.

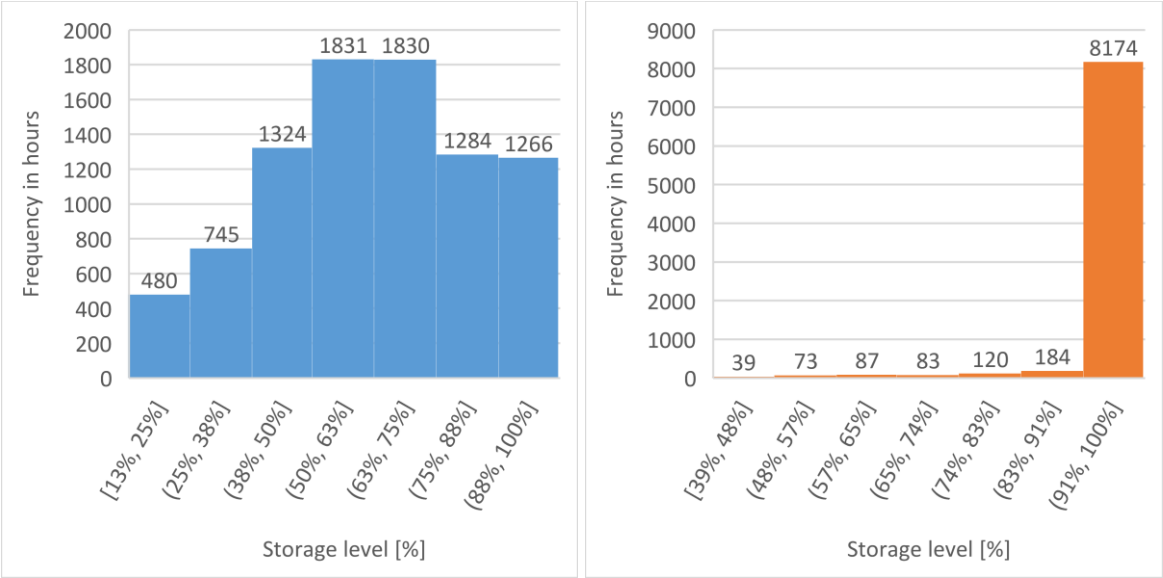

Figure 5.7 Storages level's frequencies PV-CC-BES in PLRO case, (hydrogen in "blue" and SOC in "orange").

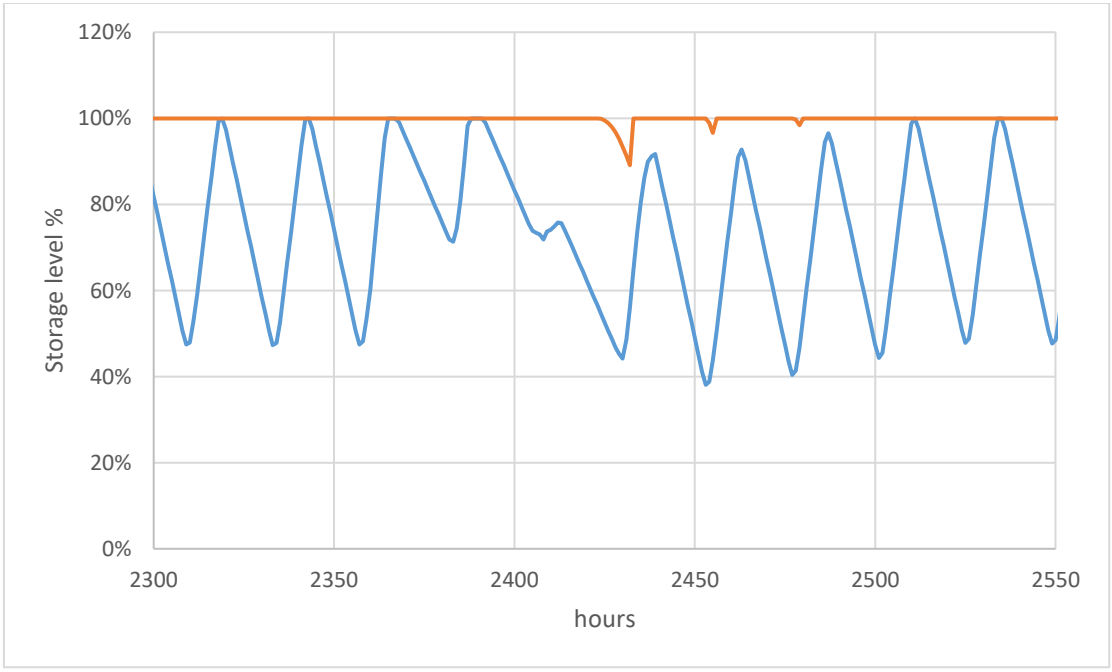

Figure 5.8 Focus of storages level in extraordinary conditions PV-CC-BES in PLRO case, (hydrogen in "blue" and SOC in "orange").

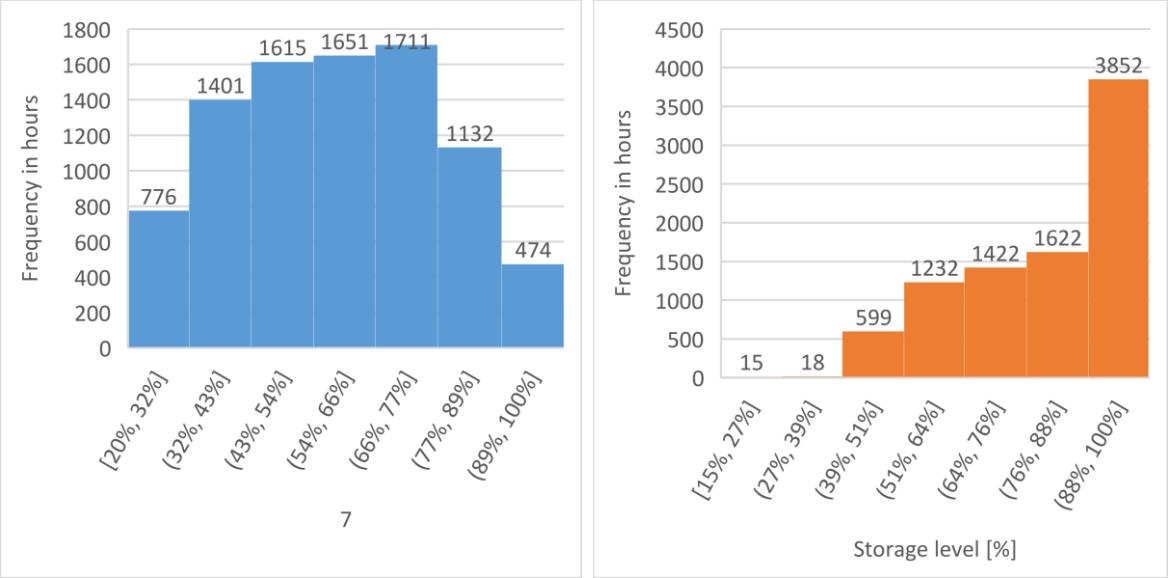

Figure 5.9 Storages level's frequencies PV-DAC-BES in PLRO case, (hydrogen in "blue" and SOC in "orange").

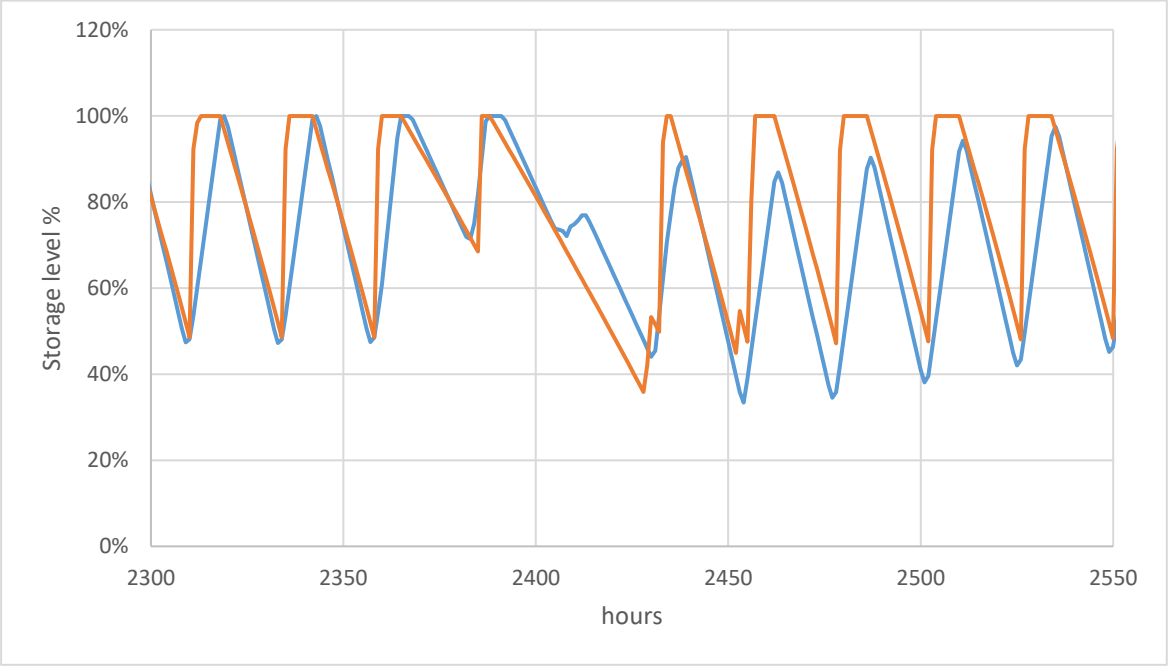

Figure 5.10 Focus of storages level in extraordinary conditions PV-DAC-BES in PLRO case, (hydrogen in "blue" and SOC in "orange").

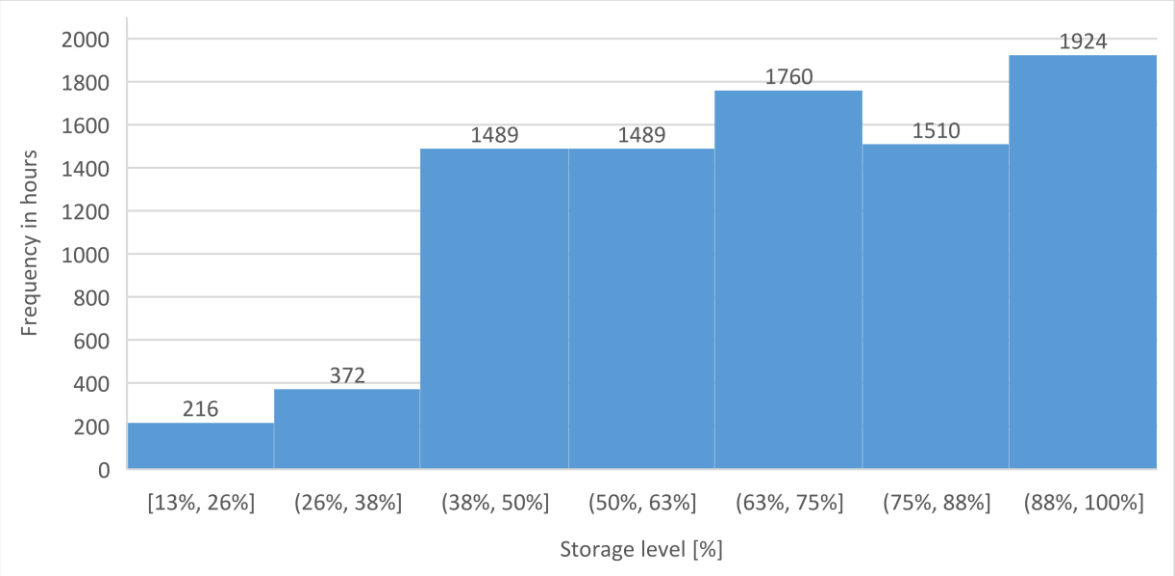

Figure 5.11 Hydrogen storage level for PV-DAC-GT in PLRO case.

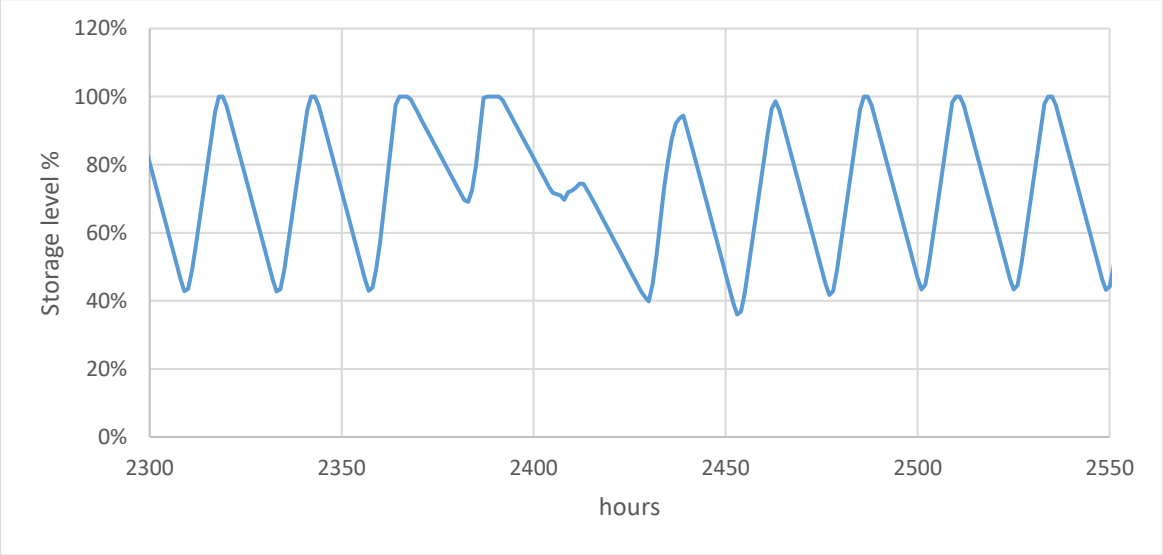

Figure 5.12 Focus of hydrogen storage level in extraordinary conditions PV-DAC-GT in PLRO case, (hydrogen in "blue" and SOC in "orange").

Table 5.6 collects the values obtained from the analysis of the hourly model.

Table 5.6 Storage sizing in PLRO case

	H_2 storage [MWh]	*Batteries [MWh]*	*Max C_{rate}*	*Load factor*
PV-CC-BES	*4337*	*13.6*	*61 %*	*95.0 %*
PV-DAC-BES	*4255*	*391*	*56 %*	*92.8 %*
PV-DAC-GT	*4879*	-	-	*95.6 %*

Load factor in Table 5.6 is the average load of the plant calculated only when the plant is working. This parameter is useful to understand the average load of the plant. This parameter

is reasonably high for all the cases and in particular it is higher in PV-DAC-GT. The absence of the batteries can be one reason for this result, because in this case partial load conditions can be caused by one factor less. On the contrary PV-DAC-BES shows the lowest load factor for the same reason, in this case the high load of the batteries turns the SOC to go sometimes under the level of Alarm (BA threshold) and causes a final lower load factor.

Another important aspect is that in this case both hydrogen storage capacity and battery capacity are lower than the previous case in Figure 5.13**.** Despite the over-sizing of the methanator, the possibility to run in partial load guarantees flexibility and lowers the capacity of the storages.

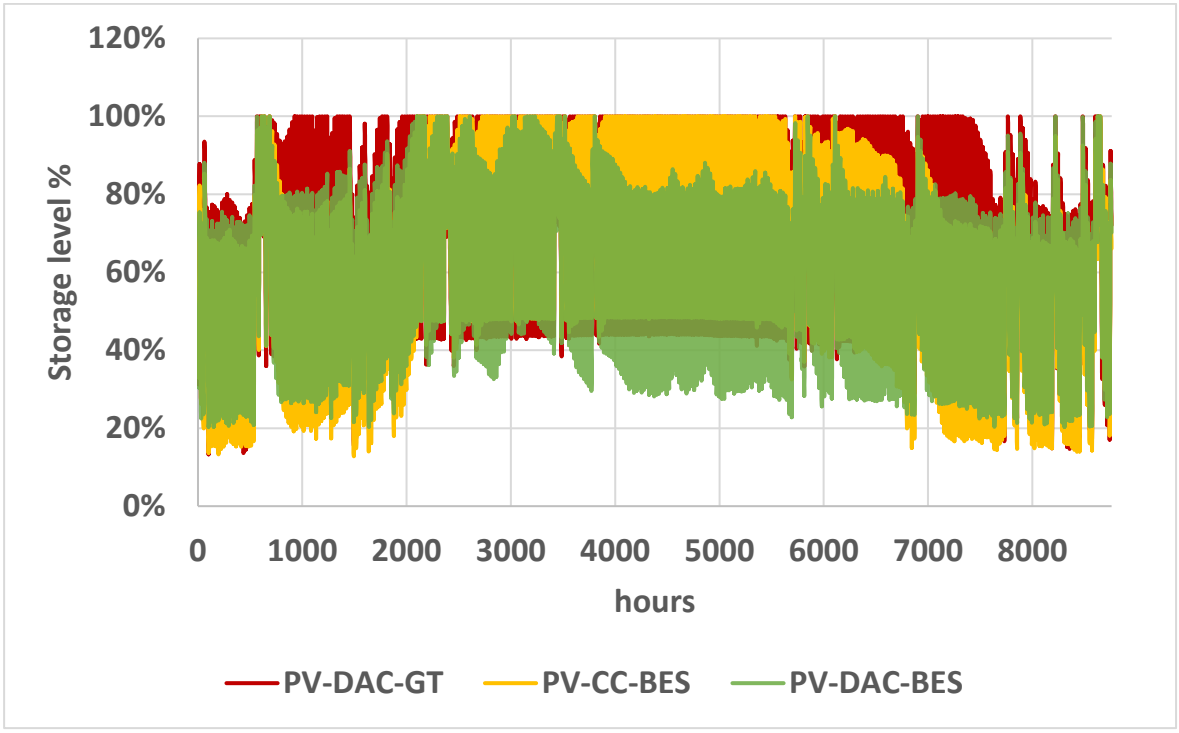

Figure 5.13 Trend of H_2 level in the storage for each supply chain.

The trend of the H_2 level in Figure 5.13 is similar in PV-CC-BES and PV-DAC-GT, and there is a perceptible seasonal variation of the average level in the hydrogen tanks. Looking at Figure 5.14 it can be noticed that the season with the highest peak (HPS) does not overlap with the region with highest average level of the tank in Figure 5.13. This behaviour is explained by the fact that HPS also presents some days with very low energy, so the storage undergoes some periods of shortage that make the level to go down frequently. On the other side the HAS present a more stable trend that let the storage to maintain a high average level.

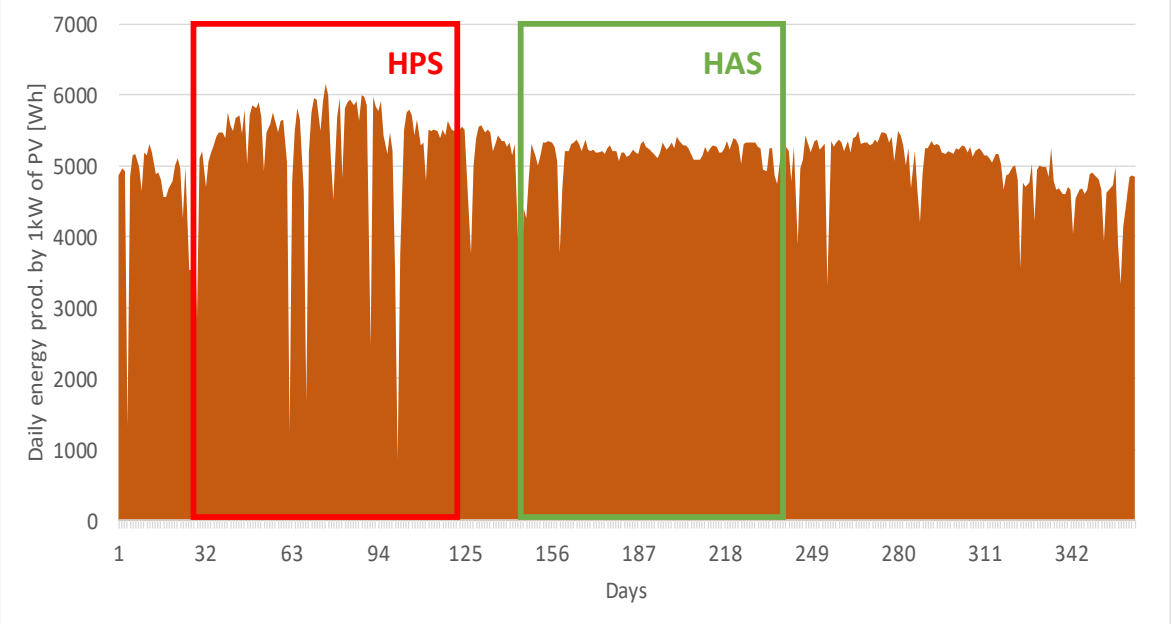

Figure 5.14 Energy per day with specific region identification, produced by 1 kW_P PV in year 2014.

Even in this case it is calculated the amount of residual hydrogen and turned into synthetic methane.

Table 5.7 Residual hydrogen at the end of the year, PLRO case

	Final level [%]	*Capacity [MWh]*	*ΔE (final – initial) [MWh]*	*SNG [MWh]*
PV-CC-BES	*66 %*	*4337*	*694*	*541*
PV-DAC-BES	*70 %*	*4255*	*851*	*664*
PV-DAC-GT	*72 %*	*4879*	*1073*	*837*

5.4 Economics

In this final case (PLRO) the total cost of investment can increase or decrease compared to the previous case (FLR). It is true that the oversizing process definitely increases the cost of some components of the plant, but the flexibility achieved with the partial load opportunity may have lowered the cost of storages. It can be noticed from Figure 5.12 that in PV-DAC-GT the investment cost is higher, while in the other two cases the higher cost of the methanator block is compensated by a lower cost of the storage systems.

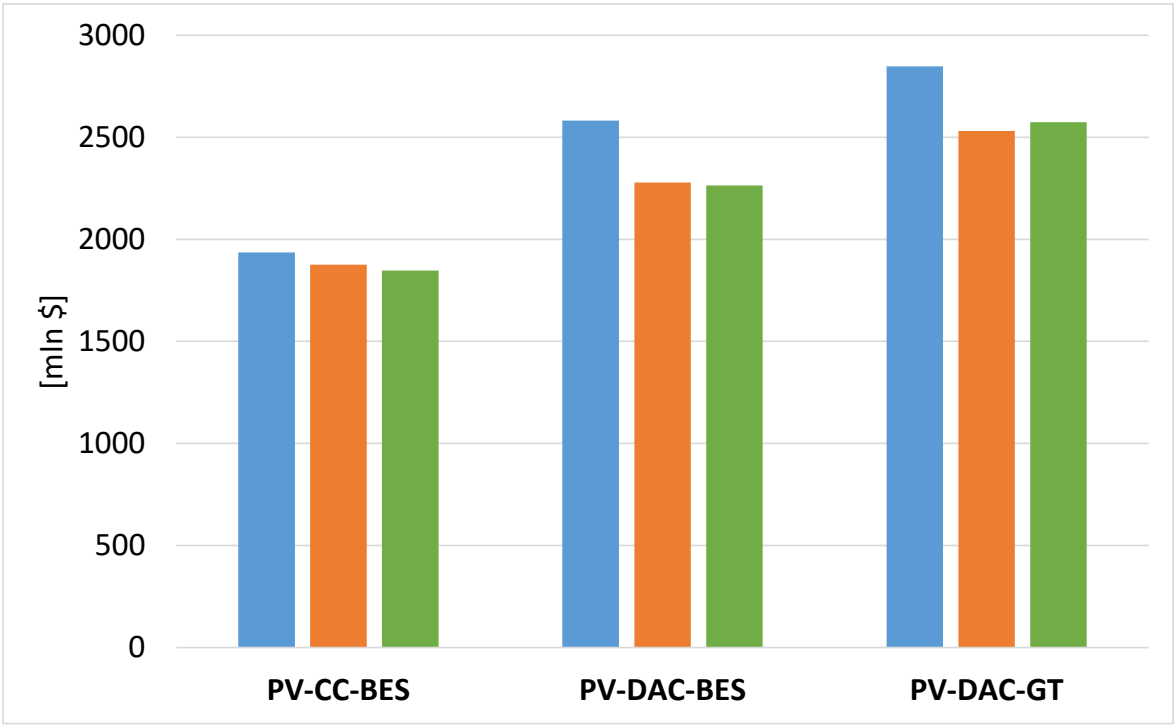

Figure 5.15 Comparison of Total investment cost in of all cases

In this case are reported the shares of cost for each supply chain as it was in FL case.

With respect to the FL case, there is an increase in the share of methanator and DAC system, but the main drivers are still PV and AEK by far.

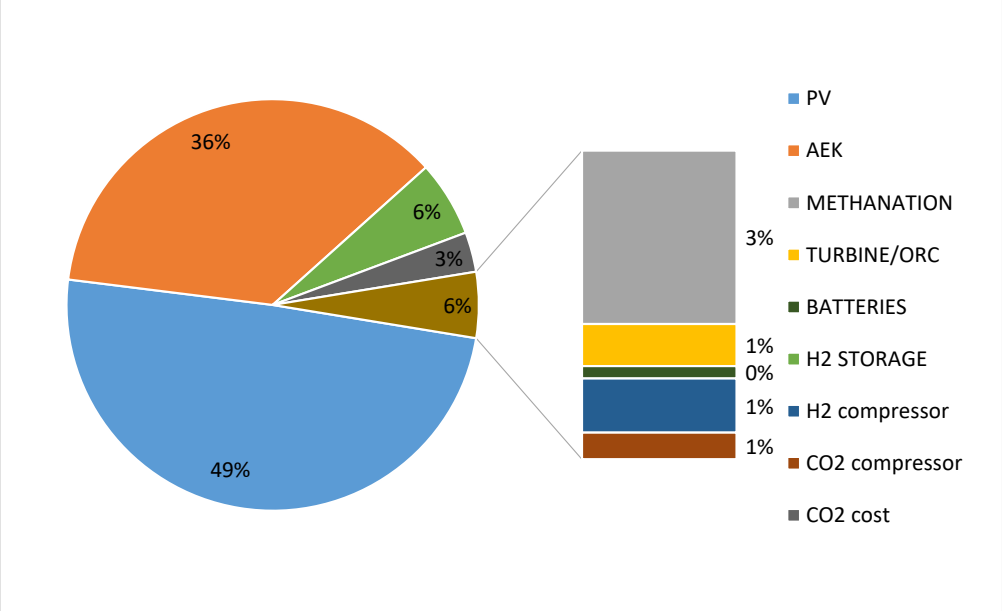

Figure 5.16 Share of costs for the PV-CC-BES configuration, PLRO case.

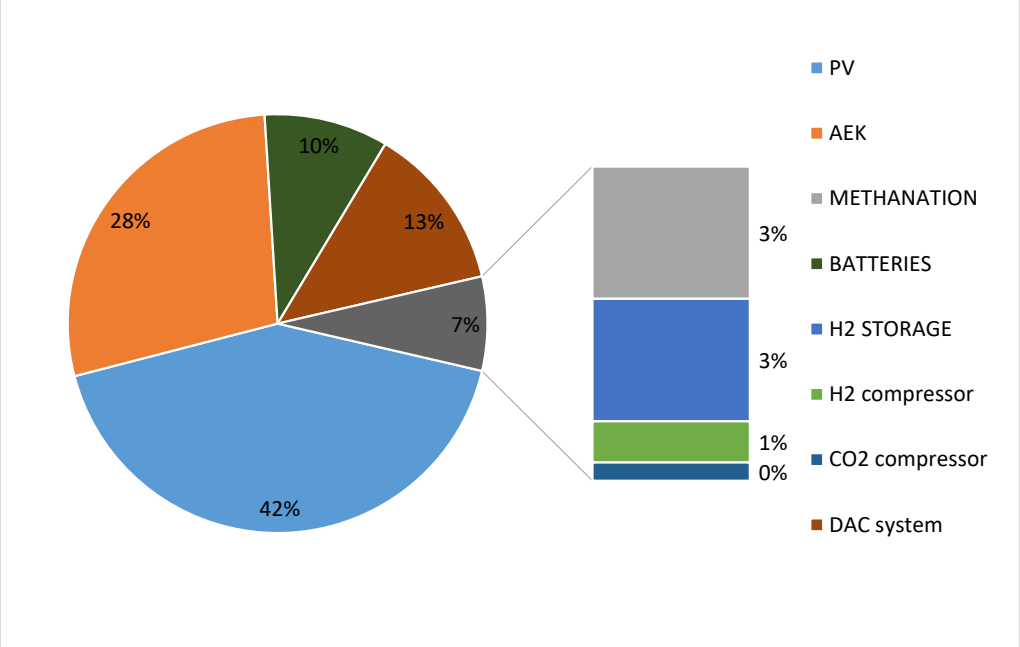

Figure 5.17 Share of costs for the PV-DAC-BES configuration, PLRO case.

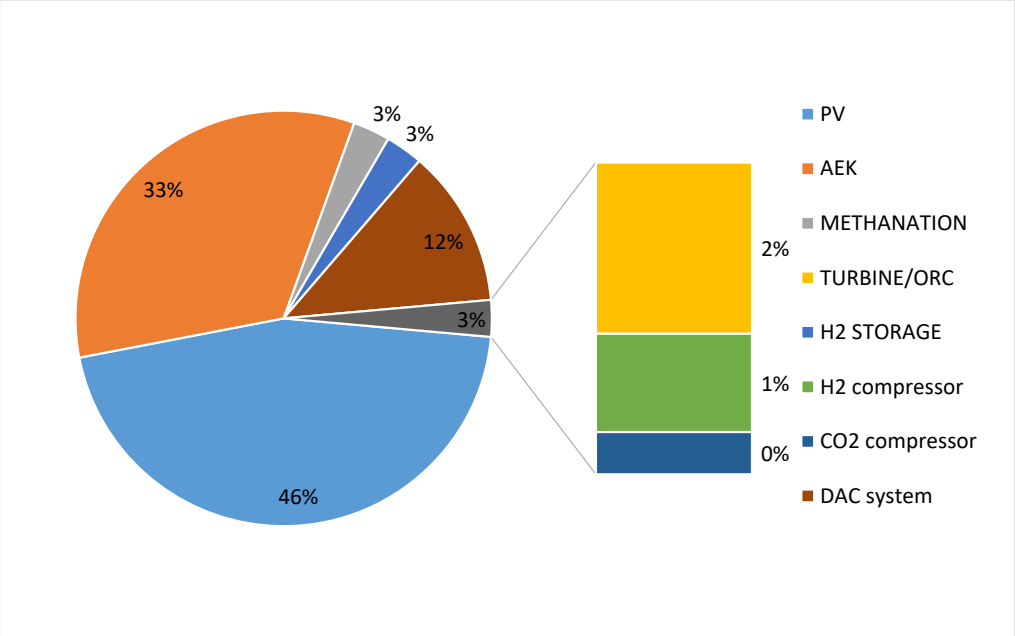

Figure 5.18 Share of costs for PV-DAC-GT, PLRO case

LCOM

In this final case, the total amount of gas produced may vary significantly respect to the previous case, in fact the different size of the methanator allows for different final productions. From the hourly model has been recorded the production hour by hour and at the end it has been summed up. To this value are added the ΔE_y calculated from the residual hydrogen left in the storage, finally this value has been multiplied by the availability.

Results are in Table 5.8.

Table 5.8 Levelized cost of syngas, PLRO case

	Annual cost [mln $]	E_y [MWh]	LCOM [$/MWh]
PV-CC-BES	206	1043842	197
PV-DAC-BES	260	1004377	259
PV-DAC-GT	290	1082715	268

In Figure 5.16 are shown the result of the entire work. First of all it appears clear that every step ahead in this analysis has resulted always in a lower LCOM, furthermore the possibility

to operate at partial load brought the best reduction in the specific cost. It means that the additional investment has turned in an additional productivity that payed back the effort.

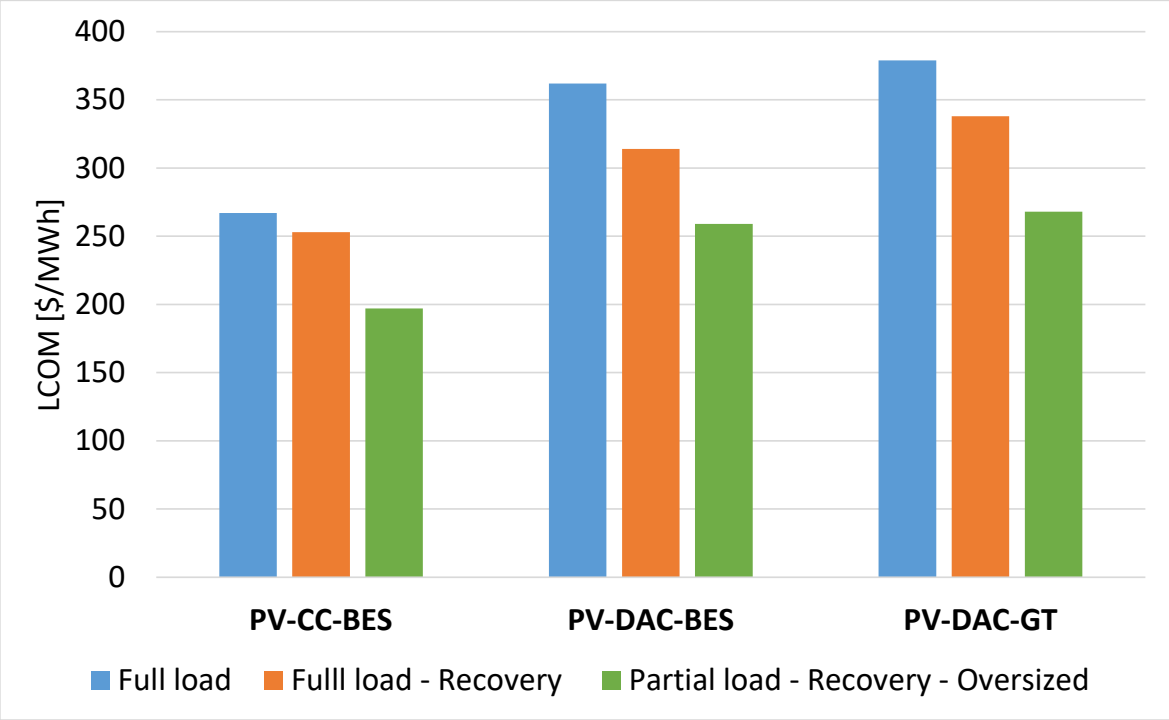

Figure 5.19 LCOM specific to each supply chain and case, FL (blue), FLR (orange) and PLRO (green).

Chapter 6 Configurations comparison and sensitivity analysis

6.1 Energy efficiency analysis

The goal of this analysis is to assess the energy efficiency of the PtG plant.

The process could be at first divided into two blocks, as Figure 5.17 suggests. The first conversion is from the solar energy to electric energy by means of the photovoltaic panels. Then from electric energy to chemical energy (synthetic gas) which is the heart of the plant, in which there is a loss of efficiency as well.

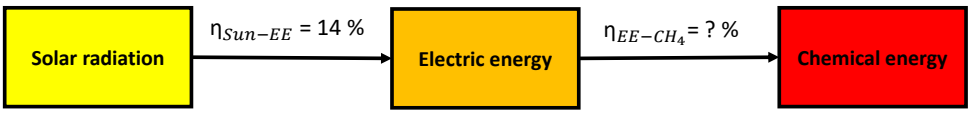

Figure 6.1 Energy conversion scheme

The efficiency that calculate the ratio between the final energy in the product with respect to the electric energy available from the PV plant is shown in Eq. 21.

$$\eta_{EE\ to\ CH_4}[\%] = \frac{Chemical\ energy\ (CH_4)}{Electric\ energy\ from\ PV} \qquad Eq.\ 21$$

Table 6.1 Conversion efficiency of all cases

		Efficiencies		
		Sun to EE	EE to CH_4	Sun to CH_4
FL	PV-CC-BES	14%	30%	4,26%
	PV-DAC-BES	14%	26%	3,59%
	PV-DAC-GT	14%	21%	3,19%
FLR	PV-CC-BES	14%	30%	4,26%
	PV-DAC-BES	14%	29%	4,12%
	PV-DAC-GT	14%	25%	3,46%
PLRO	PV-CC-BES	14%	39%	5,45%
	PV-DAC-BES	14%	35%	4,92%
	PV-DAC-GT	14%	31%	4,39%

The net efficiency of the PV plant remains the same in all cases. Efficiency depends on several variables but for the calculation of this work it is used the database PVGIS-SARAH that gives directly the power output of the PV. In this analysis the net efficiency of the PV plant is assumed equal to 14% and it is used only for this assessment. The real variable in Table 6.1 is η_{EE-CH_4}. The theorical η_{EE-CH_4} with the state of art is obtained multiplying the efficiency of the AEK (64%) with the methanator efficiency (78%). The result is 50%, but it does not take into account the energy expenditure to run BOP's and also the availability of the plant of 95%. Defining the minimum theorical energy expenditure for BOP's is complex as the power of the hydrogen compressor depends on the level of the storage level, and in the PV-CC-BES case power absorbed by the compressor is one of the main items for the auxiliaries total power.

The best η_{EE-CH_4} is achieved in PV-CC-BES case in PLRO. It is not surprising as in this case a few energy in used by BOP's because of the absence of the DAC system, which is very energy intensive.

Figure 6.2 gives a visual analysis of Table 6.1. In general, the efficiency increases after the integration and the introduction of partial load activity. Such increase does not occur in PV-CC-BES supply chain FLR case. This happens because the PV plant size doesn't change with the integration of ORC, the only difference is that the battery capacity is downsized thanks to the introduction of the additional electricity generation. So with the same nominal power of PV plant and the same yearly methane production (100 MW always at full load), the efficiency remains the same. The advantage in this case is only economic and has no impact from the energy perspective.

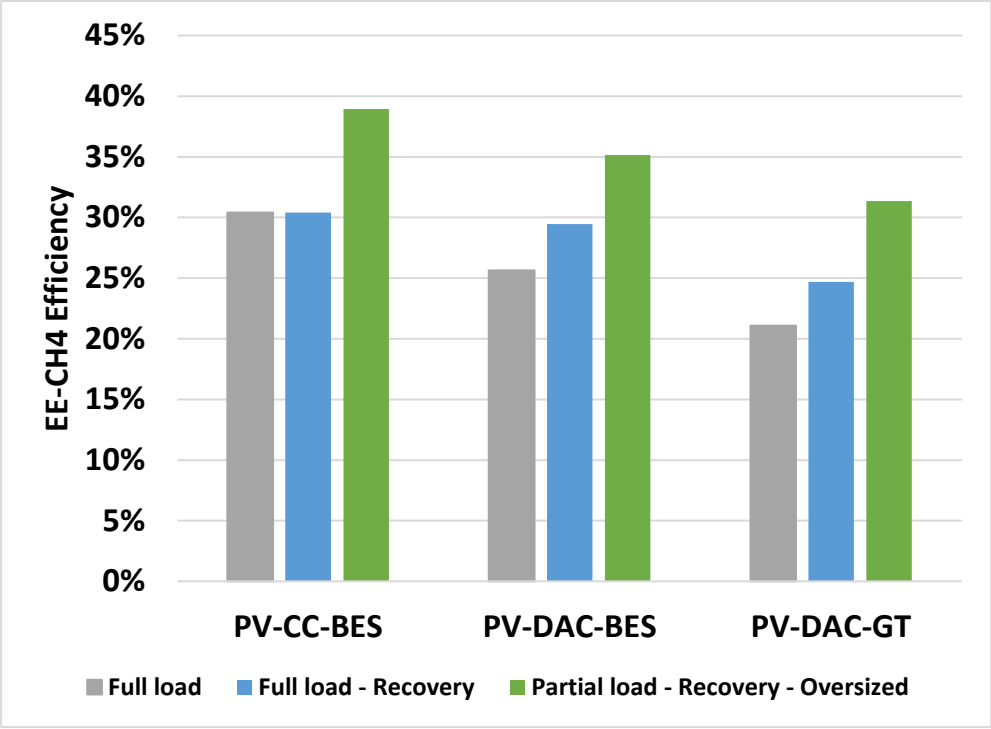

Figure 6.2 EE-CH_4 efficiency diagram

For PV-DAC-BES and PV-DAC-GT, the increase in efficiency from the FL case to the FLR comes from a better use of the electric energy from the PV plant. In particular the size of the PV plant is reduced with the introduction of HX_t, so the efficiency in Eq. 21 has the denominator which decreases while the numerator remains the same, the resulting efficiency must increase.

The step from the FLR to PLRO is different. In this case all chains show an increase in the efficiency. Now only numerator changes respect to FLR. Indeed the power block is the same

of FLR case. The oversized methanator allows the plant to transform more electric energy into syngas, so the numerator always increase and efficiency improves.

6.2 Analysis on carbon dioxide purchase cost

In this paragraph it is assessed at which cost of CO_2 the LCOM of PV-CC-BES aligns with the cost of the other two supply chains. This kind of evaluation is done only on PLRO case as it has revealed the best case.

For PV-CC-BES it has been calculated the LCOM function of the carbon dioxide price, from 40 \$/tCO_2 to 500 \$/tCO_2. Since the LCOM of PV-DAC-BES is lower than PV-DAC-GT, the breakeven price of CO_2 is lower for PV-DAC-BES. As Figure 6.3 suggests the results are 355 \$/tCO_2 for PV-DAC-BES and 400 \$/tCO_2 for PV-DAC-GT. It means that at these costs of carbon dioxide DAC technology results equally competitive. Nevertheless these costs are way higher respect to costs of carbon capture estimated in Figure 2.18, so when it is possible it is always more convenient to purchase carbon dioxide rather than capturing it from the air.

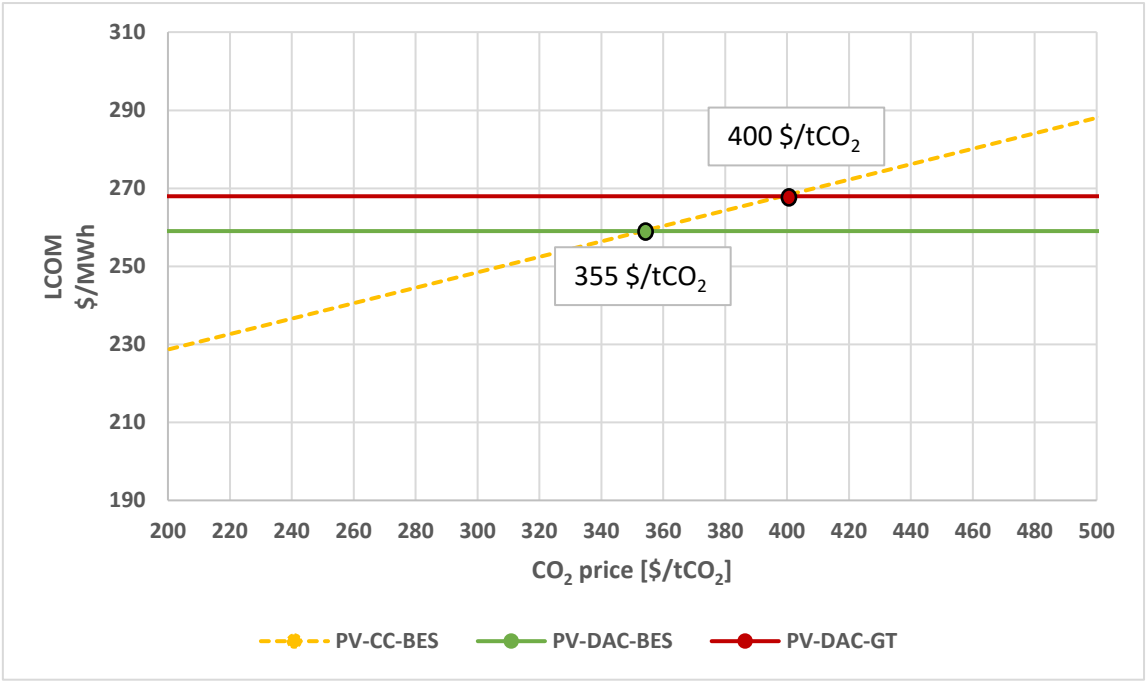

Figure 6.3 Breakeven cost of CO_2 purchased that equals the LCOM of PV-CC-BES to the other two supply chain in PLRO case

6.3 Sensitivity analysis on investment costs

In this section it is performed a sensitivity analysis on specific costs of some plant components. For this purpose the analysis considered only the four main elements: PV, AEK, DAC and Batteries. Only the PLRO case is analysed, because it is the most economically sustainable. For each item it is performed a reduction of 20% and 40% of the CAPEX and the new LCOM is assessed.

Figure 6.4 represents the LCOM for PV and AEK cost reduction. It appears that LCOM is more sensible to a variation of costs of PV rather than AEK. In particular a reduction of 40 % of the specific cost of PV lead to a reduction from 14% to 20% of the final LCOM, which is an important result.

Another interesting aspect is that a reduction in the cost of AEK lead the two DAC supply chains to converge. PV-DAC-GT has indeed the highest share of cost due two AEK, so it makes sense that it takes greater advantage from a reduction of cost of AEK rather than PV-DAC-BES.

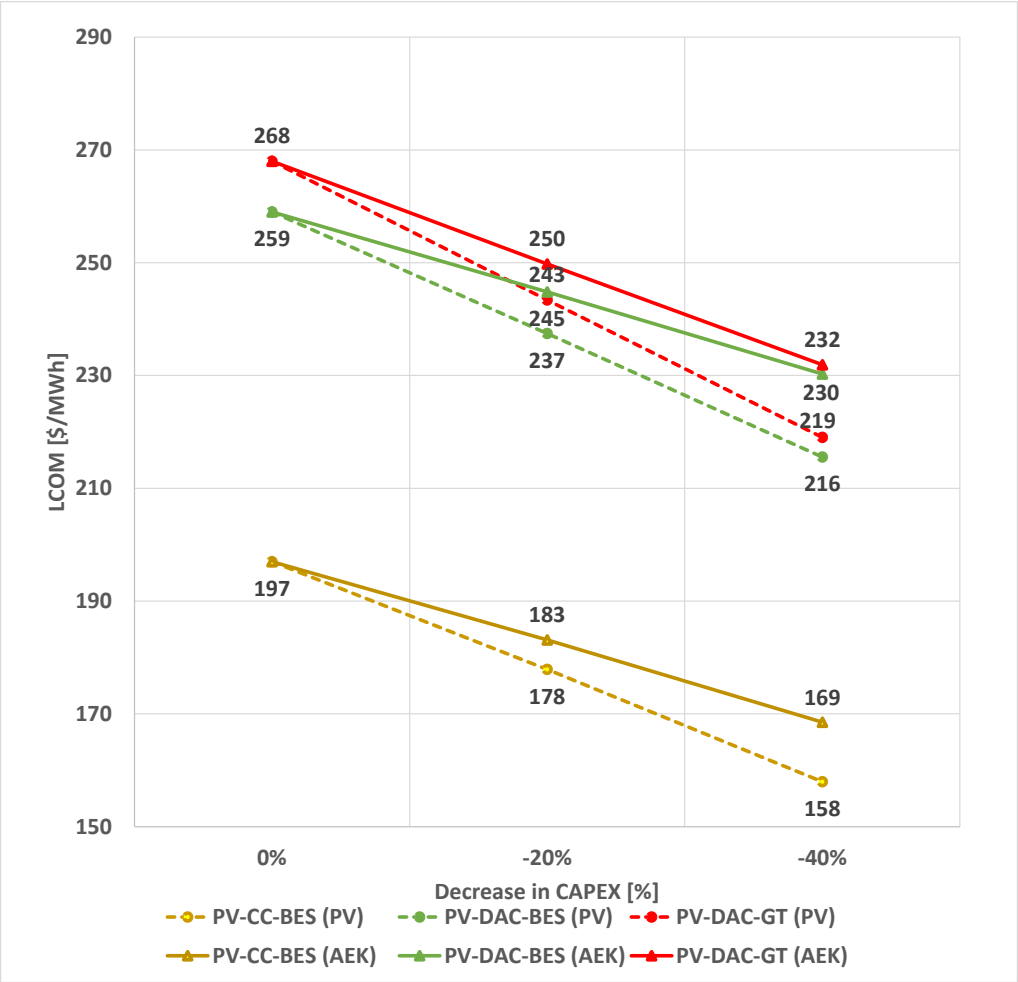

Figure 6.4 LCOM of different supply chains after a reduction in CAPEX of PV or AEK in PLRO case

The same kind of analysis is made for DAC and batteries. In this case not all chains are present as not all have batteries and DAC. PV-CC-BES is almost flat as in PLRO case the capacity of batteries is really small, PV-DAC-BES which uses both technologies is a good sample that shows that the decrease in the cost of batteries is more effective.

Both figures are in the same scale, and it appears evident that cost reduction of PV and AEK impacts way more than DAC and batteries.

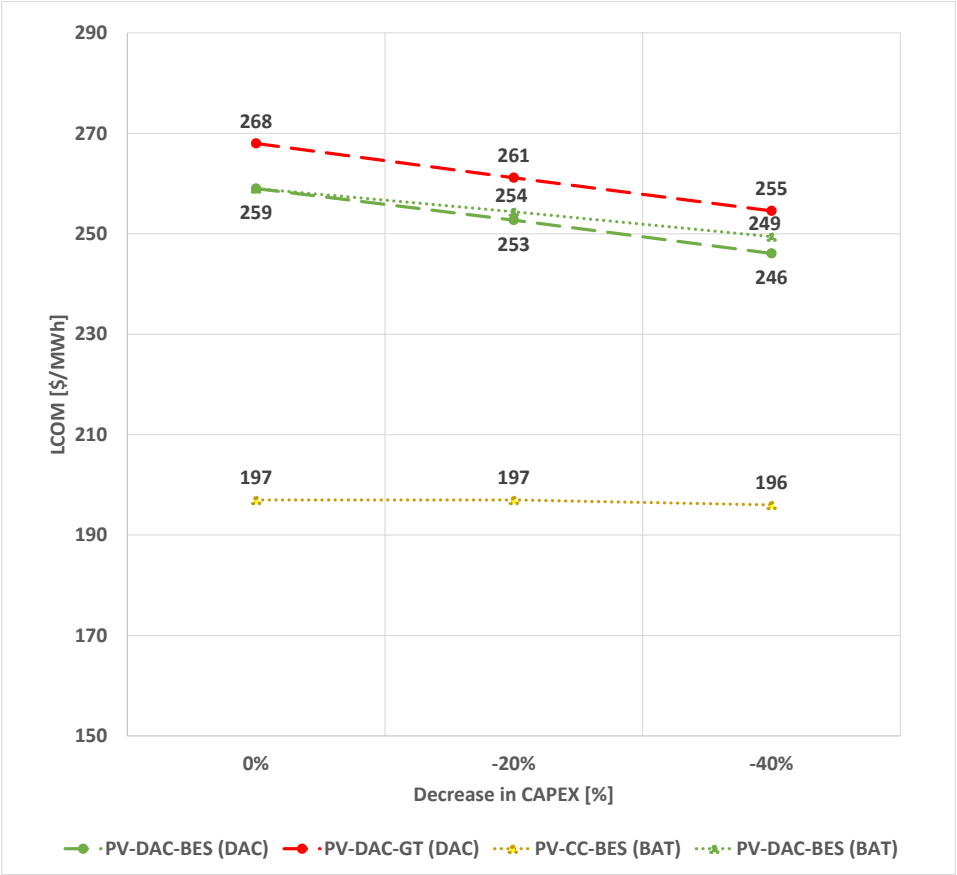

Figure 6.5 LCOM of different supply chains after a reduction in CAPEX of Batteries or DAC in PLRO case

Comparisons of configuration cases

In Table 6.2 it is shown a comparison between the nine cases. For each case the main indicators are reported. The cheapest configuration is PV-CC-BES in PLRO. The cheapest configuration results also to be the most efficient and the one that requires lower investment. Among the configurations that use DAC technology, the one using batteries results slightly better. It is also important to notice that PLRO configurations produce on average 25 % more SNG with respect to the FL types.

Table 6.2 Resume table of all cases comparing investment cost, annual production, LCOM and electric-to-chemical energy efficiency.

		Investment [mln $]	Production [GWh/y]	LCOM [$/MWh]	$\eta_{EE\text{-}CH4}$
FL	PV-CC-BES	1935	833	267	30%
	PV-DAC-BES	2582	833	362	26%
	PV-DAC-GT	2847	833	379	21%
FLR	PV-CC-BES	1875	833	253	30%
	PV-DAC-BES	2278	833	314	29%
	PV-DAC-GT	2530	833	338	25%
PLRO	PV-CC-BES	1847	1044	197	39%
	PV-DAC-BES	2264	1004	259	35%
	PV-DAC-GT	2574	1083	268	31%

Comparison between SNG and natural gas

It has been demostrated that the most profitable combination explored in this study is embodied by PLRO case. Now it is crucial to assess how much these conditions are away from the actual costs of fossil natural gas.

For this analysis it is used a reference price of 16 $/MWh as a threshold for the current cost of imported natural gas [31]. This value is then compared to the costs of synthetic methane previously calculated. The LCOM previously calculated don't take into account the cost of transport, which is instead included in the reference price. Nevertheless cost of transport for Europe for such location are in the range of 5-10 $/MWh [31], it is not such a game changer in this evaluation.

In Figure 6.6 are reported the differences in cost between PLRO case and the reference. The difference is wide, synthetic natural gas costs more than ten times its fossil equivalent. In long term it is possible that this difference in prices will get narrower thanks to a combination of reduction costs of RES and electrolysis technology, along with a gradual increase in fossil fuels cost.

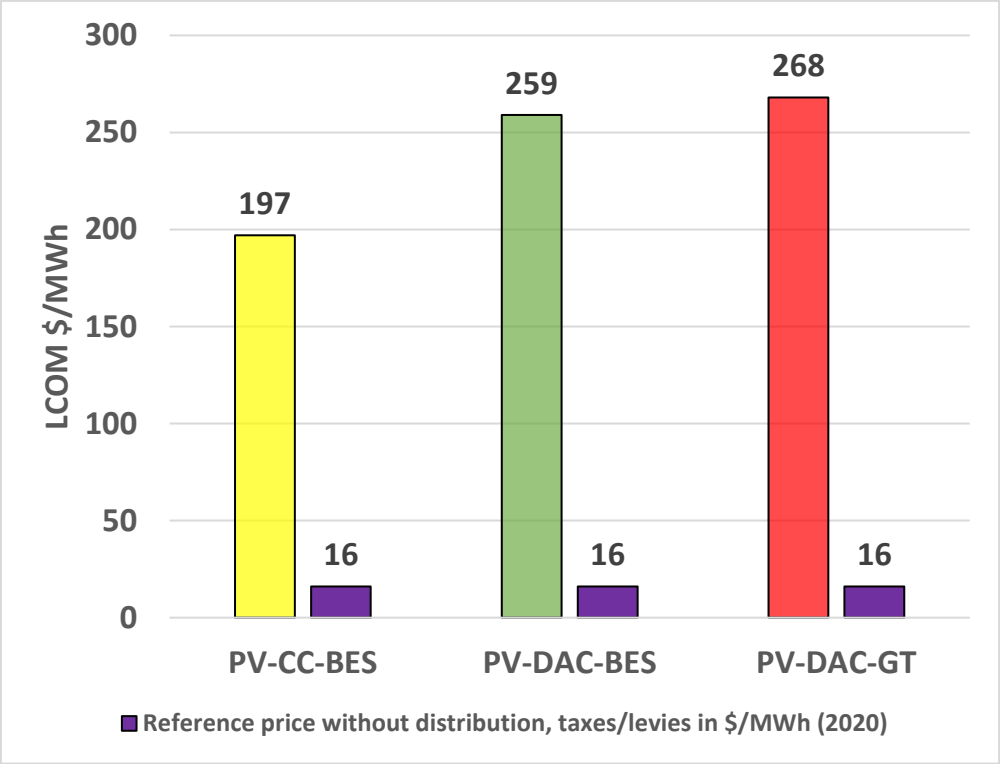

Figure 6.6 Levelized cost of synthetic methane (LCOM) in the PLRO case of each configuration (without transport), compared to the reference cost of imported natural gas (without distribution, taxes/levies).

Chapter 7 Conclusions

This work analysed a 100 MW off-grid Power-to-Gas plant based on solar PV. The plant is intended to work continuously, despite the intermittent nature of the energy source. Since there is no connection with the electric grid, some assets must be used to guarantee energy provision when the PV plant is off.

First, a review of the technologies involved has been done, followed by the location selection which had these main drivers: good irradiation, stable political situation, access to water and proximity to Oil & Gas distribution channels as well as presence of industrial settlements for carbon dioxide purchase. The selected location was Yanbu, Saudi Arabia.

Then it has been selected the set of configurations that will be explored in the analysis:

- PV-CC-BES purchases CO_2 from a supplier and uses batteries for energy storage,
- PV-DAC-BES uses a DAC system to capture carbon dioxide directly from the atmosphere and exploits batteries for electricity storage,
- PV-DAC-GT uses a DAC system but burns a part of the stored hydrogen in a gas turbine to generate electricity to run the BOP instead of using batteries.

These three supply chains are assessed in three cases, leading to a matrix of nine possible configurations. The three cases are:

- Full Load (FL): the plant always runs at full load;
- Full Load and Recovery (FLR): it is an improved version of the previous case, where the plant always operatesat full load but in addition the waste heat of the methanator is recovered and internally used;

- Partial Load with Recovery and Oversizing (PLRO): this explores the possibility to oversize the methanation block and work sometimes at partial load to achieve more flexibility.

The third case has the goal of downsizing the capacities of batteries and hydrogen storage and to recover the hydrogen that may be wasted when the storage is full and the hydrogen consumed by the methanator is lower than the quantity produced by the electrolyzer.

The analysis used a set of models for the different purposes: "days clustering" to identify the best/worst conditions in order to size the plant for continuous full load operation, hourly simulation for sizing H_2 storage and Batteries and to calculate the yearly production, daily energy simulation for the size of the methanator in PLRO. The hourly model is essential to detail the design of the storage systems, whose capacity depends upon the real weather conditions and the consumes of the plant. The capacity is decreased step by step starting from a very conservatively value until the plant experience a shut down during the year. In this way it is assessed the minimum value for each storage that allows the plant never to shut down.

Starting with the full load case (FL) it turns out that in order to produce 100 MW of SNG in steady stream condition, the plant requires 1.4-2.2 GW of PV and from 0.6 to 1 GW of electrolyzer, depending on the configuration. This massive nominal capacities cause the levelized cost of methane to be mainly driven by these two components, whose contribution represent 64-83% of the LCOM, which ranges from 265 $/MWh to 380 $/MWh. In the FL case, the configuration with carbon dioxide purchase results cheaper, so with the assumptions used appears more convenient to purchase CO_2 from exhaust of an industrial plant rather than capturing it from the atmosphere. In particular, the CC solution costs 26.3% lower than PV-DAC-BES and 29.6% less than PV-DAC-GT.

Moving forward, the analysis assessed the possibility to recover the heat released in the methanator by the exothermic reactions (FLR cases). In the PV-CC-BES configuration, this heat is used to generate electricity through an ORC system. In the other two supply chains, the heat is used to cover part of the heat demand of the DAC system. The analysis started verifying if the integration of the ORC was possible in PV-CC-BES, and how much heat

could be converted into electrical energy. In DAC configurations the heat exchanger is sized and the analysis assessed how much energy from the waste heat of the methanator could be conveyed to the DAC system to sustain the regeneration process. For CC configuration, the 65% of waste heat is conveyed to the ORC system, while in DAC configurations the 86% of the waste heat is conveyed to the DAC system, the remaining heat is discharged. Once the waste heat recovery has been evaluated, the plant components have been designed and sized in a similar way to the FL case. The result is good for all supply chains: the LCOM experiences a reduction from 5% to 13% compared to the corresponding FL cases, and the benefit is more significant in supply chains that use DAC.

Finally the PLRO case has been assessed, in which the plant is given the possibility to switch from full load to partial load (at 50%). This case has been developed because in the previous cases the capacity of the storage systems was mainly driven by the assumption of sizing the plant in order to guarantee a steady stream of 100 MW of SNG in the least favourable conditions ("worst day"). This means that if the conditions are more favourable, the methane production is choked to 100 MW due to the methanator capacity, but in principle the energy availability could allow the plant to produce more. In order to overcome this constraint, here the methanator is oversized keeping the same capacities of PV and AEK, and it is introduced the possibility to run at partial load to achieve flexibility.

An algorithm has been developed that governs the load. There are two variables that influence the algorithm, the forecasts of the upcoming 24 hours and the control of the levels of the storage of hydrogen, and electric energy if there are batteries. With the control of these two elements the plant decides to run at partial load to avoid the shutdown. The overall effect is a more efficient use of the storage systems (reduction of 20% of the capacity) and an increase of 25% on the yearly production of methane. The LCOM of this final case ranges from 197 to 268 $/MWh, i.e., a decrease of 17-22% with respect to the FLR. Even in this case the configuration with carbon dioxide provision instead of direct air capture results the least expensive.

IA sensitivity analysis was performed on the LCOM in function of investment cost of different components. As expected due to the high capacities involved, it turns out that the

LCOM is most sensitive to the investment cost of PV, a reduction of 40% of $CAPEX_{PV}$ turns into a reduction of LCOM between 17% and 20%, the same reduction for AEK causes a reduction of LCOM of 11-14%, while for DAC the reduction is of 5%. Then it has been estimated how much the carbon dioxide should cost to align the LCOM of the PV-CC-BES with the supply chain that use DAC technology. The result is that CO_2 should cost between 350-400 \$/tCO_2 to equalize the LCOM's. This indicates that DAC cost must drop significantly in order to become competitive. Anyway, this value is labile as the DAC technology is not mature and there is a wide uncertainty on future cost, especially looking at utility-scale applications.

The levelized cost of SNG for PV-CC-BES revealed 30% cheaper than the other two supply chains that uses DAC, so the independence that the DAC technology can provide has an important impact on the final cost. While there is not an appreciable difference between PV-DAC-BES and PV-DAC-GT as they are equally competitive.

Levelized costs of SNG in PLRO are then compared with a reference price of the natural gas sold in the market, in order to find the gap between the two cost. The "green" methane costs more than ten times its fossil alternative under the given scenario. In the following ten years the CAPEX of DAC is expected to decrease of more than 50% [9] , the cost of PV also is expected decrease of 20-30% [31], while it is not sure whether and how much the cost of natural gas will increase in the mid-term.

In conclusion, this work showed how components for efficient large scale production of SNG in remote regions exist and are able to exploit the large availability of low-cost RES. Anyway, the plant complexity affects the final cost and the investment costs of many components have to decrease strongly in order to make this solution applicable.

First Appendix

Legend of the graphical symbols used in the plant schemes:

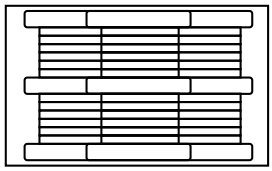

Electrolyser

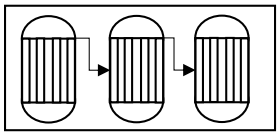

Methanator

Lamination valve

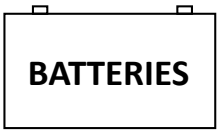

Lithium ion batteries

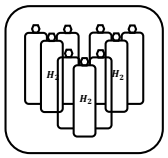

H_2 storage

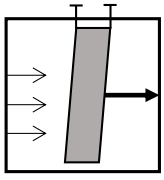

DAC system

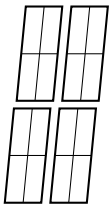

PV plant

Compressor

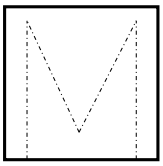

Heat exchanger

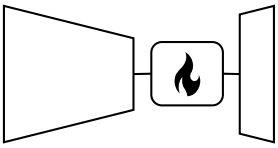

H_2 turbine

Acronyms and nomenclature

Acronyms

AEK	Alkaline Electrolyzer
BAT	Batteries
BES	Battery Energy Storage
BOP	Balance of Plant
CAPEX	Capital Expenditure
$CAPEX_a$	Annual Capital Expenditure
CC	Carbon Capture
CCS	Carbon Capture & Storage
CRF	Capital Recovery Factor
DAC	Direct Air Capture
EL	Emergency Level
FL	Full Load
FLR	Full Load with recovery
HL	Hydrogen Level
HX_m	Heat Exchanger of Methanator
IEA	International Energy Agency
LCOM	Levelized Cost of Methane
OPEX	Operational Cost
ORC	Organic Rankine Cycle
P_{AEK}	Power of Alkaline Electrolyzer

PEM	Proton Exchange Membrane
PLRO	Partial Load with Recovery and Oversizing
P_{PV}	Power of Photovoltaic plant
PtG	Power to Gas
PV	Photovoltaic
SNG	Synthetic Natural Gas
SOC	State of Charge
SOEC	Solid Oxide Electrolyzer Cell
WACC	Wheighted Average Cost of Capital

Nomenclature

$\Delta H°_R$	Standard Entalpy of reaction	kJ/mol
$R_{AEK/PV}$	Rate between Power of AEK and PV plant	-
E_{tot_left}	Energy before the median in one year	Wh
E_{tot_right}	Energy towards the median in one year	Wh
E_{tot}	Total Energy in one year	Wh
E_a	Daily Energy of "average day"	Wh
E_w	Daily Energy of "worst day"	Wh
E_b	Daily Energy of "best day"	Wh
a_{right}	Number of "average" days towards the median	-
a_{left}	Number of "average" days before the median	-
b	Number of "best" days	-
w	Number of "worst" days	-
Z_s	Compressibility fo CO2 for each stage	-
k_s	Average ratio of specific heats (Cp/Cv) of CO2 for each stage	-
R	Gas constant	kJ/kmol K
M	Molar mass of carbon dioxide	kg/kmol
T_{in}	Temperature at inlet of each stage	K°
η_{is}	Isentropic efficiency	-
β	Compression ration of each stage	-
$\dot{m}$	Mass flow rate	kg/s

A	Area	kJ/mol
Q	Heat power	-
η	Efficiency	-
E_y	Yearly energy production	MWh
ΔE	Total Energy in one year	Wh
C_{rate}	C rate of the battery	-
η_{SUN-EE}	Efficiency from solar energy to elecetric energy	-
η_{EE-CH4}	Electric energy to methane	-

Bibliography

[1] IRENA, «RENEWABLE ENERGY MARKET ANALYSIS,» *IRENA,* 2019.

[2] F. Remonato, «Integration of the methanation process within a Power-to-Gas storage system using biogas as source of CO2,» Politecnico di Milano, Milano, 2014.

[3] G. Realmonte, "An inter-model assessment of the role of direct air capture in deep mitigation pathways," *nature communications,* pp. 1-2, 2019.

[4] I. R. E. Agency, «Renewable power generation costs in 2018,» IRENA, Abu Dhabi, 2018.

[5] F. W. &. Y. X. Weijia LIU, «Power-to-gas technology in energy systems: current status and prospects of potential operation strategies,» *Journal of Modern Power Systems and Clean Energy,* 2017.

[6] A. G. I. S. A. H. J. N. S. F. O. Schmidt, «Future cost and performance of water electrolysis: An expert elicitation study,» *international journal of hydrogen energy,* 2017.

[7] World energy council, «INTERNATIONAL ASPECTS OF A POWER-TO-X ROADMAP,» *Frontier economics,* 2018.

[8] NREL, «Solar Photovoltaic Technology Basics,» [Online].

[9] M. Fasihi, «Techno-economic assessment of CO2 direct air capture plants,» *Journal of Cleaner Production,* pp. 962-970, 25 January 2019.

[10] M. Götz, "Comparison of Biological and Catalytic Methanation for Power-to-Gas Applications," Karlsruhe Institute of Technology (KIT), Karlsruhe, 2015.

[11] J. Agersborg e E. Linghed, «Integration of Power-to-Gas in Gasendal and GoBiGas,» CHALMERS UNIVERSITY OF TECHNOLOGY, Göteborg, Sweden, 2013.

[12] InformationAdministration, U.S. Energy, «Country Analysis Brief - Saudi Arabia,» 2011.

[13] SOLARGIS, ESMAP, WORLD BANK GROUP, «Global Solar Atlas,» [Online].

[14] Europen Commission, «EU SCIENCE HUB,» [Online].

[15] X. Jia, «Analyzing the Energy Consumption, GHG Emission,and Cost of Seawater Desalination in China,» *Energies,* 2019.

[16] M. U. L. Jens Perner, «The Future Cost of Electricity-Based Synthetic Fuels,» Agora Verkehrswende, Agora Energiewende and Frontier Economics (2018), 2018.

[17] D. L. McCollum, «Techno-Economic Models for Carbon Dioxide Compression, Transport, and Storage &amp,» UC Davis, 2006.

[18] Authority, Energy Market, «Review of the Vesting Contract Technical Parameters,» 2017.

[19] IEA, «IEA G20 Hydrogen report,» 2019.

[20] S. H. C. Biang Miao, «The Profitability Estimation of a 100 MW Power-to-Gas Plant,» *Elsevier,* 2018.

[21] M. G. A. L. M. S. Domenico Ferrero, «Power-to-Gas Hydrogen: techno-economic assessment of processes towards a multi-purpose energy carrier,» Elsevier Ltd, Torino, 2016.

[22] D. Pauschert, «Study of Equipment Prices in the Power Sector,» *ESMAP,* p. 23, 2009.

[23] M. Thomas Tartière, «A World Overview of the Organic Rankine Cycle Market,» *Elseviere,* 2017.

[24] E. W. Munish Chandel, «Synthetic natural gas (SNG) : Technology, Enviromental implications, and Economics,» 2009.

[25] J. K. M. L. D. U. S. Yu Wang, «Storage system of renewable energy generated hydrogen for chemical industry,» World Hydrogen Energy Conference 2012, 2012.

[26] L. B. J. v. W. H. L. N. H. E. Wim Mallon, «Costs of CO2 transportation infrastructures,» *ELSEVIER,* 2013.

[27] G. M. C. B. D. M. E. R. M. Eero Vartiainen, «Impact of weighted average cost of capital, capital expenditure,and other parameters on future utility scale PV levelised costof electricity,» *Wile Photovoltaics,* 2019.

[28] IEA Energy Technology Network, «ETSAP,» IEA Energy Technology Network, 2010.

[29] M. R. S. Koohi-Fayegh, «A review of energy storage types, applications and recent developments,» *Journal of Energy storage,* 2020.

[30] M. B. P. S. E. M. E. R. T. P. D. Casartelli, «Power block off-design control strategies for indirect solar ORC cycles,» Elsevier, 2014.

[31] M. U. A. L. Jens Perner, «The Future Cost of Electricity-Based Synthetic Fuels,» Frontier economics, 2017.

[32] J. J. K. P. S. V. S. R. W. A. Xuexiu Jia, «Analyzing the Energy Consumption, GHG Emission,and Cost of Seawater Desalination in China,» *Energies,* 2019.

[33] M. J. M. v. d. B. William Zappa, «Is a 100% renewable European power system feasible by 2050?,» *Applied Energy,* 2019.